Názov operačného programu:	OP Výskum a vývoj

NÁSLEDNÁ MONITOROVACIA SPRÁVA PROJEKTU

Názov projektu	Environmentálne aspekty urbanizovaného prostredia
Kód ITMS	26220220110
Kód rozhodnutia EK	
Prijímateľ	Univerzita Konštantína Filozofa v Nitre

Operačný program	2620002 OP Výskum a vývoj
Prioritná os	Prioritná os 2 - Podpora výskumu a vývoja
Opatrenie	2.2 Prenos poznatkov a technológií získaných výskumom a vývojom do praxe
Kód výzvy	OPVaV-2009/2.2/04-SORO
Schéma štátnej pomoci / schéma de minimis	
Názov lokálnej stratégie komplexného prístupu	

Poradové číslo následnej monitorovacej správy	2
Monitorované obdobie	04/2015 - 03/2016

1. Miesto realizácie projektu			
Región (NUTS II)		Vyšší územný celok (NUTS III)	
NUTS 2 Západné Slovensko		Nitriansky kraj	
Okres	Obec	Ulica	Číslo
Okres Nitra	Nitra	Tr. A. Hlinku	1
Existencia marginalizovaných rómskych komunít		[X] áno [ ] nie	

1. Miesto realizácie projektu			
Región (NUTS II)		Vyšší územný celok (NUTS III)	
NUTS 2 Západné Slovensko		Nitriansky kraj	
Okres	Obec	Ulica	Číslo
Okres Nitra	Nitra	Nábrežie mládeže	91
Existencia marginalizovaných rómskych komunít		[X] áno [ ] nie	

2. Príspevok k horizontálnym prioritám	
Informačná spoločnosť	[ ] áno [X] nie
Udržateľný rozvoj	[ ] áno [X] nie
Marginalizované rómske komunity	[ ] áno [X] nie
Rovnosť príležitostí	[ ] áno [X] nie

3. Finančný a časový rámec realizácie projektu			
Časový rámec realizácie projektu	Plánovaný stav (MM/RRRR)	Skutočný stav (MM/RRRR)	
Začiatok realizácie aktivít projektu	01/2011	01/2011	
Ukončenie realizácie aktivít projektu	12/2013	12/2013	
Celkové oprávnené výdavky projektu	Plánovaný stav (v EUR)	Skutočný stav (v EUR)	Stav realizácie projektu (v %)
	934 139,87	805 673,09	86,25

4. Merateľné ukazovatele projektu

Typ	Názov merateľného ukazovateľa výsledku	Merná jednotka	Počet jednotiek			
			Východiskový stav	Plánovaný stav	Stav dosiahnutý bezprostredne po ukončení realizácie aktivít projektu	Skutočný stav
Výsledok	Počet prác publikovaných v nerecenzovaných vedeckých periodikách a zborníkoch	počet	0	1	1	1
Výsledok	Počet realizovaných nástrojov na propagáciu výskumu a vývoja a popularizáciu ich výsledkov v širšej verejnosti	počet	0	2	2	2
Výsledok	Výskumníci do 35 rokov vlastnej organizácie a partnerov, ktorí využívajú poskytnutú podporu - ženy	počet	0	1	1	1
Výsledok	Výskumníci nad 35 rokov vlastnej organizácie a partnerov, ktorí využívajú poskytnutú podporu - ženy	počet	0	5	5	5
Dopad	Počet publikácií v karentovaných časopisoch	počet	0	1		1
Dopad	Počet publikácií v nekarentovaných časopisoch	počet	0	1		1
Dopad	Počet vedeckých prác publikovaných v recenzovaných vedeckých periodikách	počet	0	1		1

5. Merateľné ukazovatele projektu s relevanciou k horizontálnym prioritám

Horizontálna priorita informačná spoločnosť

Typ	Názov merateľného ukazovateľa	Merná jednotka	Východiskový stav	Plánovaný stav	Stav dosiahnutý bezprostredne po ukončení realizácie aktivít projektu	Skutočný stav

Horizontálna priorita trvalo udržateľný rozvoj

Typ	Názov merateľného ukazovateľa	Merná jednotka	Východiskový stav	Plánovaný stav	Stav dosiahnutý bezprostredne po ukončení realizácie aktivít projektu	Skutočný stav

Horizontálna priorita marginalizované rómske komunity						
Typ	Názov merateľného ukazovateľa	Merná jednotka	Východiskový stav	Plánovaný stav	Stav dosiahnutý bezprostredne po ukončení realizácie aktivít projektu	Skutočný stav
Horizontálna priorita rovnosť príležitostí						
Typ	Názov merateľného ukazovateľa	Merná jednotka	Východiskový stav	Plánovaný stav	Stav dosiahnutý bezprostredne po ukončení realizácie aktivít projektu	Skutočný stav

PRILOHA č.1

EVALUATION OF MICROCLIMATIC FACTORS IN DIFFERENT LAYOUTS OF BUILT-UP AREAS AND VEGETATION COVER OF URBAN AREAS OF NITRA MUNICIPALITY

Ján KLEIN[1], Zdenka RÓZOVÁ[2]

[1] *Department of Ecology and Environmentalistics, Faculty of Natural Sciences, Constantine The Philosopher University in Nitra, Nitra, 94974, Slovakia; e-mail:jan.klein@ukf.sk;*

[2] *Department of Ecology and Environmentalistics, Faculty of Natural Sciences, Constantine The Philosopher University in Nitra, Nitra, 94974, Slovakia; zrozova@ukf.sk*

Abstract

Many studies highlight altered climatic conditions of urban environment resulting from the presence of artificial materials at large active surface areas. These areas radiate heat (accumulated from direct solar radiation) in the periods of a negative energy balance, which occurs already during the daylight but especially after sunset. Urban vegetation affects the urban climate not only by its structure but especially by its functions. Research on microclimate dealing with relationships between vegetation cover and urban environment can bring benefits to land-use planning, as well as maintenance of urban greenery and appropriate design of its layouts, resulting in healthier environment for urban population. Our poster aims at comparing four selected layouts of urban built-up areas of the Nitra municipality in relation to microclimatic factors of air flow, surface temperature, relative air humidity and air temperature. Data on microclimatic factors were obtained by the method of surface temperature monitoring by TSI Veloci Cale 9565 – P device in 2014 (April - September). Individual built-up area layouts include Street compact built-up areas (historical), Street scattered built-up areas (houses with gardens), Scattered built-up areas (industrial zone of the town), and Mixed built-up areas adjacent to a town park. Each built-up area layout is represented by a street with a vegetation cover surface and an uncovered surface.

Different airflow in the scattered built-up area, the industrial part of town in the monitored area without vegetation is a result of an open space of the wide street. In the compact street built-up area, the airflow is restricted to its orientation. The presence of a park has an impact on the surrounding built-up areas. The dense cover of the high shrubs eliminates the airflow and it maintains relative air humidity high and it can decrease the air temperature even by 4.1°C. More compact structures of trees in the park have a climatic impact on the adjacent built-up areas. Broadleaf trees have a greater microclimatic effect than the coniferous ones.

Key words: urban climate, urban vegetation, built-up area layout, microclimatic factors

Introduction

Urban climate was created as a result of replacing natural soil by vast areas of impermeable roads, pavements, parking places, roofs of walls with dense and artificial surface of solid and dense structure (Kuttler, 2008). Different thermal characteristics of active surfaces lead to the absorbing of heat in time of positive energy balance. The result is that central urban zone is warmer than surrounding land. (Scudo et. al., 2002). The factor of densely built-up area is considered to be one of the key reasons of UHI effect. (Kantzioura - Kosmopoulos - Zoras, 2012). Differences in temperature are also attributed to urban geometry – the size, shape and

orientation of buildings and streets as well as the nature of urban areas – their albedo, thermal capacity of materials, thermal conductivity and humidity (Landsberg, 1981). In urban environment there is the change of geometry of active surface. Increasing of area of active surface and predominance of surfaces with vertically orientation are significant as well. These aspects lead to increasing of quantity of absorbed shortwave radiation and to reflections (Voogt, 2003). Even temperatures of horizontal earth surfaces are more significant than surface temperatures. Wind direction and speed combined with street orientation, as well as the effect of trees, increase of the height/width ratio, increase of the albedo of earth surface and walls, have the greatest impact on street canyon microclimate in relation to temperatures of air and surfaces (Andreou - Axarli, 2012). Urban climate is directly connected to street axes configuration, height of buildings and their attributes. Relationship of urban morphology and microclimate change and air quality within a town centre also affects thermal comfort of pedestrians (Krüger - Minella - Rasia, 2011). Changes to urban conditions often cause environment quality deterioration and can result in damage to health of the citizens of towns (Kuttler, 2008). Vegetation plays the significant role in the forming of microclimate and thermal comfort (Scudo et. al., 2002). Vegetation has a significant impact on energy balance, as even though green areas have low albedo, thus absorbing a great part of emanating radiation, they maintain a lower temperature than usual regarding hard surfaces, as they are cooled by evapotranspiration (Pearlmutter et al. 2014). Vegetation improves environmental variables like solar radiation, temperatures of surrounding surfaces, temperature and humidity of air and wind speed, which are also important for thermal comfort of people due to their qualities – limited emission of direct solar radiation on surrounding buildings and surfaces, air cooling by evapotranspiration and wind speed reduction (Akbari - Pomerantz - Taha, 2001). Spangenberg et al. (2008) confirm the cooling effect of park vegetation in comparison with the open town square average by 2°C and in comparison with the street canyon by 2.5°C during midday while the maximum difference was 6°C. The relative air humidity was also 10 % higher in the park with the compared areas. However, by continuing the research by simulation of incorporation of trees in a street canyon by the particular method had a restricted cooling effect on the air temperature (1.1°C) but it also lead to a significant cooling of the street surface above 12°C. By comparing the surface type as well as the localities, Keresztesová – Rózová (2013) recorded a provable impact of vegetation on the local microclimate. With the increasing number of green areas the surface temperature is decreased as well as the relative air humidity is increased. Reháčková – Pauditšová (2006) found out the difference in surface temperatures between the tree cover and the open stand. Even a solitary tree has a significant cooling effect on the surface in warm summer days (Reháčková – Pauditšová, 2006). In the park, this difference was smaller or rather it created more balanced surface temperature (Rózová et al., 2013). Significant impact on the wind direction has vegetation with structure and type of canopy. Vegetation areas in urban environment work as a thermal stabilizer. Crowns of trees in dense canopy keep the air temperature in the spring period. Significant microclimatic function of vegetation is to provide partially obscuration (Bahnová, Rózová, 2014).

The paper aims at comparing microclimatic factors in different vegetation structures as well as within four street corridors representing different types of built-up areas of the town of Nitra. Partial evaluation of the ongoing research has been recorded for the period from April to September.

Materials and methods

Four localities in the town of Nitra were selected. Each locality within a whole street block represents a different urban structure. Particular monitored locality with two monitored areas

with different plant structure represents a relatively homogenous character of a built-up area. They are particular streets predominantly oriented in north-south direction with different vegetation representations. The orientation has been taken into consideration according to the h/w ratio (height/width) for the microclimatic effect of trees to be shown at the largest extent as possible (Andreou, 2014). Individual localities representing certain types of urban built-up areas were selected as follows:

1. Compact layout in the town historical centre, representing typical street canyon (Farska street, Fig. 1). It is a street with 10 to 15 m high historical terraced buildings (Locality 1).
2. Detached layout – family houses with gardens (Moyzesova street, Fig. 2). Detached single-storey family houses with front yards are most frequently represented in this layout. (Locality 2).
3. Industrial layout, industrial part of town (Bratislavska street, Fig.3). It is a broad and open street with a four-lane road, up to 8 m high buildings and spacious parking places with grassy islands (Locality 3).
4. Mixed layout adjacent to the town park (Jesenskeho street, Fig.4). It is a relatively narrow street (10 – 20 m) and its corridor on the southern part is created by buildings up to the height of 10 m with a gradual continuing to the park on the northern part (Locality 4).

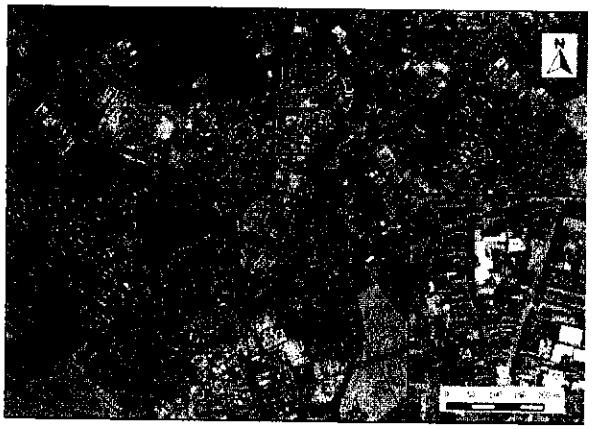

Fig. 1 Compact layout (historical), Farska street – Locality 1

Fig. 3 Industrial layout in industrial part of town, Bratislavska street – Locality 3

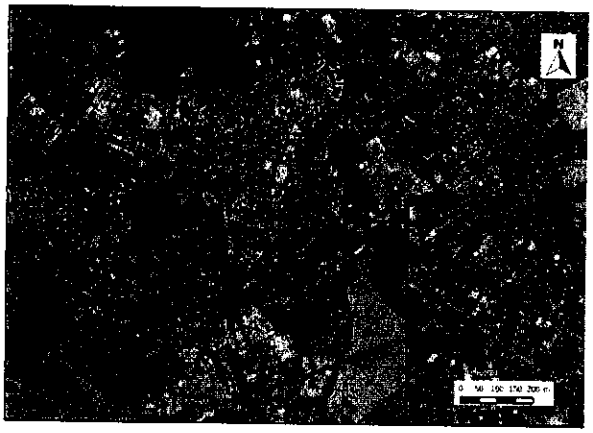

Fig. 2 Detached layout- family houses with gardens, Moyzesova street – Locality 2

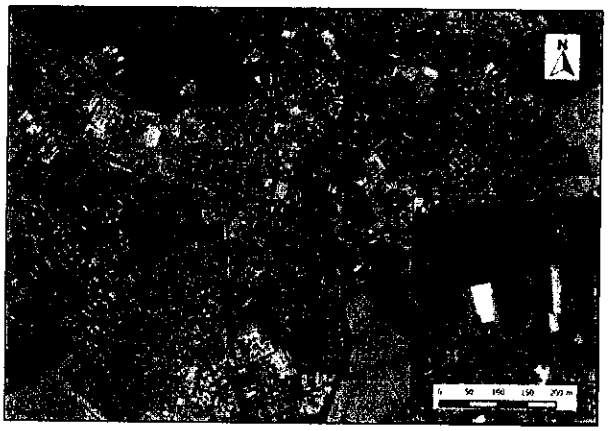

Fig. 4 Mixed layout adjacent the town park, Jesenskeho street – Locality 4

All monitored surfaces in monitored areas are asphalt as the most frequently represented type of surface in urban environment in general. Each locality comprises two monitored areas – an area without vegetation cover, respectively with minimum cover, and an area with vegetation cover. Vegetation cover is represented by plants, particularly trees, representing public greens.

Measurements were carried out by anemometer TSI Veloci Cale 9565 – P (air temperature, relative air humidity, airflow, temperature of horizontal surfaces) once a week, two times a day – at midday and in the evening. The day interval anticipates also the accumulation process and it records the culmination of the air temperature during the day for more accurate results (Klein – Rózová, 2014). Monitored day is characterised by anticyclone weather, respectively by a prevalence of direct solar radiation, as the surface and adjacent air layers are intensely heated by solar radiation during the day. The evening measurements were adapted to the day time during the monitored time period – one hour after the sunset. We compared differences in measured values in the monitored areas with vegetation cover and without vegetation within a single street canyon as well as differences between localities, respectively in different layouts of built-up areas. Data used for this research were recorded in the period from April to June. Data for March were not used as a result of incomparable days (starting vegetation period) because of statistical evaluation. Measurements were statistically evaluated by the one-way ANOVA test and confirmed by the Tukey HSD test. They were compared within monitored areas as well as localities in Statistica 7.

Results and discussion

In evaluating the data of measured microclimatic factors – airflow, air temperature, relative air humidity and surface temperature – among the selected localities, we have used one-way analysis ANOVA. The methodology has been set in such way that the measured data would catch the presupposed microclimatic effects of vegetation.

Statistically significant difference in the airflow depending on the locality has been shown in the locality 3 and 1 (Fig. 5) by using the one-way ANOVA test, $p<0,05$ (Tab.1, Fig.5). The locality 3, shattered built-up area – industrial part of town, represents the biggest share of open built-up areas in which the highest values of airflow has been recorded. The great airflow has been also recorded in the locality 1 – just in the narrow street canyon that might be caused by restriction of the air flow only to direction of the street canyon. In the locality 3, the airflow had a completely different extent of medians that shows a great significance of trees in catching the airflow. Akbari – Pomerantz – Taha (2001) point in a similar way to trees having been reducing the speed and direction of the wind.

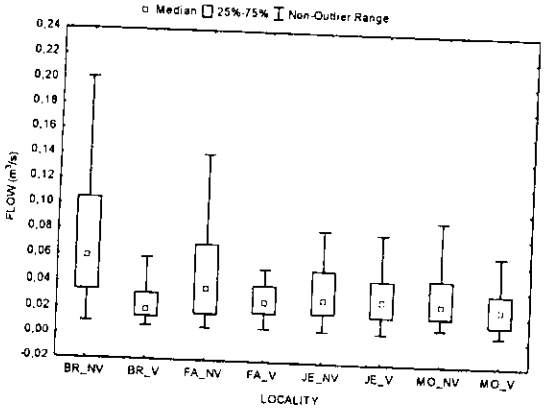

Fig. 5 Comparison of airflow in localities and monitored areas, BR (locality 3), FA (loacality 1), JE (locality 4), MO (locality 2); V (vegetation), NV (non-vegetation)

Effect	SS	Degr. Of F.	MS	F	p
Intercept	0,511179	1	0,511179	320,1972	0,000000
Locality	0,064985	7	0,009284	5,8151	0,000003
Error	0,395920	248	0,001596		

Tab. 1 One-way ANOVA, $p<0,05$, variable air flow, all localities

We have not found any statistically significant difference in the air temperature factor depending on the locality (Fig. 6). The biggest average difference between the air temperature with and without vegetation cover has been in the locality 3 (1,2°C), (Tab. 2) which represents the difference in comparison with the spring season (Klein – Rózová, 2014). All the medians of values had a close development. The lowest average difference in the air temperature was in the locality 4 (0,6°C), (Tab. 2). Small differences in the air temperature are caused by the impact of the neighbouring park. The average air temperature difference between the vegetation cover and the areas without vegetation in the localities was 0,84°C. Almost all the higher differences of the air temperature (above 2°C) were recorded in the locality 3 – industrial layout, industrial part of town. The maximum measured air temperature difference between the vegetation cover and the areas without vegetation was 4,1°C.

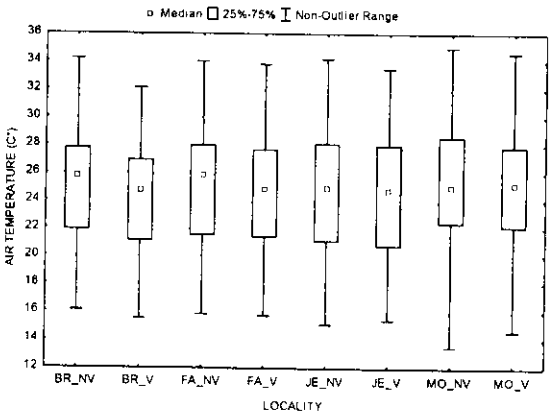

Fig. 6 Comparison of air temperatures in localities and monitored areas; BR (locality 3), FA (loacality 1), JE (locality 4), MO (locality 2); V (vegetation), NV (non-vegetation)

LOCALITY	Δ F (m3/s)	Δ AT (°C)	Δ H (%)	Δ ST (°C)
3 (Bratislavska)	0,052	1,272	5,179	5,977
1 (Farska)	0,036	0,701	1,923	5,770
4 (Jesenskeho)	0,027	0,603	2,444	1,813
2 (Moyzesova)	0,025	0,803	2,041	4,184

Tab. 2 Comparison of average differences of values of microclimatic factors between the vegetation cover and the areas without vegetation in all localities, Δ F – air velocity, Δ AT – air temperature, Δ H – relative humidity, ΔST – surface temperature

In the factor of relative humidity we have not found any statistically significant difference depending on the locality (Fig. 7) The greatest average difference in the air humidity between the vegetation cover and the area without vegetation was also in the locality 3 (5,1 %) (Tab. 2). The medians between the localities showed only minimum differences. The maximum values are interesting. The biggest difference in the air humidity was 15,1% and the above 10 % differences have been reached five times – all in the locality 3 – industrial layout, industrial part of town. It might be caused by the highest values of the airflow just in this locality. The

monitored area with vegetation cover represents a dense cover of high shrubs that eliminates the airflow and keeps the air humidity higher.

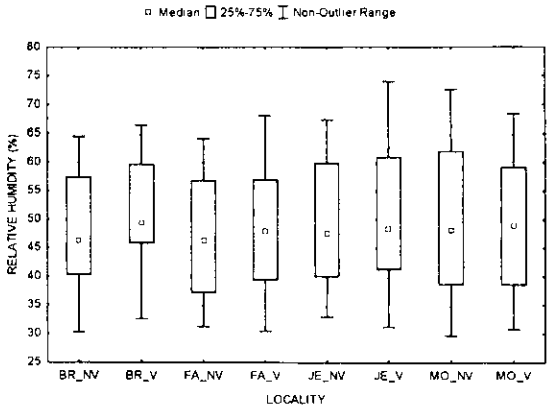

Fig. 7 Comparison of relative air humidity in localities and monitored areas; BR (locality 3), FA (loacality 1), JE (locality 4), MO (locality 2); V (vegetation), NV (non-vegetation)

In the microclimatic factor of surface temperature, we have recorded statistically significant difference depending on the locality and the presence of the vegetation one-way ANOVA, $p<0,05$, (Tab.2, Fig.8). All the surfaces are made from asphalt with high thermal capacity. By this effect, the asphalt influences the ground level of the atmosphere by the fact that it emits the transformed accumulated heat (Středa – Středová – Rožnovský, 2011). In the localities 1 to 3, the impact of trees on surface temperature became evident in the given structures. Raháčková – Pauditšová (2006) state that even a solitary tree has a significant cooling effect on the surface in warm summer days. In the industrial layout, industrial part of town the highest values in the surface temperature factor and the airflow factor have been reached by which the airflow impact on the surface temperature has not been shown. This is connected with the built-up structure where we can take the town geometry into consideration. Andreou – Axarli (2012) found out that for the air temperature and the surface temperature goes that the speed and direction of wind are influenced by street orientation, tree plantation, raising the H/W ratio and raising the albedo. The average surface temperature difference was 4,4°C between the vegetation cover and the area without vegetation. The highest values were recorded in the locality 1 and locality 3 with the maximum of 11,1°C that is in accordance with the results of Spangenberg et al. (2008).

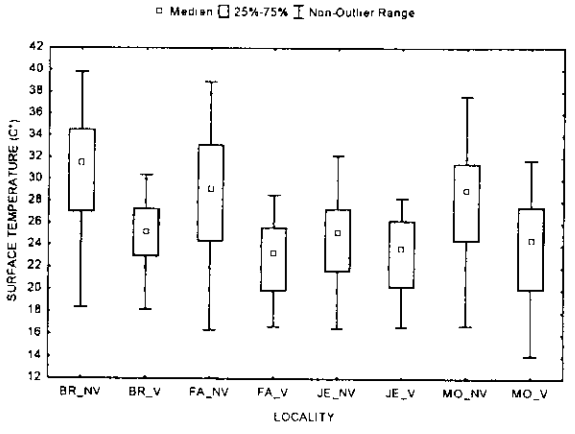

Fig. 8 Comparison of surface temperatures in localities and monitored areas; BR (locality 3), FA (loacality 1), JE (locality 4), MO (locality 2); V (vegetation), NV (non-vegetation)

Effect	SS	Degr. Of F.	MS	F	p
Intercept	172115,0	1	172115,0	7850,501	0,000000
Locality	1859,9	7	265,7	12,119	0,000000
Error	5437,2	248	21,9		

Tab. 3 One-way ANOVA, $p<0,05$, variable suface temperature, all localities

Locality 1 – Compact layout in the town historical centre

Farska street represents a typical "street canyon" – a narrow street with 10 to 15 metres long buildings in the terraced built-up area. The width of the street reaches only 8 metres. The monitored area with vegetation cover represents tress in the alley creating "canopy layer". They have a substantial impact on the airflow (Bahnová, Rózová, 2014) which is restricted to the direction of the street canyon. The monitored area with vegetation cover in this locality reached the lowest values of medians in comparison with the equivalent areas in the other localities. The subject structure of the cover in combination with the town geometry has the greatest cooling effect on the surface temperature. The effect of trees on reducing maximum air temperature is approximately 0.5 °C, while the effect on maximum horizontal ground temperature is 10 °C (Andreou - Axarli, 2012).

Locality 2 – Detached layout – family houses with gardens

In Moyzesova street, there are separately standing single-storey family houses with front gardens. The centre of the street is supplemented by 8 metres wide green zone with double tree alley. Here we can see numerous representation of the vegetation not only in the street area. The monitored area with the vegetation cover is comprised by coniferous trees. The range of air temperatures was highest just in this locality while the medians of air temperature values in the cover were slightly higher than outside the cover. The coniferous trees evince lower microclimatic effect. Abreu-Harbich – Labaki – Matzarakis (2012) state that the deciduous species provide better microclimatic characteristics than the permanent species.

Locality 3 – Industrial layout, industrial part of town

It is a wide open street with a four-lane road lined by buildings up to 8 metres long and extensive car parks with grassed over small islands. The monitored area without vegetation evinced very high values of the airflow not only as a result of the vegetation absence but also the town geometry. For wider streets with lower buildings the shadow effect of trees is very important (Andreou, 2014) that was shown in the surface temperature factor. The difference between the medians of the surface temperature has reached the highest value between the areas with and without vegetation cover. The dense high bushes in this locality are able to lower the air temperature by 4,1°C.

Locality 4 – Mixed layout adjacent to the town park

Jesenského street is relatively narrow (10 – 20 m) and it is created by building up to 10 metres long. In the north part it continuously passes to the town park in which the monitored area with vegetation cover is situated. The airflow had almost the same range at both of the areas. Factors of air temperature and relative air humidity had relatively the same course. The ranges of values correspond to the structure or the cover presence. The monitored area with a small portion of vegetation had lower values than the equivalent areas of the other localities. It is similarly stated by Yu – Hien (2006) that the cooling effects of parks are reflected not only in the lower temperatures in park but also in the lower temperatures in the surrounding area.

Conclusion

Ground thermal monitoring in the town of Nitra has been performed in four localities with diverse built-up structure. The localities were represented by the monitored area with and without vegetation cover. The data collecting were implemented in the vegetation season of April to September. The microclimatic factors – surface temperature, air temperature, relative air humidity and airflow were recorded. The data were statistically evaluated one-way ANOVA ($p<0,05$) where the statistically significant differences depending on the locality and the vegetation presence have been found out in the airflow and surface temperature factors.

The scattered tree cover in the open street built-up area – family houses with gardens does not have an impact on the total mesoclimate of the locality of given structure as closeness to the park in the mixed layout adjacent to the town park which keeps all the monitored microclimatic factors in relatively close development for the total mesoclimate of the locality. More compact tree structures in park have a climatic impact on the adjacent built-up areas. Broadleaf trees have a greater microclimatic effect than the coniferous ones. The higher representation of the broadleaf trees in the open street built-up area – family houses with gardens showed itself in the relative air humidity which was higher in the area with shattered representation of broadleaf trees than in the monitored cover of coniferous trees. The airflow is influenced by the vegetation cover structure and by the street configuration. The dense cover of high shrubs substantially eliminates the airflow and it keeps the relative air humidity higher and it is able to lower the air temperature by 4,1°C. The monitored area without vegetation cover in the industrial layout, industrial part of town showed very high values of the airflow not only as a result of the cover absence but also as a result of the town geometry. The substantial impact of trees on the airflow became evident in the compact historical built-up area even when in street canyon the airflow is restricted to its orientation. The airflow did not have an impact on the surface temperature, but it influences the air temperature. The air temperature and the relative air humidity did not show any statistically significant difference in the values between the localities. The time range of the year data does not show any significant differences in comparison with the spring season (Klein – Rózová, 2013). The vegetation has an impact on the environment mainly in the physiological maturity in the given vegetation season.

Acknowledgement

This study is the result of the project implementation: Environmental aspects of the urban environment ITMS 26220220110 supported by the Research & Development Operational Program funded by the ERDF and the result of the project: VEGA 1/0042/12 Analysis of selected environmental factors in relation to possible health risks.

References

Abreu-Harbich, L., V., de, Labaki, L., C., Matzarakis, A., 2012. Different Trees and configuration as microclimate control strategy in Tropics. ICUC8 – 8th International Conference on Urban Climates, 2012, UCD, Dublin Ireland

Akbari, H., Pomerantz, M., Taha, H., 2001. Cool surfaces and shade trees to reduce energy use and improve air quality in urban areas. Elsevier Science Ltd., *Solar Energy* Vol. 70, No. 3, pp. 295 – 310.

Andreou, E., 2014. The effect of urban layout, street geometry and orientation on shading conditions in urban canyons in the Mediterranean. Renewable Energy 63, Elsevier, pp. 587 – 596.

Andreou, E., Axarli, K., 2012. Investigation of urban canyon microclimate in traditional

and contemporary environment. Experimental investigation and parametric analysis. *Renewable Energy* 43 (2012), pp. 354 – 363.

Bahnová, K., Rózová, Z., 2014. Microclimatic conditions of housing estate Chrenova 1 in Nitra city. In: Rožnovský, J., Litschmann, T., (eds): Mendel a bioklimatologie. Brno, 3. – 5. 9. 2014, ISBN 978-80-210-6983-1

Kantzioura, A., Kosmopoulos, P., Zoras, S., 2012. Urban surface temperature and microclimate measurements in Thessaloniki. *Energy and Buildings* 44, pp. 63-72.

Keresztesova, S., Rózová, Z., 2013. Influence of vegetation on surface temperature in urban areas. Folia oecologica, vol. 40, no.1, ISSN 1336-5266

Klein, J., Rózová, Z., 2014. Impact of Vegetation on Microclimate in Different Layouts of Built-Up Areas in Urbanised Environment of Nitra Municipality in Spring Period. In: Rožnovský, J., Litschmann, T., (eds): Mendel a bioklimatologie. Brno, 3. – 5. 9. 2014, ISBN 978-80-210-6983-1

Krüger, E. L., Minella, F.O., Rasia, F., 2011. Impact of urban geometry on outdoor thermal comfort and air quality from field measurements in Curitiba, Brazil. *Building and Environment* 46 (2011), pp. 621 – 634.

Kuttler, W., 2008. The urban climate – Basic and applied aspects. In: Marzluff, J., M., Schulenberger, E., Endlicher W., Alberti, M., Bradley, G., Ryan, C., ZumBrunnen, C., Simon, U., ed., 2008: Urban ecology. Springer, New York, 807p., ISBN 978-0-387-73411-8

Landsberg, E. H., 1981. The urban climate, International geophysics series vol. 28, academic press, INC, New York, 277 p., ISBN 0-12-435960-4

Pauditšová, E., Reháčková, T., 2006: *Praktické skúsenosti s hodnotením mikroklimatickej funkcie vegetácie v urbánnom prostredí.* In: Sídlo-park-krajina IV. Kultúrna vegetácia v sídlach a v krajine. SPU, pp. 227-235, ISBN 80-8069-809-0

Pearlmutter, D., Erell, E., Snir, K., Shashua-Bar, R., 2014. The moderating effects of urban vegetation on pedestrian thermal stress in a hot-arid environment. *Urban Climate News*, (51), pp. 13-18.

Reháčková, T., Pauditšová, E., 2006. Vegetácia v urbánnom prostredí. Cicero, Bratislava, ISBN 80-969614-1-1

Rózová, Z. et al., 2013. Environmentálne aspekty urbanizovaného prostredia. FPV UKF v Nitre, 390 p., ISBN 978-80-558-0388-3

Scudo G., Dessi, V., Rogora, A., 2002. *Evaluation of radiant conditions in urban spaces.* In: Designing open spaces in the urban environment: a bioclimaticapproach. 2002, p. 12-17, ISBN 960-86907-2-2

Spangenberg, J., Shinzato, P., Johansson, E., Duarte, D., 2008. Simulation of the influence of vegetation on microclimate and thermal comfort in the city of São Paulo. Rev. SBAU, v. 3, n. 2, pp. 1 – 19.

Středa, T., Středová, H., Rožnovský, J., 2011. *Temperature Regime of the Urban Environment.* In: Středová, H., Rožnovský, J., Litschmann, T. (eds): Mikroklima a mezoklima krajinných struktur a antropogenních prostředí. Skalní mlýn, 2. – 4.2. 2011, ISBN 978-80-86690-87-2

Středová et al. 2011. Microclimate and mezoclimate of towns, microclimate of vegetation. [Mikroklima a mezoklima měst, mikroklima porostů], ČHMÚ, Praha, 102 p. ISBN 978-80-86690-90-2

Voogt, J. A., Oke, T. R., 2003. *Thermal remotesensing of urban climates.* Remote Sensing of Environment, 86, s. 370 – 384 .

Yu, C., Hien, W., N., 2006. Thermal benefits of city parks. Energy and Buildings 38, Elsevier, pp. 105–120.

Evaluation of Microclimatic Factors in Different Layouts of Built-Up Areas and Vegetation Cover of Urban Areas of Nitra Municipality

Ján KLEIN, Zdenka RÓZOVÁ

Department of Ecology and Environmentalistics, Faculty of Natural Sciences, Constantine The Philosopher University in Nitra, Nitra, 94974, Slovakia; e-mail:jan.klein@ukf.sk; zrozova@ukf.sk

Many studies highlight altered climatic conditions of urban environment resulting from the presence of artificial materials at large active surface areas. These areas radiate heat (accumulated from direct solar radiation) in the periods of a negative energy balance, which occurs already during the daylight but especially after sunset. Urban vegetation affects the urban climate not only by its structure but especially by its functions. Research on microclimate dealing with relationships between vegetation cover and urban environment can bring benefits to land-use planning, as well as maintenance of urban greenery and appropriate design of its layouts, resulting in healthier environment for urban population. Our poster aims at comparing four selected layouts of urban built-up areas of the Nitra municipality in relation to microclimatic factors of air flow, surface temperature, relative air humidity and air temperature. Data on microclimatic factors were obtained by the method of surface temperature monitoring by TSI Veloci Cale 9565 – P device in 2014 (April - September). Individual built-up area layouts include *Street compact built-up areas* (historical), *Street scattered built-up areas* (houses with gardens), *Scattered built-up areas* (industrial zone of the town), and *Mixed built-up areas* adjacent to a town park. Each built-up area layout is represented by a street with a vegetation cover surface and an uncovered surface.

Different air flow in scattered built-up areas (i.e. an industrial zone of the town) on monitored surface without vegetation results from the open space of a broad street. Air flow in the street compact built-up areas is restricted to its orientation. Irregular values in air flow predominantly occurred in monitored areas without vegetation. The highest values of the factor of surface temperature were recorded in scattered built-up areas. Air temperature medians in the street compact built-up areas in the historical town centre were higher in monitored area with vegetation cover, in which lower air flow medians were recorded.

Acknowledgement

This study is the result of the project implementation: Environmental aspects of the urban environment ITMS 26220220110 supported by the Research & Development Operational Program funded by the ERDF and the result of the project: VEGA 1/0042/12 Analysis of selected environmental factors in relation to possible health risks.

PRÍLOHA č. 2

DE GRUYTER
OPEN

Ekológia (Bratislava)
Vol. 34, No. 4, p. 392–402, 2015
DOI:10.1515/eko-2015-0035

ACCUMULATION OF SOLAR RADIATION DEPENDING ON TYPE OF SURFACE IN THE URBAN ENVIRONMENT OF THE CITY NITRA

KATARÍNA BAHNOVÁ , ZDENKA RÓZOVÁ

Department of Ecology and Environmental Sciences, Faculty of Natural Sciences, Constantine the Philosopher University in Nitra, Trieda A. Hlinku 1, 949 74 Nitra, Slovak Republic; e-mail: katarina.bahnova@ukf.sk, zrozova@ukf.sk

Abstract

Bahnová K., Rózová Z.: Accumulation of solar radiation depending on type of surface in the urban environment of the city Nitra. Ekológia (Bratislava), Vol. 34, No. 4, p. 392–402, 2015.

The diversity of active surfaces in urban environment is an alarming element of microclimatic conditions at the time of positive energy balance. The accumulation of solar and reflected radiation are forming local climate – microclimate. Vegetation areas in the urban environment have the capability to eliminate extreme demostrations of local climate. The impact of transpiration causes an increase in the relative air humidity, reducing the effect of solar radiation. The result is the elimination of surface temperature in vegetation. The aim of this study is to evaluate the potentiality of accumulation of solar radiation depending on the vegetation structure and the type of surface in research areas A1–B1–C1, A2–B2–C2 between intervals 6:30 a.m.–12:30 p.m., 12:30 p.m.–9:30 p.m. The legwork ran in summer period June–August 2013 in residential area Chrenova 1 in the city Nitra.

Key words: microclimate, surface temperature, vegetation structure.

Introduction

According to Wardoyo et al. (2011), the urban environment is specific to hard surface, typical urban geometry, vegetation areas and variability of surface materials. These factors form and influence microclimate. For every active surface, it is typical that there is a transformation of the energy of the shortwave radiation to the thermal energy. A part of this energy goes to sub base of active surface and vice versa. The active surface is the main climatic factor (Středová et al., 2011). Vegetation plays a significant role in the formation of microclimate and thermal comfort. The surface temperature of vegetation influences the thermal balance through the blazing change (Scudo et al., 2002). Different types of surfaces in the urban environment have different impacts on vegetation. The outflow and sedimentation change, depending on the type of material (Godefroid, Koedam, 2004). Miller and Hobs (2002) point out to possibilities of modeling specific area changes in the urban environment. Solar radiation forms the climatic regime of the Earth and influences the environment. The total solar radiation impinging on the surface of the Earth is global radiation. Global radiation has two components – direct and diffuse radia-

tion (Chmelík, Pribulová, 2005). Tree vegetation uses 2% of solar energy on photosynthesis, 60–80% is absorbed by leaves and 5–15% is reflected back to space. The rest of the solar energy goes through leaves. A certain amount of radiation is used for warming up the particular parts of a tree. Trees with thin crowns can receive 60–80% of solar radiation. Through the trees with compact crowns penetrates 2–3% of solar radiation (Pauditšová, Reháčková, 2006). Albedo is the difference between absorbed and issued heat. Plants have value of albedo that is higher compared with compact areas. The values of albedo differ depending on the type of vegetation and surface. Vegetation generally has value of albedo 15–30%, conifers 10–20% and dry soil 20–30%. Thermal balance is influenced by the level of transparency of vegetation (density of crown, size of leaves and their orientation) (Pauditšová, Reháčková, 2006). In the urban environment are large concentration of surfaces that are strongly overheated and have large thermal capacity. The result is the accumulation of heat in the city environment (Hudeková, 2012). The temperature of the active surface directly infulences the thermal conditions on the ground and the marginal layer of the atmosphere (Středová et al., 2011). Different thermal characteristic of the active surfaces lead to increased heat absorption during the period of positive energy balance. Due to this modification, the built-up areas can be warmer than the surrounding land. According to Oke (1997), the specific thermal conditions are related to albedo and air pollution. Vegetation areas do not accumulate heat. After the opening of the stomata and during assimilation, the temperature of stomata matches the air temperature or drops down under this temperature (Slováková, Mistrík, 2007). According to Small and Miller (2010), vegetation influences the city conditions of the environment. Vegetation areas have an impact on the energy demand and the formation of thermal heat islands. In certain conditions, plants directly under the sun overheat as well, but this is just short-term overheating, because the evaporation of water from the leaves decreases the temperature of assimilating organs, when they are removed from direct sun. Leaves close their stomata to prevent excessive evaporation, which causes even more overheating of leaves. It is important to mention that overheated dry soil, asphalt, concrete, walls of the buildings, tin roofs, or body shells of cars radiate the heat even though the sun is not shining (Čaboun, 2008). The formation of thermal conditions in built-up areas is related to specific characteristics of the urban environment. In the urban environment, there is a change of geometry of an active surface. The expansion of active surface and vertical surfaces is also significant (Voogt, Oke, 2003).

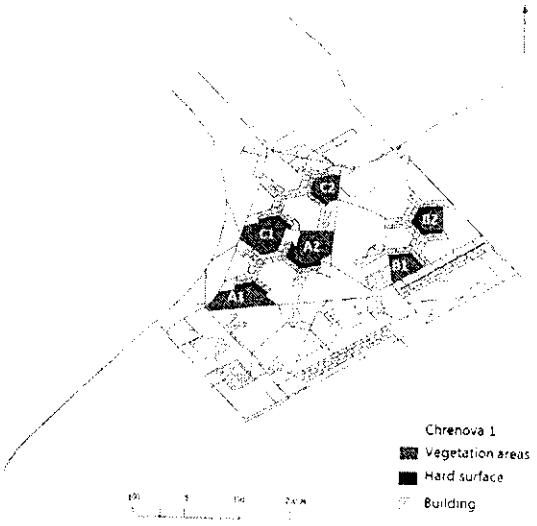

Fig. 1: Research areas

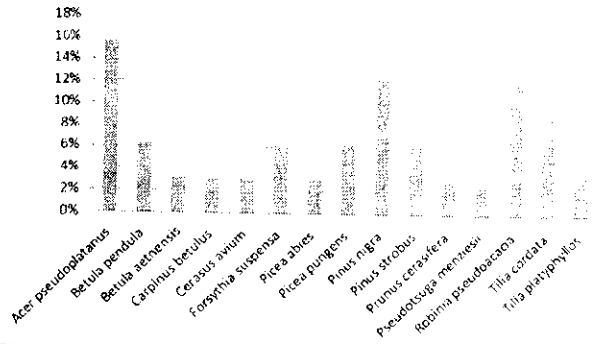

Fig. 2. Percentage of types of vegetation in vegetation area – Locality A1.

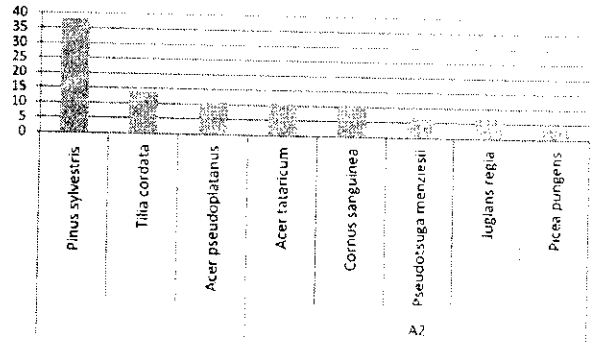

Fig. 3. Percentage of types of vegetation in vegetation area – Locality A2.

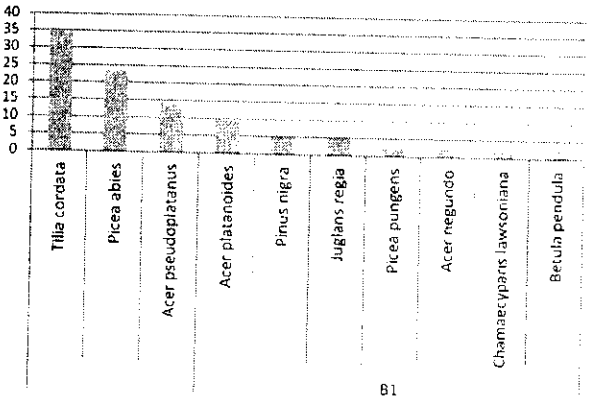

Fig. 4. Percentage of types of vegetation in vegetation area – Locality B1.

Material and methods

The legwork was accomplished in residential area of Chrenova 1. The selected localities consisted of three apartment complexes – A,B,C. In apartment complex A – localities A1, A2; in apartment complex B – localities B1, B2; in apartment complex C – localities C1, C2. Research areas include vegetation area, hard surface and block of flat (Fig. 1).

In research areas were accomplished the measurments:

1.in vegetation area - with touch probe and 2 m above the surface

2.on hard surface – with touch probe and 2 m above the surface

Structure of vegetation areas

Locality A1: The vegetation in the locality A1 is bilayer with 50 trees. The monitoring point is located in dense and relatively closed canopy of 26 trees with continuity on the open lawn. The highest part has the type *Acer pseudoplatanus* – 16% (Fig. 2).

Locality A2: The vegetation in the locality A2 is three-layered with 33 trees; it is structured into five formations with a central lawn. The vegetation area is open to the inside of residential area. The monitoring point is located in sparse vegetation with 7 trees. The highest percentage has *Pinus sylvestris* – 38% (Fig. 3).

Locality B1: The vegetation in the locality B1 is three layered with 46 trees. The trees are organized into three small clusters on the left side. In the middle of the vegetation area is the lawn with solitaire tree. The monitoring point is located in vegetation with a dense canopy of crowns with 9 trees. The highest percentage has *Tilia cordata* – 34.9% (Fig. 4).

Locality B2: The vegetation in area B2 is three layered. It is organized into two clusters, with a dense canopy of crowns. The number of trees in the vegetation area is 11. The monitoring point is located in the central lawn near the children's playground. The

highest percentage has *Pseudotsuga menziesi* – 35.8% (Fig. 5).

Locality C1: The vegetation in the locality C1 is three layered with 68 trees. The tree vegetation is organized into five clusters. The lawn is open near the river Nitra. The monitoring point is located in the cluster of three trees with a sparse canopy of crowns. The highest percentage has *Juglas regia* – 42.8% (Fig. 6).

Locality C2: The vegetation area in the locality C2 is a typically bounded area by inside of the residential area. In the vegetation area are 22 trees organized into five clusters with a sparse canopy of crowns. The monitoring point is located in the central lawn. The highest percentage has *Taxus baccata, Pseudotsuga menziesii, Tilia cordata* - 25% (Fig. 7).

Measurements in research areas

In research areas A1, A2, B1, B2, C1, C2 were accomplished measurements with Anemometer TSI Veloci Calc 9565 – P; it is a method of surface thermal monitoring. Twenty measurements were made at 3-second intervals at both the monitoring points for statistical evaluation.

Monitoring of microclimatic factors:

1. air temperature (2 m above the surface)
2. surface temperature (with touch probe)
3. relative humidity (2 m above the surface).

Measured values of microclimatic factors during the summer we evaluated with Statistica 7. We used the analysis of variance (ANOVA) one-way and Tukey HSD test (honest significant difference test).

Results

The aim of this study is to evaluate the capability of accumulation of solar radiation depending on the structure

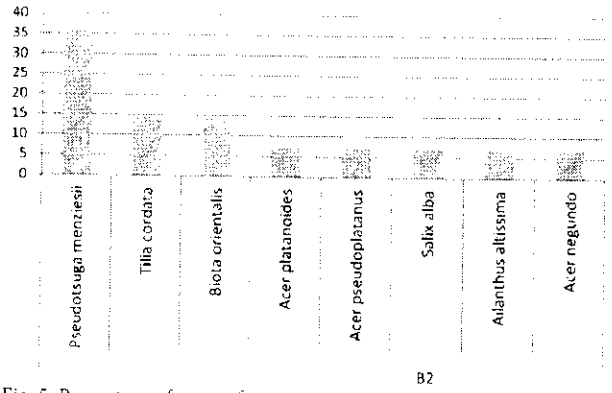

Fig. 5. Percentage of types of vegetation in vegetation area – Locality B2.

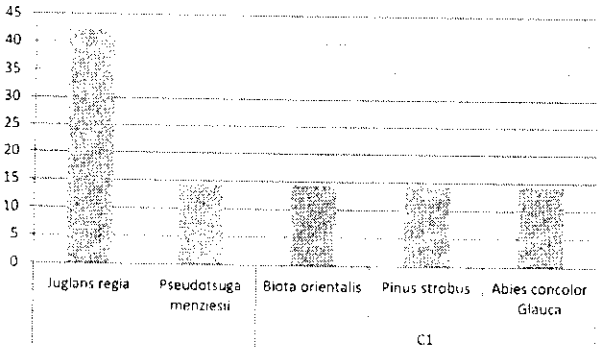

Fig. 6. Percentage of types of vegetation in vegetation area – Locality C1.

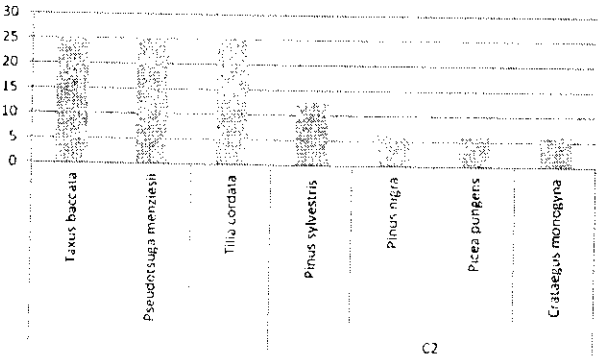

Fig. 7. Percentage of types of vegetation in vegetation area – Locality C2.

of vegetation area and the form of surface in the research areas A1–B1–C1, A2–B2–C2 between intervals – 6:30 a.m. –12:30 p.m., 12:30 p.m.–9:30 p.m. The legwork vas accomplished during the summer June – August 2013 (Table 1) in residential area of Chrenova 1 in city Nitra.

Table 1. Time of measurements in summer period.

MONTH	JUNE	JULY	AUGUST
TIME	5:40 a.m.	6:00 a.m.	6:15 a.m.
	12:30 p.m.	12:30 p.m.	12:30 p.m.
	9:30 p.m.	9:45 p.m.	9:00 p.m.

In Fig. 8 are the significant differences in surface temperature in the interval 6:30 a.m. - 12:30 p.m. between the localities A2–B2 and A2–C2. During the time of positive energy balance was the difference of surface temperature on the research area A2 – 8.95 °C; on the research area B2 – 13.49 °C; on research area C2 – 14;35 °C. The vegetation area A2 had 33 trees. The measurement point is located in a sparse canopy of vegetation with 7 trees. The surface temperature on research area A2 was 26.3 °C at the time 12:30 p.m. It was also the lowest value. The significant value was the relative air humidity at the time 6:30 a.m. The maximum relative air humidity was 76% on the research area A2. The degree of saturation of air by water vapour in vegetation depends on the quantity and the function of the vegetation. Significant is the relation between humidity and air temperature, higher humidity = lower temperature. The lowest value of relative air humidity was 69% in locality B2 at the time 6:30

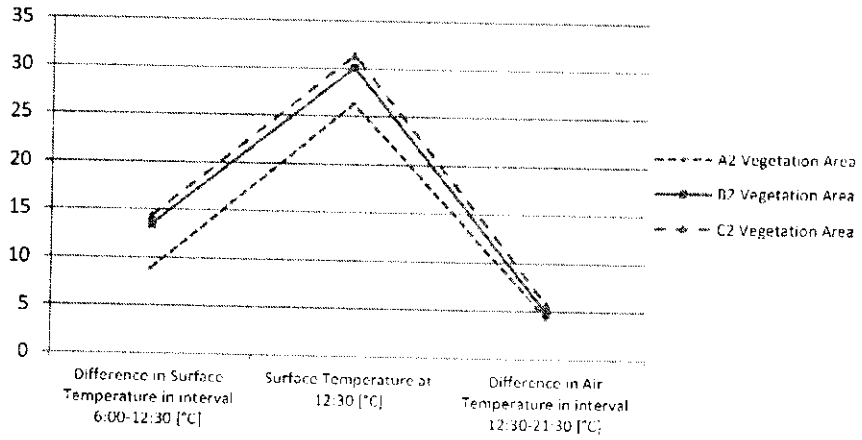

Fig. 8. Difference in surface temperature (°C) in vegetation areas A2, B2, C2 with north-east orientation depending on vegetation structure in interval 6:00 a.m.–12:30 p.m.; surface temperature (°C) in vegetation areas A2, B2, C2 with north-east orientation depending on vegetation structure at 12:30 p.m.; difference in air temperature (°C) in vegetation areas A2, B2, C2 with north-east orientation depending on vegetation structure in interval 12:30 p.m.–9:30 p.m..

a.m.. The localities B2, C2 are dominated by open lawns with sparse vegetation. During the time of positive energy balance, these areas accumulate more solar radiation due to which the surface temperature rises. The difference of surface temperature between vegetation area with trees and the lawns without trees was 5–6°C in the interval 6:00 a.m.–12:30 p.m.. The structure of vegetation was a significant factor between localities A2–B2 (Tukey HSD test, $p=0.04$, $p<0.05$), and localities A2–C2 (Tukey HSD test, $p=0.01$). The significant statistic value in air temperature was evaluated in the interval 12:30 p.m.–9:30 p.m. (Tukey HSD test, $p=0.02$, $p<0.05$).

In Fig. 9 is the evaluated difference of temperature in monitoring point of hard surface between localities A1, B1, C1. We evaluated the surface temperature at the time 12:30 p.m. and the difference between air and surface temperature in the monitoring point of hard surface in the interval 12:30 p.m.– 9:30 p.m. The statistically significant value was the difference of surface temperature between localities A1–B1 in the interval 6:00 a.m.–12:30 p.m., (Tukey HSD test, $p=0.04$, $p<0.05$). In the research area A1, the temperature in the monitoring point of hard surface increased up to 8.12 °C. In the vegetation area A1 were 50 trees in the dense canopy, after which the hard surface continued. Trees with south-west orientation in the dense canopy provided partial shading on the hard surface during the time of positive energy balance – in the interval 6:00 a.m.–12:30 p.m. The accumulation of solar radiation in this research area was the lowest compared to localities B1 and C1. Between localities A1–C1 was noticed significant statistical difference of surface temperature at the time 12:30 p.m. (Tukey HSD test $p=0.02$, $p<0.05$). The value of surface temperature in the research area A1 was 25.88°C, and in the research area C1 was 30.69 °C at the time 12:30 p.m. In the interval 12:30 p.m.– 9:30 p.m., we evaluated the cooling effect on the

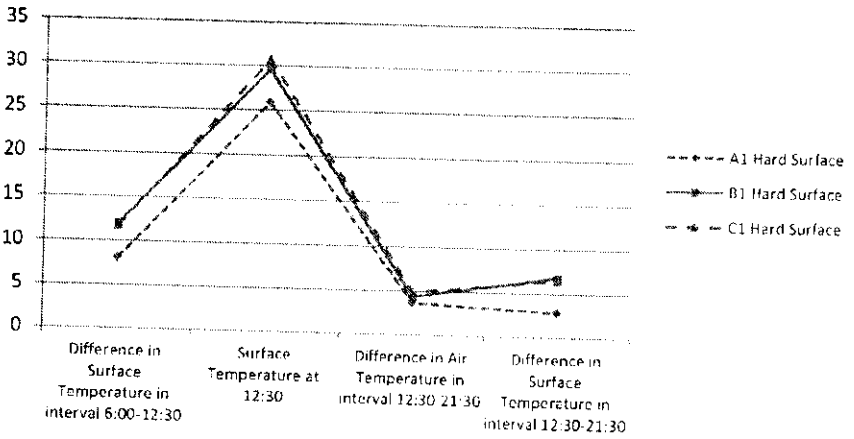

Fig. 9. Difference in surface temperature (°C) on hard surface A1, B1, C1 with south-west orientation in interval 6:00–12:30; surface temperature (°C) on hard surface A1, B1, C1 with south-west orientation at 12:30; difference in air temperature (°C) on hard surface – localities A1, B1, C1 with south-west orientation in interval 12:30 p.m.–9:30 p.m.; difference in surface temperature (°C) on hard surface – localities A1, B1, C1 with south-west orientation in interval 12:30 p.m.–9:30 p.m..

hard surface temperature among localities A1, B1, C1. The lowest difference of surface temperature in the interval 12:30 p.m.–9:30 p.m. was in the locality A1 – 2.83 °C. The difference of surface temperature in the locality B1 was – 6.83 °C. In the locality C1, the difference of surface temperature in the interval 12:30 p.m.–9:30 p.m. was 6.51 °C. Statistical significance was confirmed between localities A1–B1 (Tukey HSD test, $p=0.0002$, $p<0.001$) and localities A1–C1 (Tukey HSD test, $p=0.0005$, $p<0.001$). In the interval 12:30 p.m.–9:30 p.m., we evaluated the cooling effect – air temperature above the hard surface among localities A1, B1, C1. The lowest difference in air temperature above hard surface was in the locality A1 – 3.63 °C. In this locality were 50 trees with a dense canopy of crowns (Fig. 2). During the time of negative energy balance, the air temperature cooled down the least in the locality A1. It was a result of the vegetation with the transpiration impact that maintained the air temperature. The vegetation area regulates the maximum differences in vegetation and its surroundings when the sun is not shining. We confirmed the significant statistical difference in air temperature above the hard surface between localities A1–C1 (Tukey HSD test, $p=0.02$, $p<0.05$).

In Fig. 10 are the compared values of the surface temperature among localities A1, B1, C1 in the monitoring point of the vegetation area and the hard surface at the time 12:30 p.m.. The lowest temperature of the surface in the vegetation area was measured in the locality A1 – 26.04 °C, and the highest temperature in the locality B1 – 26.7 °C. The highest surface temperature on the hard surface was measured in the locality C1 – 30.68 °C. The difference in surface temperature between the monitoring points of vegetation area and the hard surface was 4.3 °C. In the monitoring point of the hard surface was observed the lowest of surface temperature in the locality A1 – 25.88 °C. The minimum difference in surface temperature between monitoring points of the vegetation area and the hard surface of the locality A1 was 0.16 °C. The locality A1 had the maximum number of trees among all the research areas.

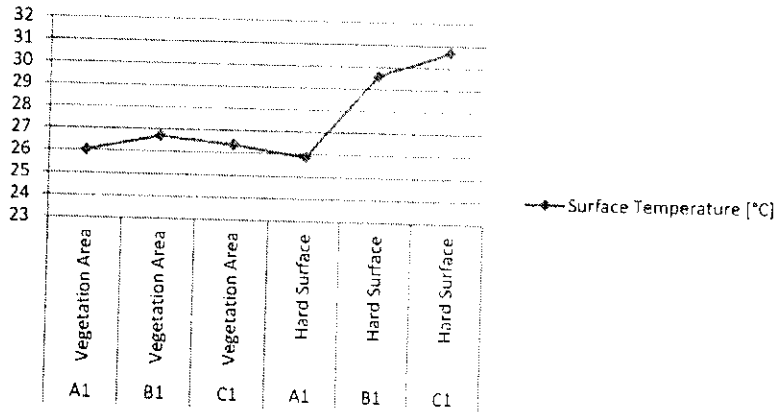

Fig. 10. Difference in surface temperature (°C) in vegetation areas – localities A1, B1, C1 and hard surface – localities A1, B1, C1, with south-west orientation in summertime at 12:30 p.m..

In Fig. 11 are the compared values of the surface temperature among localities A2, B2, C2 in the monitoring points of the vegetation area and the hard surface at the time 12:30 p.m. The lowest surface temperature in monitoring point vegetation area was measured in the locality A2 – 26.3 °C and the highest surface temperature in the locality C2 – 31.56 °C. The highest surface temperature – 35.42 °C in monitoring point of hard surface was measured in the locality B2 and the lowest surface temperature in the locality A2 – 31.31 °C. The highest difference in surface temperature between the vegetation area and the hard surface was – 5.32 °C in the locality B2.

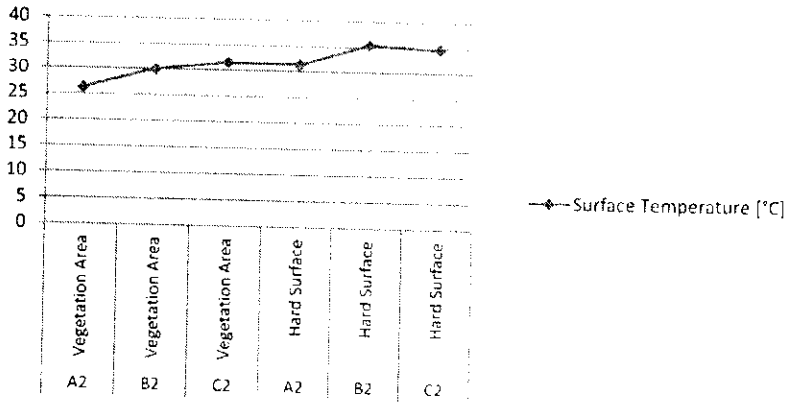

Fig. 11. Difference in surface temperature (°C) in vegetation area – localities A2, B2, C2 and hard surface – localities A2, B2, C2 with north-east orientation in summertime at 12:30 p.m..

In Table 2 are evaluated the impact of orientation towards cardinal points in surface temperature in the measurement point in vegetation area for all localities – A1, B1, C1 with south-west orientation, localities A2, B2, C2 with north-east orientation. Statistically significant were differences in surface temperature depending on the orientation between localities A1–C2 (Tukey HSD test, p=0.007, p<0.01), localities B1–C2 (Tukey HSD test, p=0.03, p<0.05) and localities C1–C2 (Tukey HSD test, p=0.01).

Table 2. Values of surface temperature (°C) in vegetation areas A1, A2, B1, B2, C1, C2 depending on orientation in summertime at 12:30 p.m.

Tukey HSD test; **Vegetation Area - 12:30 Surface Temperature**							
	Locality	**{1} - 26.042**	**{2} - 26.303**	**{3} - 26.711**	**{4} - 30.102**	**{5} - 26.383**	**{6} - 31.566**
1	A1		0.999983	0.998427	0.125630	0.999939	**0.007955**
2	A2			0.999852	0.158374	1.000000	**0.010268**
3	B1				0.304504	0.999953	**0.032583**
4	B2					0.186331	0.940067
5	C1						**0.013689**
6	C2						

In Table 3 are evaluated the impact of orientation towards cardinal points in the surface temperature in the measurement point on hard surface for all localities, A1, B1, C1 with south-west orientation, localities A2, B2, C2 with north-east orientation. Statistically significant were differences in the surface temperature depending on the orientation between localities A1–B2 (Tukey HSD test, p=0.0004, p<0.001) and A1–C2 (Tukey HSD test, p=0.0008, p<0.001).

Table 3. Values of surface temperature (°C) on hard surface-localities A1, A2, B1, B2, C1, C2 depending on orientation in summertime at 12:30 p.m.

Tukey HSD test; **Hard Surface - 12:30 Surface Temperature**							
	Locality	**{1} - 25.883**	**{2} - 31.318**	**{3} - 29.592**	**{4} - 35.426**	**{5} - 30.685**	**{6} - 34.711**
1	A1		0.104098	0.497031	**0.000459**	0.212715	**0.000895**
2	A2			0.961853	0.397635	0.999686	0.582248
3	B1				0.085179	0.995435	0.156335
4	B2					0.252277	0.999529
5	C1						0.402843
6	C2						

Discussion

In this study, we evaluated the capability of accumulation of solar radiation depending on the type of surface in city Nitra. The active surfaces in the urban environment are the main microclimatic factors. The microclimatic function of vegetation and monitoring its specific demonstrations is nowadays the current tool for elimination of extreme weather demonstrations, especially in the urban environment. The capability to absorb solar radiation during the time of positive energy balance depends on the vegetation structure, the canopy of trees and the quantity. In Fig. 8, the surface temperature increased by 13.49 °C in the vegetation area B2 with the dominant lawn in the interval 6:00 a.m.–12:30 p.m. In the vegetation area C2, the surface temperature increased by 14.35 °C. In the vegetation area A2, the monitoring point is located in a sparse canopy of 7 trees. Here the surface temperature increased by only 8.95 °C. We evaluated the statistical significance in surface temperaure depending on the vegetation structure by using ANOVA one-way analysis and Tukey HSD test. According to Čaboun, 2008, the way the vegetation modifies direct solar radiation influences the thermal regime. On average, the difference in the surface temperature between the vegetation area with and without trees (with the lawn) was 5–6 °C. The correlation between vegetation structure and surface temperature was confirmed by the authors (Keresztesová et al., 2013). They recorded the lowest surface temperature during summertime in city park of Nitra. The changes of relative air humidity are related to the air temperature. According to Tužinský, 2002, is higher relative air humidity in the tree vegetation, in the part of trunk – the morning type of humidity. The highest relative air humidity is in the surface of the soil. It was confirmed in the vegetation area A2 with the trec vegetation. Here the value of relative air humidity was 76% at the time 6:30 a.m. Compared with the value of relative air humidity in the vegetation area B2, without the trees vegetation, it was only 69%.

The vegetation area A1 is the locality with the maximum of trees – 50 species in the dense canopy of crowns . We monitored the surface temperature on the hard surface near the vegetation area (Fig. 1). Trees with the dense canopy provide partial obscuration of the hard surface at the time of positive energy ballance – interval 6:30 a.m.–12:30 p.m. Here we evaluated the lowest accumulation of the surface temperature compared with localities B1 and C1. Between localities A1–C1, at the monitoring point of the hard surface, we evaluated the significant statistical difference in the factor of surface temperature at the time 12:30 p.m. too. In the locality A1, it was 25.88 °C, and in the locality C1, it was 30.69 °C, (Tukey HSD test, $p=0.02$, $p<0.05$). The lowest cooling effect of air temperature we evaluated was in locality A1 at the time of negative energy balance (the difference of air temperature in the interval 12:30 p.m.–9:30 p.m. –3.63 °C). A significant factor is the ability of vegetation with the transpiration impact to maintain the air temperature. It means to regulate the maximum differences in the vegetation and the surroundings, hard surface, when sun is not shining.

Conclusion

The aim of this study was to evaluate the capability of accumulation of solar radiation depending on vegetation structure and quality of areas A1–B1–C1, A2–B2–C2 in intervals 6:00 a.m.–12:30 p.m., 12:30 p.m.–9:30 p.m. We accomplished the legwork in summertime, June–August 2013 in residential area Chrenova 1 by using methods of the surface thermal monitoring. We evaluated the measurements values by using the ANOVA one-way analysis and Tukey HSD test in the software Statistica 7. The relationships between the vegetation structure and the surface temperature were shown as statistically significant. The accumulation of the solar radiation on vegetation area without the trees was higher – on average by 6 °C. The factor of relative air humidity was significant in the locality A1 – with the largest amount of species in the dense canopy of crowns. Research results refer to the ability of vegetation to positively influence microclimate in the urban environment. Quantification of the measurement data, statistical analysis and its generalization will provide in the future possibilities of how to solve problems related to extreme demonstrations of climatic changes in the urban environment.

Acknowledgements

This study is the result of the project implementation: Environmental aspects of the urban environment (Environmentálne aspekty urbanizovaného prostredia) ITMS 26220220110 supported by the Research & Development Operational Program funded by the ERDF.

References

Čaboun, V. (2008). Vegetation impact on decreasing of surface temperature and air temperature during the extreme heat (in Slovak). In J. Rožnovský & T. Litschmann (Eds.), *Bioklimatologické aspekty hodnocení procesů v krajině*. Mikulov, 9.– 11.9.2008.

Chmelík, M. & Pribulová A. (2005). Solar UV radiation significantly influences theenvironment (in Slovak). *Enviromagazín*, 3, 28–29.

Godefroid, S. & Koedam N. (2004). Interspecific variation in soil compactionsensitivity among forest floor species. *Biol. Conserv.*, 119, 207–217. DOI: 10.1016/j.biocon.2003.11.009.

Hudeková, Z. (2012). *After-effects of climate changes in urban environment and the urban planning (in Slovak).* Online. http://www.urbion.sk/dosledky-zmien-klimy-v-urbanizovanomprostredi-a-uzemne-planovani/

Keresztesová, S., Strelková, M. & Rózová Z. (2013). Impact of vegetation on surfacetemperature in the city Nitra (in Slovak). In M. Heinrichová & T. Reháčková (Eds.), *Aktuálne problémy krajinnej architektúry a krajinného plánovania* (pp. 94–99). Bratislava: Veda, vydavatelstvo SAV.

Miller, J.R. & Hobbs R.J. (2002). Conservation where people liveand work. *Conserv. Biol.*, 16, 330–337. DOI: 10.1046/j.1523-1739.2002.00420.x.

Oke, T.R. (1997). Urban climates and global environmental change. In R.D. Thompson & A.H. Perry (Eds.), *Applied climatology: Principles and practice* (pp. 273–287). London: Routledge.

Pauditšová, E. & Reháčková T. (2006). Practical experiences with the evaluation of microclimatic function of vegatation in urban environment (in Slovak). In *Sídlo - Park - Krajina IV. Kultúrna vegetácia v sídlach a v krajine* (pp. 227–235). Zborník vedeckých prác a referátov. Nitra: SPU.

Scudo, G., Dessi, V. & Rogora A. (2002). Evaluation of radiant conditions in urban spaces. In M. Nikolopoulou (Ed.), *Designing open spaces in the urban environment: a bioclimatic approach* (pp. 12–17). Greece: CRES.

Slováková, E. & Mistrík I. (2007). *Physiological processes of plants in stress conditions (in Slovak).* Bratislava: Univerzita Komenského.

Small, C.H. & Miller R.B. (2010). *Monitoring the urban environment from space.* Digital Cities II.

Středová, H., Bokwa, A, Dobrovolný, P. et al. (2011). *Urban microclimate and mesoclimate, stand microclimate (in Czech).* Praha: Český hydrometeorologický ústav.

Tužinský, L. (2002). *Bioclimatology (in Slovak).* Zvolen: Technická univerzita.

Voogt, J.A. & Oke T.R. (2003). Thermal remote sensing of urban climates. *Remote Sens. Environ.*, 86, 370–384. DOI: 10.1016/S0034-4257(03)00079-8.

Wardoyo, J., Suprapti, A. & Wediningsih H. (2011). Vegetation configuration as microclimate control strategy in hot humid tropic urban open space. S E N V A R + I S E S E E I-3 December 2008, International seminar in sustainable environment & architecture.

PRÍLOHA č. 3

FUNKČNÉ VYUŽITIE VNÚTROBLOKOVÝCH PRIESTOROV SÍDLISKA CHRENOVÁ 1 V NITRE

Katarína Bahnová, Mária Dobišová, Zdenka Rózová
Katedra ekológie a environmentalistiky, Univerzita Konštantína Filozofa v Nitre, katarina.bahnova@ukf

Abstract

Housing Estate Chrenova 1 started up between 1964-1968. Seventies were the first wave of this type of building in Slovakia, as a result of increasing of industrialization and urbanization. In Chrenova 1 Estate the aim of architectural design was to selected backyards as a centre of repose with social function. The main goal of this paper is refer about function utilisation of backyards in Chrenova 1. In selected spaces are located vegetated areas with not only recreation and social function but also with microclimatic function. Structure of vegetated areas (number of trees, species diversity and canopy of crowns) influences the microclimatic conditions in time of possitive energy balance. Microclimatic conditions in backyards of Housing Estate Chrenova 1 were observed by using the method of surface thermal monitoring in summer session 2014. Selected microclimatic factors (air flow, air temperature, relative air humidity, surface temperature) were evaluated by using the software Statistica 7.

Key words: urban environment, housing estate, microclimate, vegetation area, function

Úvod a cieľ

Miera a rozsah globálnych zmien v životnom prostredí, či už hovoríme o skleníkových plynoch, globálnej klimatickej zmene, odlesňovaní alebo degradácii biodiverzity, sú riadené rastom populácie. Predovšetkým s nárastom mestského obyvateľstva, rastie tiež podiel prostriedkov využívaných týmito obyvateľmi. (GRIMMOND, 2007). Súčasťou urbánnej vegetácie sa v kontexte vývoja miest stávajú rôzne typy plôch s vegetáciou, ktorých gradient siaha od pôvodných rastlinných spoločenstiev, resp. ich zvyškov, cez rôzne typy človekom zámerne vytvorených a udržiavaných plôch, až po nevyužívané plochy s vegetačnou pokrývkou v rôznom stupni sukcesného vývoja. Sídlisko Chrenová 1 vznikalo v sedemdesiatych rokoch minulého storočia. Hlavným architektom projektu bol Michal Maximilián Scheer. Už v samotnom architektonickom návrhu sa počítalo s vyčlenením vnútroblokových priestorov, ktoré budú poskytovať vyhovujúce zázemie obyvateľom sídliska. Meandrová štruktúra zástavby vytvorila samostatné, z časti uzavreté priestory, ktoré mali plniť prevažne sociálnu a rekreačnú funkciu. V súčasnosti v týchto priestoroch evidujeme vegetačné plochy. Cieľom tohto príspevku je poukázať na funkčnosť dvoch vybraných vnútroblokových priestorov sídliska Chrenová 1, nielen z hľadiska sociálneho, či rekreačného, ale aj z hľadiska plnenia mikroklimatickej funkcie vo vzťahu k formovaniu lokálnej klímy mestskej časti Chrenová 1.

Materiál a metódy

Vegetácia v urbanizovanom prostredí

Vegetácia v urbanizovanom prostredí je významným sprírodňujúcim a estetickým prvkom ľudských sídiel. Tu sa uplatňujú jej funkcie, či už ekologické, sociálne a z časti tiež hospodárske. Má vplyv na zlepšovanie mikroklimatických podmienok, produkuje kyslík a iné biologicky účinné látky. Absorbuje škodlivé látky z ovzdušia, znižuje hladinu hluku, prašnosť a imisivitu, pozitívne ovplyvňuje fyzikálny stav ovzdušia, poskytuje priestor a vhodné podmienky na

rekreáciu človeka. Esteticky a kompozične dotvára krajinný obraz mesta a pôsobí pozitívne tiež na fyziologický a psychický stav človeka (SUPUKA, 2002). Podľa WAGNER (1982), verejná zeleň sídlisk pozostáva z uličnej zelene, zelene verejných budov, z mestských parkov a prstenca zelene začleňujúcej sídlisko do okolitej krajiny. Zeleň obytného súboru by svojimi funkciami mala zabezpečovať obyvateľom čo najvyššiu kvalitu okolitého prostredia.

Vegetačné plochy vo vzťahu k mikroklíme

Podľa BEDNÁŘ (1993), je mikroklíma definovaná ako klíma malého priestoru. Zasahuje priestor nad aktívnym povrchom i pod ním. Mikroklíma je najčastejšie formovaná homogénnym aktívnym povrchom. Práve aktívny povrch, na ktorom prebieha premena slnečnej energie na tepelnú je hlavným mikroklimatotvorným činiteľom (STŘEDOVÁ, ET. AL., 2011). Existencia mikroklímy je závislá na vyšších kategóriách klímy, za silného prúdenia sa nemusí vôbec vyvíjať. Vo formovaní mikroklímy a tepelného komfortu hrá významnú úlohu vegetácia. Jej povrchová teplota ovplyvňuje tepelnú bilanciu prostredníctvom sálavých výmen (SCUDO ET. AL., 2002). SHASHUA a HOFFMAN, (2000) chápu mikroklímu ako celok tvorený čiastkovými faktormi a to: teplotou vzduchu, vlhkosťou vzduchu, prúdením vzduchu, tlakom vzduchu a znečistením vzduchu. Podľa GODEFROID - KOEDAM (2007), druhové zloženie a vitalitu vegetačných plôch ovplyvňuje predovšetkým hustota zástavby v mestskom prostredí. MILLER – HOBS (2002), poukazujú na účinok jednotlivých častí zastavaného prostredia, napríklad na obytné priestory verzus komerčné priestory a možnosti modelovania špecifických priestorových zmien v urbanizovanom prostredí. Rôzne typy zástavby majú rôzny vplyv na distribúciu rastlín v mestskej matrici. Citlivosť niektorých druhov v husto zastavanom území je vyššia, ako v polootvorených či otvorených zastavaných častiach miest (GODEFROID – KOEDAM, 2003).

Terénny výskum

Terénny výskum sme realizovali v letnej sezóne (jún - august 2014). Metódou pozemného termálneho monitoringu pomocou prístroja Anemometer TSI Veloci Calc, sme sledovali mikroklimatické podmienky vo vybraných vnútroblokových priestoroch (Blok 1 – Blok 2) sídliska Chrenová 1. Namerané mikroklimatické faktory (prúdenie vzduchu [l/s], teplotu vzduchu [°C], teplotu povrchu [°C] a relatívnu vlhkosť vzduchu [%]) sme štatisticky a graficky vyhodnotili v softvéri Statistica 7, pre porovnanie mikroklimatických podmienok v jednotlivých vnútroblokoch sme použili Mann-Whitney test.

Výsledky

Vnútroblokové priestory sídliska Chrenová 1 v Nitre vznikli za účelom plnenie sociálnej či rekreačnej funkcie. V súčasnosti sú však obyvateľmi sídliska minimálne využívané, dôvodom je absencia rozsiahlejších rekonštrukčných opatrení (renovácia detského ihriska, doplnenie drobného mobiliáru). Okrem malých prídomových záhrad, či súkromnej okrasnej výsadby je ich prvotná funkcia značne potlačená. Vo vybraných vnútroblokoch (Blok 1 – Blok 2) evidujeme vegetačné plochy s rôznou štruktúrou porastu (Graf 1, Obr. 1, Graf 2, Obr. 2). Vo vzťahu k formovaniu mikroklímy majú významný vplyv najmä plošné usporiadanie drevín, zápoj, druhové zloženie a tiež typ realizovaných manažmentových opatrení.

Cieľom tohto príspevku je poukázať na funkčnosť vybraných vnútroblokových priestorov z hľadiska plnenia mikroklimatickej funkcie vo vzťahu k formovaniu lokálnej klímy mestskej časti Chrenová 1.

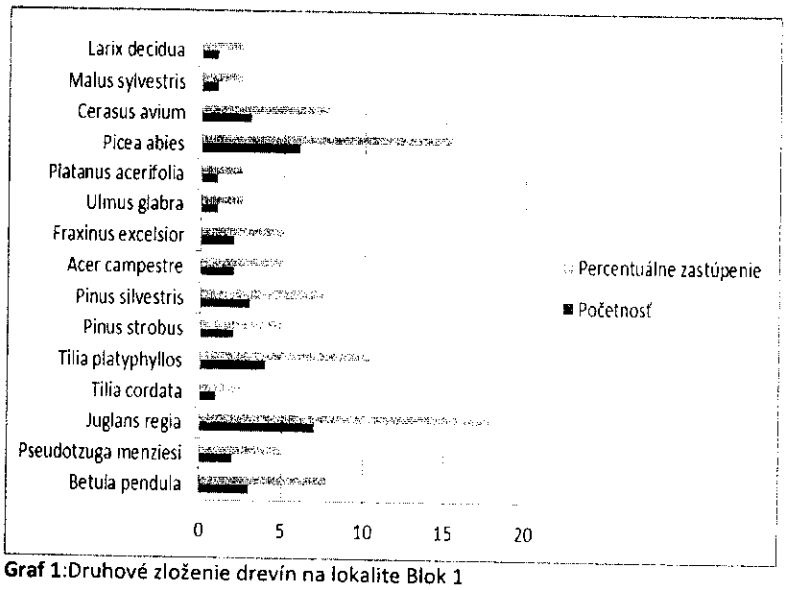

Graf 1:Druhové zloženie drevín na lokalite Blok 1

Najvyššie percentuálne zastúpenie na lokalite Blok 1 má druh *Juglans regia* (18%). Porast na vybranej lokalite je dvojvrstvový v hustom relatívne uzavretom zápoji s počtom drevín 39.

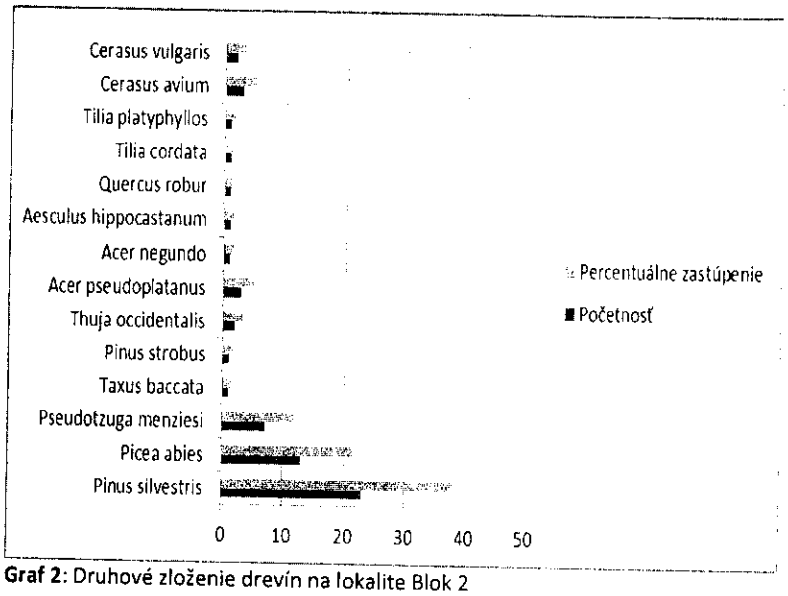

Graf 2: Druhové zloženie drevín na lokalite Blok 2

Najvyššie percentuálne zastúpenie na lokalite Blok 2 má druh *Pinus silvestris* (38,2 %). Porast na vybranej lokalite je dvojvrstvový s počtom drevín 60.

Štatistické hodnotenie mikroklimatických podmienok vybraných vnútroblokových priestorov sídliska Chrenová 1 v Nitre

Mikroklimatické faktory: prúdenie vzduchu, teplota vzduchu, teplota povrchu a relatívna vlhkosť vzduchu sme vyhodnotili v programe Statistica 7, pre porovnanie jednotlivých vnútroblokových priestorov sme použili Mann-Whitney test.

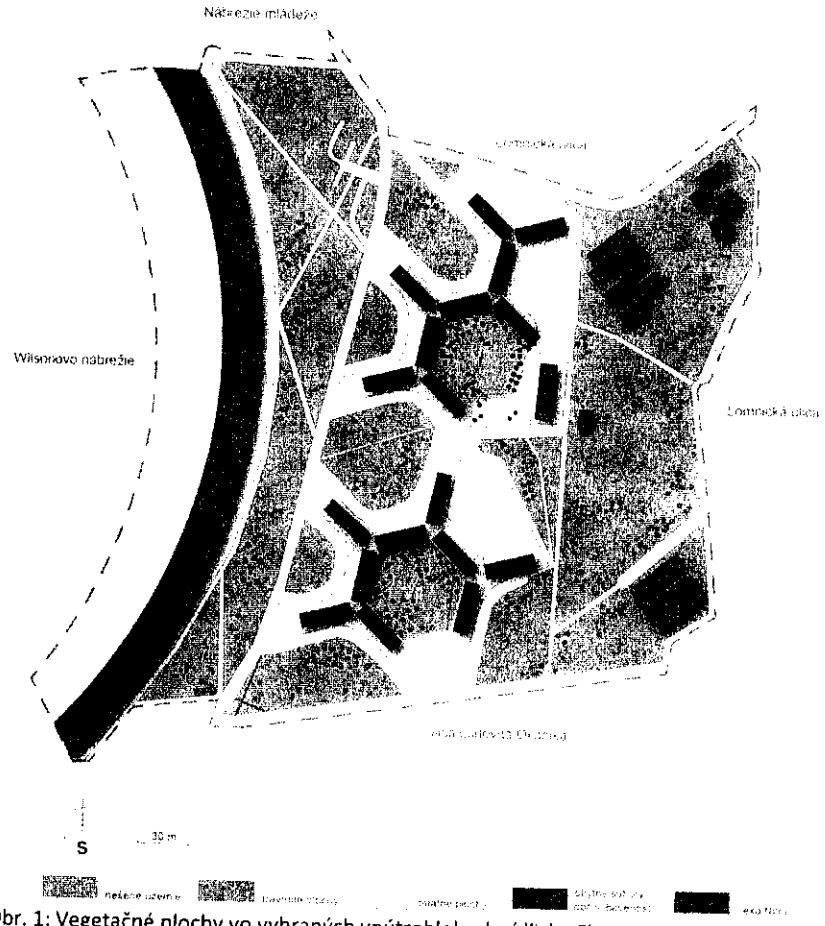

Obr. 1: Vegetačné plochy vo vybraných vnútroblokoch sídliska Chrenová 1 v Nitre

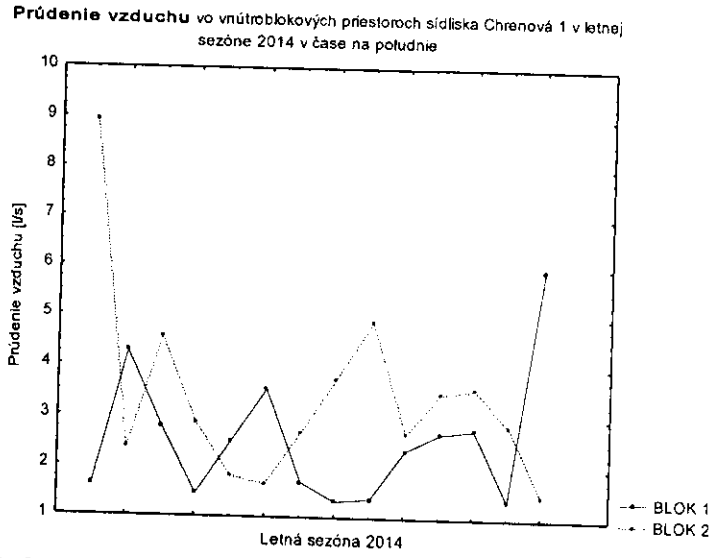

Graf 3: Trendová krivka pre mikroklimatický faktor prúdenie vzduchu v letnej sezóne 2014 pre vybrané lokality Blok 1 – Blok 2

Prúdenie vzduchu vo vybraných vnútroblokoch v letnej sezóne 2014 znázorňuje trendová krivka (Graf 3), vzhľadom na štruktúru porastu a charakter jednotlivých plôch evidujeme na

vybraných plochách hodnoty Blok 1 medián 2,6 - Blok 2 medián 3,4. Tu možno poukázať na funkciu vegetácie ako vetrolamu, kde vnútroblok Blok 1 tvorí vegetácia v hustom uzavretom zápoji s najvyšším zastúpením druhu *Juglans regia*.

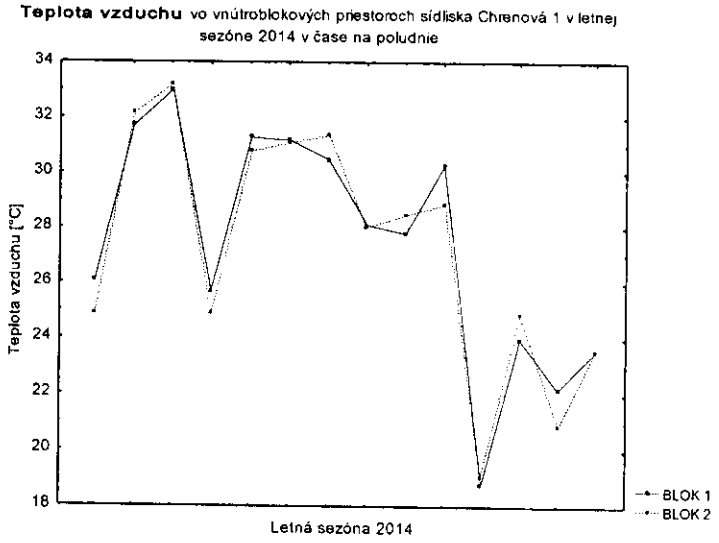

Graf 4: Trendová krivka pre mikroklimatický faktor teplota vzduchu v letnej sezóne 2014 pre vybrané lokality Blok 1 – Blok 2

Teplota vzduchu počas letnej sezóny 2014 vo vnútroblokových priestoroch sídliska Chrenová 1 v Nitre bola takmer vyrovnaná, Blok 1 medián 27,5 [°C] - Blok 2 medián 27,3 [°C]. Oproti priemernej teplote vzduchu sídliska Chrenová 1 rozdiel predstavuje Blok 1 (27,5) – Chrenová 1 (28,1) – 0,6 [°C], Blok 2 (27,3) – Chrenová 1 (28,1) – 0,8 [°C]. Ako znázorňuje trendová krivka počas letnej sezóny 2014 (Graf 4), rozdiel medzi jednotlivými vnútroblokmi predstavuje približne 1 [°C] pre vybrané dni merania.

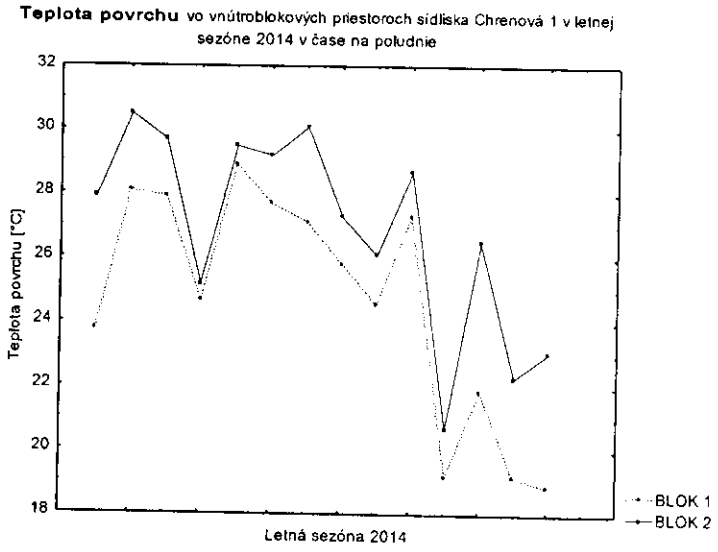

Graf 5 : Trendová krivka pre mikroklimatický faktor teplota povrchu v letnej sezóne 2014 pre vybrané lokality Blok 1 – Blok 2

Významným mikroklimatickým faktorom je teplota povrchu. Na mikroklimatické podmienky vplýva tiež variabilita aktívnych povrchov v urbanizovanom prostredí. V čase pozitívnej

energetickej bilancie sa umelé povrchy výrazne prehrievajú, čoho dôsledkom je sálavá výmena tepla medzi povrchom a prostredím. Na lokalite Blok 1 sme zaznamenali hodnotu mediánu 24,7 [°C], na lokalite Blok 2 26,9 [°C]. Funkčná vegetácia pôsobí ako tepelný stabilizátor, poskytuje tieň a tiež prirodzene udržiava vlhkosť v poraste vplyvom transpirácie. Dôsledkom je rozdiel v teplote povrchu medzi vybranými lokalitami – 2,2 [°C].

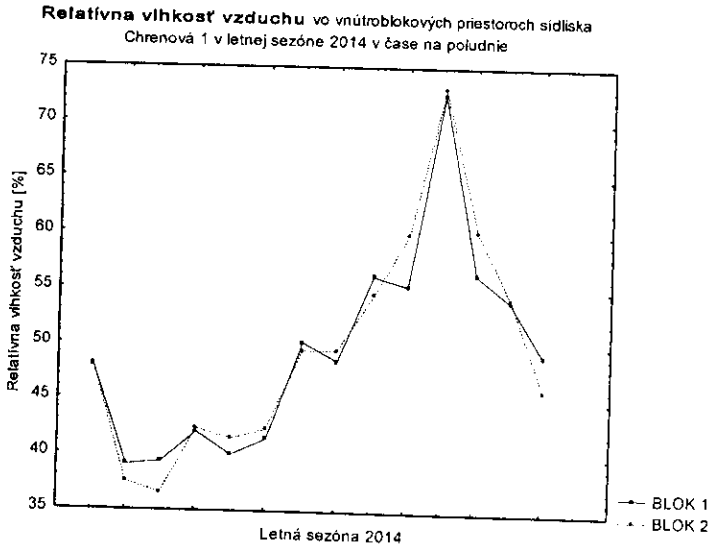

Graf 6: Trendová krivka pre mikroklimatický faktor teplota povrchu v letnej sezóne 2014 pre vybrané lokality Blok 1 – Blok 2

Zvýšenie relatívnej vlhkosti vzduchu pod porastovým krytom nastáva dôsledkom zníženej teploty, transpirácie rastlín a zamedzenia prúdenia vzduchu, ktoré udržiava takto vytvorenú vlhkosť v ovzduší. Väčší rozdiel badať pod listnatými ako pod ihličnatými drevinami (ČABOUN, 2008). Medzi vybranými vnútroblokovými priestormi neboli zaznamenané výrazné rozdiely v mikroklimatickom faktore relatívna vlhkosť vzduchu počas letnej sezóny 2014 (Graf 6). Hodnoty mediánu predstavujú rozdiel iba 0,2 % Blok 1 (49,5 %) – Blok 2 (49,7 %). Pri porovnaní priemernej vlhkosti medzi vybranými lokalitami a sídliskom Chrenová 1 (43,9%) evidujeme rozdiel 5,7 %. Na termálny komfort má významný vplyv práve zvýšenie relatívnej vlhkosti vzduchu, čo človek pociťuje (s výnimkou veľmi teplých dní) ako zníženie teploty.

Diskusia a záver

Cieľom tohto príspevku bolo poukázať na funkčnosť vybraných vnútroblokových priestorov z hľadiska plnenia mikroklimatickej funkcie vo vzťahu k formovaniu lokálnej klímy mestskej časti Chrenová 1. Terénny výskum prebehol v letnej sezóne 2014 metódou pozemného termálneho monitoringu vo vybraných vnútroblokových priestoroch Blok 1 – Blok 2. Sledovali sme mikroklimatické faktory prúdenie vzduchu, teplotu vzduchu, teplotu povrchu a relatívnu vlhkosť vzduchu, v čase pozitívnej energetickej bilancie (na poludnie – 12:30). Mikroklimatické podmienky boli vyhodnotené softvérom Statistica 7, pre porovnanie vybraných lokalít výskumu sme použili Mann-Whitney test. Vo formovaní mikroklímy má významný vplyv vegetácia. Vplyvom transpirácie dochádza k udržiavaniu vlhkosti v poraste, čo priaznivo pôsobí na pocitovú teplotu a poskytuje termálny komfort obyvateľom v letných mesiacoch. Vegetačné plochy svojou štruktúrou plnia v prostredí funkciu vetrolamu a pôsobia tiež ako tepelný stabilizátor. Z trendových kriviek pre jednotlivé mikroklimatické faktory možno poukázať na význam vegetačných plôch vo vzťahu k formovaniu lokálnej klímy mestskej časti sídliska

Chrenová 1 (Graf 5 – Teplota povrchu, Graf 6 – Relatívna vlhkosť vzduchu). V čase výrazných klimatických zmien a extrémnych prejavov počasia, je dôležité zamerať sa na efektívne opatrenia a manažment funkčných plôch vegetácie, ktoré poskytujú celý rad funkcií priaznivo ovplyvňujúcich kvalitu života v urbanizovanom prostredí.

Poďakovanie: Tento príspevok vznikol vďaka finančnej podpore z projektu Vega 1/0042/12 Analýza vybraných environmentálnych faktorov vo vzťahu k možným environmentálnym rizikám.

Literatúra

BEDNÁŘ, J. et al. 1993. Meteorologický slovník výkladový terminologický. 1.vyd. Praha : Academia.)

ČABOUN, V., 2008: Vplyv vegetácie na znižovanie teploty povrchov a ovzdušia pri extrémnych horúcavách. In: Rožnovský, J., Litschmann, T. (ed): „Bioklimatologické aspekty hodnocení procesu v krajine", Mikulov 9. – 11.9.2008, ISBN 978-80-86690-55-1

GODEFROID, S. - KOEDAM, N., 2003. How important are large vs. small forest remnants for the conservation of the woodland flora in an urban context? In: Global Ecology Biogeography . p. 12, 12:287–298

GODEFROID, S.- KOEDAM, N., 2007. Urban plant species patterns are highly driven by density and function of built-up areas. In: Landscape Ecol, 2007, Springer science+Business media B. V., 22:1227-1239, p. 13, 10980-007-9102-x

GRIMMOND, C. S. B, 2007: Urbanization and global environmental change- Local effects of urban warming. In: Geographical journal, 2007. 173- 83-88

MILLER, J.R. - HOBBS, R.J., 2002 Conservation where people live and work. In: Conservation Biology, p. 12, 16:330–337

WAGNER, B. 1982. Teorie vývoje a tvorba krajiny 1.,Všeobecný význam zelene v životě člověka a společnosti, Praha: SPN, 79 p.

SHASHUA - BAR, L. – HOFFMAN, M. E., 2000. Vegetation as a climatic component in the design of an urban street. An empirical model for predicting the cooling effect of urban green areas with trees. In: Energy and Buildings, p. 11, 31: 221-235

SCUDO ET., AL., 2002: Evaluation of radiant conditions in urban spaces. In: Designing open spaces in the urban environment: a bioclimatic approach. 2002, p. 12-17, ISBN 960- 86907-2-2

STŘEDOVÁ, H., BOKWA, A, DOBROVOLNÝ, P., et., al. 2011: Urban microclimate and mesoclimate, stand microclimate. (Mikroklima a mezoklima měst, mikroklima porostů), Český hydrometeorologický ústav, Praha, 1. vyd., 102 s. ISBN 978-80-86690-90-2.

SUPUKA, J., 2002: Regulatívy plošného zastúpenia vegetačných štruktúr v mestských sídlach. In: Acta Environmentalica Universitatis Comenianae, Bratislava, 2002, s. 189-195

Bahnová, K., Dobišová, M., Rózová, Z. 2015: Funkčné využitie vnútroblokových priestorov sídliska Chrenová 1 v Nitre. In: Zborník recenzovaných príspevkov vedeckej konferencie Krajinná architektúra a krajinné plánovanie v perspektíve, Ústav krajinnej a záhradnej architektúry, Fakulta architektúry , STU v Bratislave, 1. – 2. október 2015, s. 75-82, ISBN 978-80-227-4443-0

PRÍLOHA č. 4

Šiška et al. (eds): TOWARDS CLIMATIC SERVICES
Nitra, Slovakia, 15th – 18th September 2015

THE IMPACT OF VEGETATION STRUCTURE ON MICROCLIMATIC CONDITIONS IN URBAN ENVIRONMENT OF NITRA CITY

KATARÍNA BAHNOVÁ, ZDENKA RÓZOVÁ

Department of Ecology and Environmental Sciences, Constantine the Philosopher University in Nitra, Tr. A. Hlinku 1, 949 74, Nitra, Slovakia

Trend of nowadays is decreasing of green areas related to increasing urbanization and spatial requirements of urban population. According to Wardoyo (2011) is urban environment specific to hard surface, typical urban geometry, vegetated areas and variability of surface materials. In urban environment is large concentration of surfaces which are strongly overheated and have large thermal capacity. As a result is the accumulation of heat in the city environment (Hudeková, 2012). One of the factors that influences the local climate conditions in relation to environmental risks are vegetated areas in urban environment. Vegetated areas in urban environment have the capability to eliminate extreme demostrations of local climate. The impact of transpiration causes increasing of the relative air humidity reduces the effect of solar radiation. As a result is the elimination of surface temperature in vegetation. The aim of this study was to evaluate the potentiality of impact of vegetation structure and type of surface on microclimatic conditions. The legwork ran in summer period June-August 2013 and 2014 in residential area Chrenova 1 in the city Nitra by using the method of thermal surface monitoring. Microclimatic conditions and climatic factors, air temperature [°C], relative air humidity [%], air flow [l.s^{-1}], surface temperature [°C], we observed in six localities – vegetated areas of Housing Estate Chrenova 1. Our measurments were realized during the standard atmospherical conditions (anticyclonal type of weather).

Keywords: vegetation, microclimate, urban environment

INTRODUCTION

Vegetation plays the significant role in the forming of microclimate and thermal comfort in urban environment.Surface temperature of vegetation influence the thermal balance through the blazing change (Scudo et. al., 2002). Different type of surface in urban environment have the different impact on vegetation. The outflow and sedimentation is changing depending on the type of material (Godefroid, Koedam, 2004). Tree vegetation uses 2 % of solar energy on photosynthesis, 60-80 % absorbs by leafs and 5-15 % reflects back to space. The rest of solar energy goes trough leaves. The certain amount of radiation is being used for warming up the particular parts of the tree. Trees with thin crowns can receive 60-80 % of solar radiation. Through the trees with compact crowns penetrates 2-3% of solar radiation (Reháčková, Pauditšová, 2006). Different thermal characteristic of active surfaces lead to raising of heat absorption in period of positive energy balance. Due to this modification the built-up areas can be warmer than surrounding land. According to Oke (1997) the specific thermal conditions are related to albedo and to the air pollution. Vegetation areas dont accumulate heat. After the opening of stomata and during the assimilation the temperature of stomata matches with the air temperature or drops down under this temperature (Slováková, Mistrík, 2007).

MATERIALS AND METHODS

In research areas of Housing estate Chrenova 1 we realized the inventory of species in spring session 2013 and 2014. We evaluated structure of vegetated area, foliation and species diversity, percentage, high of trees and canopy of crowns by using the method of Machovec (1987).

Structure of vegetated areas

Locality A1: Vegetation in the locality A1 is bilayer with 50 trees. Monitoring point is located in dense and relative closed canopy of 26 trees with continuity on the open lawn. The highest part has the type *Acer pseudoplatanus* – 16 % .

Locality A2: Vegetation in the locality A2 is three-layer with 33 trees, it is structured into 5 formations with central lawn. Vegetated area is opened to the inside of residential area. Monitoring point is located in sparse vegetation with 7 trees. The highest percentage has *Pinus sylvestris* – 38 %

Locality B1: Vegetation in the locality B1 is three - layer with 46 trees. Trees are organized into 3 small clusters on the left side. In the middle of the vegetated area is the lawn with solitaire tree.Monitoring point is located in vegetation with dense canopy of crowns with 9 trees. The highest percentage has *Tilia cordata* – 34,9 % .

Locality B2: The vegetation in the vegetated area B2 is three - layer, it is organized into 2 cluster with dense canopy of crowns. Number of trees in vegetated area is 11. Monitoring point is located in central lawn near the children's playground. The highest percentage has *Pseudotsuga menziesi* – 35,8 %.

Locality C1: Vegetation in the locality C1 is three-layer with 68 trees. Tree vegetation is organized into 5 clusters. The lawn is open near the river Nitra. Monitoring point is located in the cluster of 3 trees with sparse canopy of crowns. The highest percentage has *Juglas regia* – 42,8 %.

Locality C2: The vegetated area in locality C2 is typical bounded area by inside of residential area. In vegetation area are 22 trees organized into 5 clusters with sparse canopy of crowns. Monitoring point is located in central lawn. The highest percentage has *Taxus baccata, Pseudotsuga menziesii, Tilia cordata* – 25 %.

Measurments in research areas

The legwork ran in summer sessions June-August 2013 and 2014 in residential area Chrenova 1 in the city Nitra by using the method of thermal surface monitoring with instrument Anemometer TSI Veloci Calc. Microclimatic conditions and climatic factors, air temperature [°C], relative air humidity [%], air flow [l.s^{-1}], surface temperature [°C], we observed in six localities – vegetated areas of Housing Estate Chrenova 1. Our measurments were realized during the standard atmospherical conditions (selected days with anticyclonal type of weather) at 6:00 a.m. and 12:30 p.m.. Microclimatic factors were statisticaly evaluated in software Statistica 7 by using the Kruskal –Wallis analyse.

RESULTS

We compared differences in microclimatic factors between selected vegetated areas depending on vegetation structure in times 6:00 a.m. (one hour after sunrise in summer sessions 2013-2014), 12:30 p.m. (at noon in summer sessions 2013-2014) and overheating of surface in time of positive energy balance (in interval 6:00 a.m. – 12:30 p.m. in summer sessions 2013-2014).

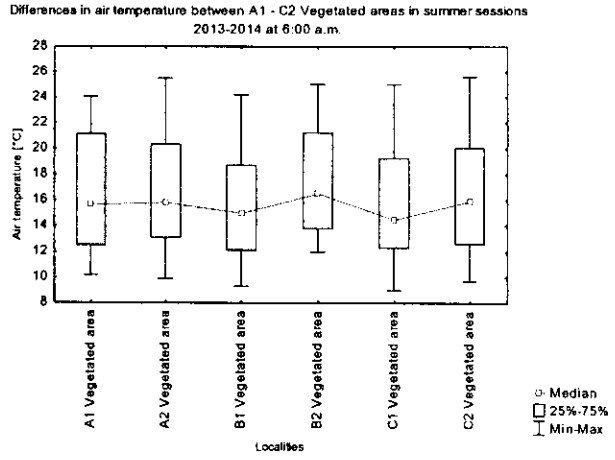

Fig. 1: Microclimatic factor air temperature in vegetated areas A1 – C2 in summer sessions 2013-2014

In the Fig. 1 we compared microclimatic factor air temperature at 6:00 a.m. (one hour after sunrise in summer sessions 2013-2014) between all selected vegetated areas with different vegetation structure. The lowest value of air temperture at 6:00 a.m. we noticed in Vegetated areas (B1, C1 – 15,9 [°C]). In these localites dominated leaf trees, in B1 Vegetated area - the highest percentage has *Tilia cordata* – 34,9 %, in C1 Vegetated area - The highest percentage has *Juglas regia* – 42,8 %. The highest value of air temperature at 6:00 a.m. was noticed in B2 Vegetated area (17,5 [°C]). In Vegetated area B2 is three –layer vegetation with 11 trees, it is minimum number of trees between all selected vegetated areas.

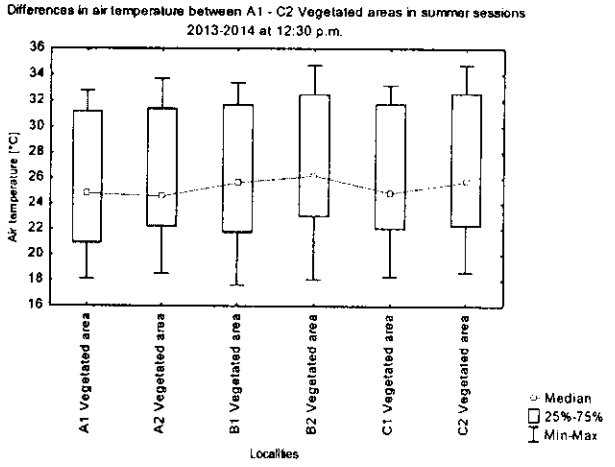

Fig. 2 : Microclimatic factor air temperature in vegetated areas A1-C2 in summer sessions 2013-2014

In the Fig.2 we compared microclimatic factor air temperature at 12:30 p.m (at noon in summer sessions 2013-2014) between all selected vegetated areas with different vegetation structure. Median values of air temperature were appropriately balanced in range 25,7 – 27,3 [°C]) for all research areas. Statistically significant diferences were not recorded.

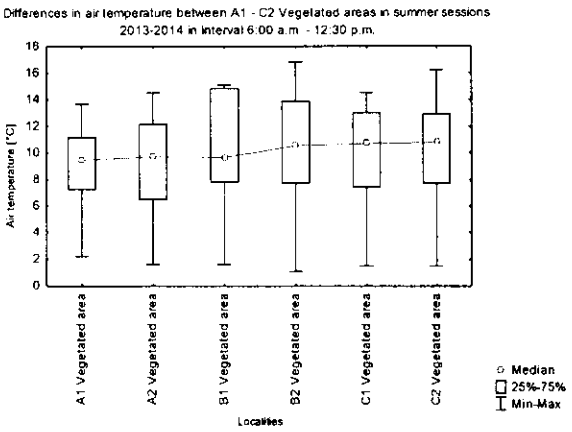

Fig. 3: Differences in air temperature between vegetated areas A1-C2 in interval 6:00-12:30 in summer sessions 2013-2014

In the Fig. 3 we evaluated microclimatic factor air temperature in interval 6:00 a.m. – 12:30 p.m. in time of positive energy balance for selected vegetated areas of housing estate Chrenova 1. In the research area A1 value of air temperature increased up to 9,2 [°C]). Vegetation in the locality A1 is bilayer with 50 trees. Monitoring point is located in dense and relative closed canopy of 26 trees with continuity on the open lawn. Trees vegetation in dense canopy has the function of thermal stabilizer, as a result is the lowest increase of air temperature in vegetation between selected vegetated areas.

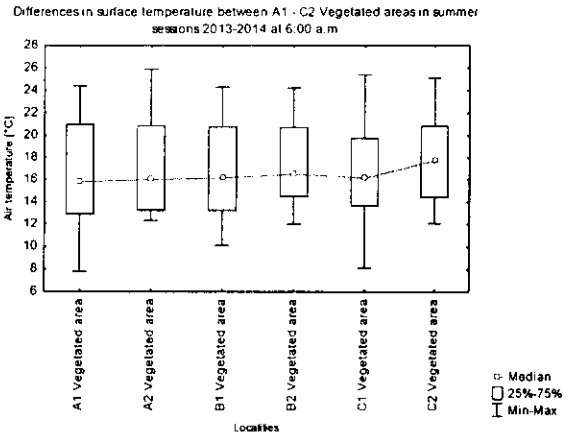

Fig. 4: Microclimatic factor surface temperature in vegetated areas A1-C2 in summer sessions 2013-2014

In the Fig. 4 we compared microclimatic factor surface temperature at 6:00 a.m. (one hour after sunrise) for selected vegetated areas depending on vegetation structure. The highest median values of surface temperature was noticed in vegetated area C2 with central lawn. This locality is typical bounded area by inside of residential area.

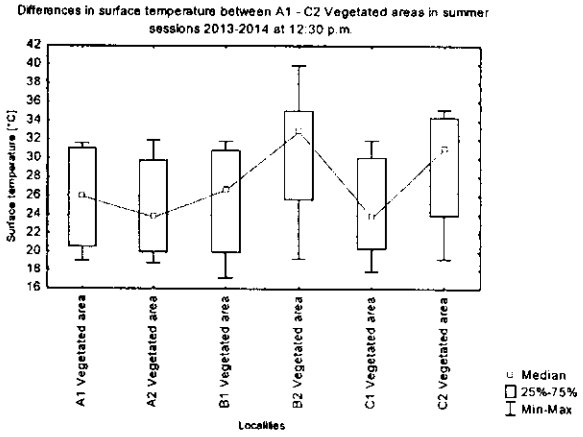

Fig. 5: Microclimatic factor surface temperature in vegetated areas A1-C2 in summer sessions 2013-2014

In the Fig. 5 we evaluated microclimatic factor surface temperature at 12:30 p.m. (at the noon) in time of positive energy balance, when the overheating of different type of surfaces is significant. The highest median value of surface temperature was in vegetated area B2 – 30.9 [°C], with dominance of open lawn, number of trees is 11. The highest percentage has *Pseudotsuga menziesi* – 35,8 %. The lowest median value of surface temperature was observed in vegetated area C1-24,8 [°C].

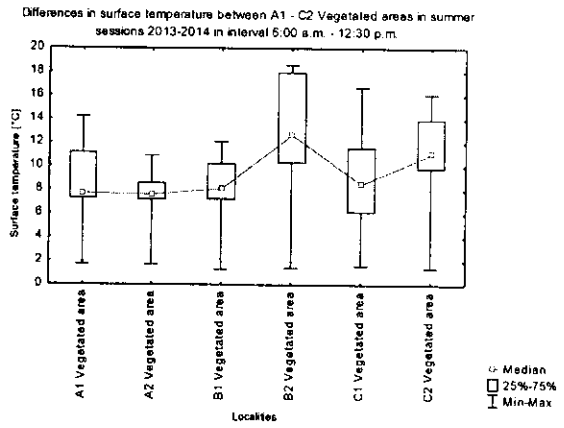

Fig. 6: Differences in surface temperature between vegetated areas A1-C2 in interval 6:00-12:30 in summer sessions 2013-2014

In the Fig. 6 we evaluated increasing of surface temperature depending on vegetation structure between selected vegetated areas A1-C2 in summer sessions 2013-2014. Statistically significant differences were recorded between vegetated areas A2-B2 (7,6-12,7 [°C], in p-level, p=0,01, p<0,05). Between localities B1-B2 was recorded statistically significant difference in p level (p=0,03, p<0,05). Number of trees in vegetated area B2 is 11. Monitoring point is located in central lawn near the children's playground. The capability to absorb solar radiation in time of positive energy balance is depending on the vegetation structure, the canopy of trees and quantity (Čaboun, 2008).Very important factor which influences overheating of surface is managment of vegetated areas in urban environment. Vegetated areas with the dominant lawn and uncovered clusters of soil can by overheat in time of positive energy balance equally as hard surfaces.

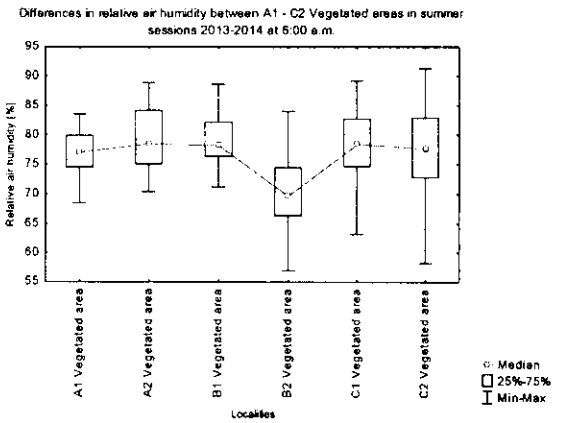

Fig. 7: Microclimatic factor relative air humidity at 6:00 a.m. in vegetated areas A1-C2 in summer sessions 2013-2014

In the Fig. 7 we compared microclimatic factor relative air humidity at 6:00 a.m. between selected vegetated areas A1-C2. The changes of relative air humidity are related to the air temperature. According to (Tužinský, 2002) is higher relative air humidity in the part of trunk – the morning type of humidity. Statisticaly significant differences in factor relative air humidity were recorded between vegetated areas A2-B2 (79,4 % - 69,9 %, p=0,009, p<0,01), B1-B2 (78,9 – 69,9 %, p=0,01), B2-C1 (69,9 – 78,2 %, p=0,02, p<0,05), B2-C2 (69,9 – 77,8 %, p=0,04, p<0,05). On process of transpiration has significant impact air temperature, characters of growth and temperature in growth, LAI index, radiation balance and air humidity. Characters of growth are represented with number of trees, species diversity (coniferous or foliose trees), age of growth and canopy (Škvarenina et.al, 2013). The lowest median values of relative air humidity at 6:00 a.m. was recorded in vegetated area B2 with dominance of *Pseudotsuga menziesi* – 35,8 %.

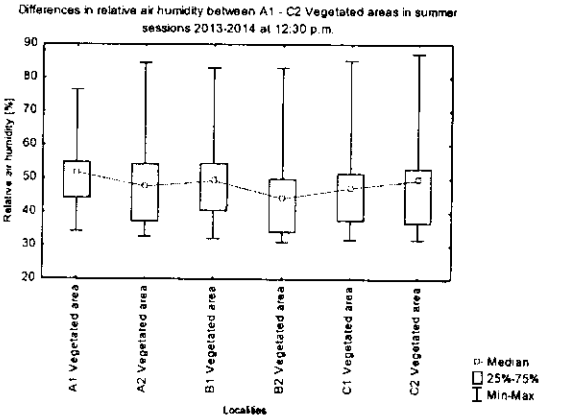

Fig. 8: Microclimatic factor relative air humidty in vegetated areas A1-C2 in summer sessions 2013-2014

On microclimatic factor of relative air humidity in vegetated areas has the significant impact canopy of crown, number of trees and species diversity. Thermal balance is influenced by the level of transparency of vegetation - density of crown, size of leaves and their orientation (Rcháčková, Pauditšová, 2006). In the Fig. 8 we compared median values of relative air humidity at 12:30 p.m. in summer sessions 2013-2014. The highest value of relative air humidity was in vegetated area A1 with 50 trees in dense canopy, the lowest value of relative air humidity was in vegetated area B2 with dominance of open lawn with minimum of trees vegetation between selected research area.

CONCLUSION

The aim of this study was to evaluate impact of vegetation structure on microclimatic conditions in urban environment of Nitra. Research areas were selected in Housing estate Chrenova I. In vegetated areas A1-A2-B1-B2-C1-C2 we realized measurments by using method of thermal surface monitoring with instrument Anemometer TSI Veloci Calc. We observed microclimatic factors air temperature, surface temperature and relative air humidity in time of positive energy balance (at 6:00 a.m. – one hour after sunrise, at 12:30 p.m. – at the noon). For evaluating of microclimatic factors was used software Statistica 7 – Kruskal-Wallis analyse. We compared microclimatic condition depending on vegetation structure between selected vegetated areas. Statistically significant differences were recorded in microclimatic factor surface temperature in interval 6:00 a.m. -12:30 p.m. between vegetated areas A2-B2 (7,6-12,7 [°C] in p-level, $p=0,01$, $p<0,05$) and between localities B1-B2 in p level ($p=0,03$, $p<0,05$). These results indicate, that vegetated areas with the dominant lawn and uncovered clusters of soil can by overheat in time of positive energy balance equally as hard surfaces. According to Wardoyo (2011) is urban environment specific to hard surface, typical urban geometry, vegetated areas and variability of surface materials. For every active surface is typical that there is a transformation of the energy of the shortwave radiation to the thermal energy. Accumulation of solar radiation and reflected radiation are forming microclimate. In urban environment is large concentration of surfaces which are strongly overheated and have large thermal capacity. Vegetation areas in urban environment have the capability to eliminate extreme demostrations of local climate. In time of marked climate changes, that influence quality of live in urban environment, is important dedicated to effectively management of vegetated areas. Functional planting and proposals are the tool for eliminate of negative impact of increasing temperature and extremes of weather in urban environment. Significant capability of vegetation for thermal comfort of residents is to keep relative air humidity by transpiration. Relation between air temperature, relative air humidity and velocity of air have the impact on wind chill factor. On process of transpiration has significant impact air temperature, characters of growth and temperature in growth, LAI index, radiation balance and air humidity). In certain conditions plants are on direct sun overheating too, but this is just short-term overheating. In selection of woody species with positive adaptation on climate change is applicable to planting of foliose trees, invasive species are unsuitable, because higher air temperature has the impact on their spreading (Záborská a kol., 2014 in Hegei, Šteiner, 2014).

Acknowledgement

This study is the result of the project implementation: VEGA 1/0042/12 Analysis of selected environmental factors in relation to possible health risk and the project supported by University Grant Agency of Faculty of Natural Sciences, Constantine the Philospher University in Nitra - VIII/3/2015.

LITERATURE

Čaboun, V., 2008: Vplyv vegetácie na znižovanie teploty povrchov a ovzdušia pri extrémnych horúcavách. In: Rožnovský, J., Litschmann, T. (ed): „Bioklimatologické aspekty hodnocení procesu v krajine", Mikulov 9. – 11.9.2008, ISBN 978-80-86690-55-1

Godefroid, S., Koedam, N., 2004: Interspecific variation in soil compaction sensitivity among forest floor species. In: Conservation Biology, 2007, p. 14, 119:207–217

Hegei, L., Šteiner, A., 2014. Adpatácia na zmenu klímy – naliehavá úloha miest, Karpatský rozvojový institute, Košice 2014, 128 s.

Machovec, P., 1987: Hodnocení vzrostlé zelene v mestských parcích. Praha: Vydavatelstvo ŽP, 1987. pp 134-139

Oke, T. R. 1997: Urban climates and global environment change in applied climatology, routledge. London – New York, s. 273 – 287

Reháčková, T., Pauditšová E., 2006: Practical experiences with the evaluation of microclimatic function of vegatation in urban environment. (Praktické skúsenosti s hodnotením mikroklimatickej funkcie vegetácie v urbánnom prostredí). In: Sídlo - Park – Krajina IV. KULTÚRNA VEGETÁCIA V SÍDLACH A V KRAJINE. 2006, Zborník vedeckých prác a referátov. SPU Nitra, s. 227-235, ISBN 80-8069-809-0

Scudo, G., Dessi, V., Rogora, A., 2002: Evaluation of radiant conditions in urban spaces. In: Designing open spaces in the urban environment: a bioclimatic approach. 2002, p. 12-17, ISBN 960-86907-2-2

Slováková, L., Mistrík, I., 2007: Physiological processes of plants in stress conditions. (Fyziologické procesy rastlín v podmienkach stresu), Univerzita Komenského Bratislava 2007, s. 232. ISBN 978-80-223-2322-2.

Škvarenina,J., Hríbik, M., Škvareninová, J., Fleischer, P., 2013 Globálne zmeny klímy a lesné ekosystémy, Technická univerzita vo Zvolene, 2013, s.123, ISBN 978-80-228-2595-5

Tužinský, L., 2002: Bioclimatology. (Bioklimatológia), Technická Univerzita Zvolen, Lesnícka fakulta, Katedra prírodného prostredia, 2002, p. 140, ISBN 80-228-1150-5

Wardoyo, J., ET. AL. 2011. Vegetation Configuration as Microclimate Control Strategy In Hot Humid Tropic Urban Open Space. S E N V A R + I S E S E E 1-3 December 2008, International seminar in sustainable environment & architecture

Záborská, Z., Schvalb, M., Jerguš, M., Dobrucká, A., 2014: Prípadová štúdia z procesu adaptácie na zmenu klímy mestskej časti Košice – Západ, s. 90-102, In: Adpatácia na zmenu klímy – naliehavá úloha miest, Karpatský rozvojový institute, Košice 2014, 128 s

PRÍLOHA č. 5

Bahnová, K., Dobišová, M., Rózová, Z., 2015: Vegetated areas in relation to formation of local climate – an example of the city Nitra. In: The Abstracts of the 17th International Symposium "Landscape and Landscape Ecology", 27-29 May 2015, Nitra, Slovakia, Institute of Landscape Ecology, Slovak Academy of Sciences. p. 10, ISBN 978-80-89325-27-6

Vegetated areas in relation to formation of local climate – an example of the city Nitra

Katarína BAHNOVÁ, Mária DOBIŠOVÁ, Zdenka RÓZOVÁ

Department of Ecology and Environmental Sciences, Constantine the Philosopher University in Nitra, Slovakia, e-mail: katarina.bahnova@ukf.sk; maria.dobisova@ukf.sk; zrozova@ukf.sk

Trend of nowadays is decreasing of green areas related to increasing urbanization and spatial requirements of urban population. One of the factors that influences the local climate conditions in relation to environmental risks are vegetated areas in urban environment. The aim of this study is to specify the relation between functional areas with vegetation in the central city zone and categories of climate in the city Nitra. Climate as a significant environmental factor is defined by categories in urban environment (e.g.: Grimmond, 2007) as: climate of the city (climatic conditions of the city Nitra), local climate (climate of selected city district– housing estate Chrenova 1) and microclimate (specific climate of small area – selected residential blocks of housing estate Chrenova 1). The significant data source for assignment of climate of city Nitra is the numerical model supported by (Ukrainian centre of environmental and water projects, 2006), that effectively minimises the estimation error of meteorological data by using the Kalman filter. For assignment of local climate we used the method of thermal surface monitoring. Acquired data were evaluated as average values for the selected city district. Microclimate conditions were monitored by using thermal surface monitoring in six localities in the housing estate Chrenova 1 during the spring and summer session 2013.

Acknowledgement This study is the result of the project implementation: Environmental aspects of the urban environment ITMS 26220220110 supported by the Research & Development Operational Program funded by the ERDF and the result of the project: VEGA 1/0042/12 Analysis of selected environmental factors in relation to possible health risks.

PRÍLOHA č. 6

Journal of the Ceramic Society of Japan 123 [9] 874-879 2015 Paper

The influence of heat on elastic properties of illitic clay Radobica

Miroslav JANKULA,* Tomáš HÚLAN,* Igor ŠTUBŇA,* Ján ONDRUŠKA,* Rudolf PODOBA,** Peter ŠÍN,*** Peter BAČÍK**** and Anton TRNÍK*,*****,†

*Department of Physics, Constantine the Philosopher University in Nitra, A Hlinku 1, 94974 Nitra, Slovakia
**Department of Structural Ceramics, Institute of Materials Research, Slovak Academy of Sciences, Watsonova 47, 040 01 Košice, Slovakia
***Department of Physics, Faculty of Civil Engineering, Slovak University of Technology, Radlinského 11, 81368 Bratislava, Slovakia
****Department of Mineralogy and Petrology, Faculty of Natural Sciences, Comenius University, Mlynská dolina, 842 15 Bratislava, Slovakia
*****Department of Materials Engineering and Chemistry, Czech Technical University in Prague, Thákurova 7, 16629 Prague, Czech Republic

Brick clay from a locality Radobica, Central Slovakia, which was exploited for brick manufacturing in the past, was investigated for its possible reuse in the brick industry. The crystalline phases of the green sample were 48% of quartz, 37% of illite, 13%, of Na-feldspar and 2% of calcite. The measurements of Young's modulus of clay samples were performed during heating up to 1100°C and also at room temperature on samples preheated at temperatures from 100 to 1100°C. It was found during firing that 1) the physically bound water is released in 3 steps (up to 300°C) and reaches ~2.5 wt %. The thermal expansion is decelerated by setting the crystal closer at low temperatures. Young's modulus increases in its values (~36%) which is a result of the closer structure that is created via release of the physically bound water. 2) The mass loss during dehydroxylation (450–750°C) is ~3 wt %. The superposition of dehydroxylation and $\alpha \rightarrow \beta$ transformation of quartz creates a step ~3% of the relative thermal expansion. Young's modulus slightly decreases in its values, the dehydroxylation does not influence this trend. 3) Above 900°C, the intensive contraction due to sintering is observed and a steep increase (250%) of Young's modulus takes place in this temperature interval. The irreversible changes of the Young's modulus measured at room temperature after firings at the temperatures from the interval 100–1100°C give a different picture. Dehydroxylation affects Young's modulus very significantly decreasing its values from 7.8 GPa (at 400°C) to 4.3 GPa (at 700°C). After dehydroxylation, the sintering increases Young's modulus. Since the porosity remains relatively high (~30%) and a part of the glassy phase in the sample fired at 1100°C is relatively low (25%), the Young's modulus is low even after firing at 1100°C (9.3 GPa).

Key-words : Illitic clay, Elastic properties, Mechanical strength, Thermal analyses

[Received January 29, 2015; Accepted May 26, 2015]

1. Introduction

Clays, which contain kaolinite and/or illite, are essential ingredients for building ceramic manufacture for its plasticity, workability and green strength.[1] The most common natural additional minerals included in clays are quartz, carbonates, feldspar, iron oxides and sulfides. In addition, clays usually contain some organic material. The structural features of the ceramics are developed during the shaping/molding the green ceramic product and its drying, and finally the structure and properties of the ceramic product are consolidated during the firing, in which physical and chemical processes occur among the different minerals.[2)–4)] Required mechanical properties of the building ceramics are associated mainly with mechanical strength and Young's modulus which are the most important. These two parameters are largely dependent on structural characteristics that develop during firing.[2),5)]

Young's modulus and mechanical strength are important not only for building applications but also for a regime of the firing process where determine the maximum rate of heating. In spite of the importance of Young's modulus for firing the building ceramic products, it was studied during heating and cooling very rarely. As far as we know, Young's modulus of the green ceramic sample was measured during heating only for porcelain mixture,[6)] for heat-proof stove ceramics[7)] and for almost pure illite.[8)] Some common features can be observed in a development of Young's modulus: 1) a loss of the remainders of the physically bound water from pores increases the Young's modulus of the green ceramic mass in a significant measure. For example, Young's modulus of the green porcelain mixture increases ~30%;[6)–8)] 2) no significant changes of Young's modulus were observed in the dehydroxylation region;[8)] 3) $\alpha \rightarrow \beta$ transformation of quartz at 573°C, which is characterized with intensive expansion and sharp decrease of Young's modulus of quartz grains in the ceramic mixture,[9)] does not influence elastic properties of the green ceramic sample during its heating;[7),10)] 4) sintering, which starts at ~700°C, increases the Young's modulus.[6),11)]

In addition to direct observating the influence of heat on the mechanical properties during heating, a commonly used way how to find these relationships is the measurement of the mechanical properties after firing.[1),4)] To determine the suitability of some clay for ceramic productions, different tests are performed at room temperature on samples fired at temperatures higher than

† Corresponding author: A. Trnik; E-mail: atrnik@ukf.sk, anton.trnik@fsv.cvut.cz

DOI http://dx.doi.org/10.2109/jcersj2.123.874

700°C. The mechanical strength, porosity, irreversible shrinkage and absorbability are probably most often measured mechanical quantities. Development of the phases during firing is experimentally studied through thermal analyses, mainly: differential thermal analysis (DTA), thermogravimetry (TGA), thermodilatometry (TDA) and X-ray diffraction (XRD).[1),4),12)-16)]

The material of the present investigation is the clay from locality Radobica, Central Slovakia. The clay was exploited for brick manufacturing in the past. Its re-exploiting can be attractive in a new ceramic mixture with a fly-ash, which is a perspective waste raw material for a green ceramic body.[16)] The goal of this paper is a study of the elastic properties of this clay during thermal treatment and also as a function of the firing temperature.

2. Experimental

2.1 Samples

The clay used to prepare the samples was excavated from a depth more than 1.2 m (at smaller depths the samples contained a large amount of organic mass and sample properties intensively varied). The clay was ground and mixed with distilled water to obtain a plastic mass with the water content 25 mass %. Cylindrical samples were prepared with a laboratory extruder. After open air free drying, the samples contained ~2 mass % of the physically bound water.

2.2 Measurement methods

The phase analysis was performed by powder X-ray diffraction using a diffractometer BRUKER D8 Advance with a Cu anticathode ($\lambda\alpha_1 = 1.54060$ Å), accelerating voltage 40 kV, and beam current 40 mA. For a quantitative analysis the Rietveld method was used with a corundum internal etalon. A content of quartz was also checked with DSC and content of illite with TGA.

A picture of the fracture area was obtained with a scanning electron microscope (SEM) Auriga Compact FIB-SEM from the Carl Zeiss Company, using an accelerating voltage 5 kV. Prior to the SEM observation, the samples were treated by carbon vapor deposition.

DTA and TGA were performed by the analyzer Derivatograph 1000[17)] on compact bodies with dimensions of ⌀12 × 20 mm and mass ~3.5 g. A reference compact sample for DTA, which had approximately the same size and mass as the measured green clay sample, was made from pressed Al_2O_3 powder. The experiments were repeated three times for each sample type to ensure reproducibility of our results. As blank curves, we used data from a second measurement of the same material under identical conditions. Therefore, any reversible processes that take place in the material cannot be registered in these two thermal analyses.

The relative expansion in dependence on the temperature was determined using a horizontal alumina push-rod dilatometer.[18)] Dimensions of the samples were ⌀12 × 40 mm.

Using the experimental results of TDA $\varepsilon = \Delta l/l_0 = \Delta d/d_0$, and TGA $\mu = \Delta m/m_0$ (l_0, d_0 and m_0 are the length, diameter, and mass of the green sample, respectively), the bulk density was calculated as

$$\rho = \rho_0 \frac{1+\mu}{(1+\varepsilon)^3}, \tag{1}$$

where ρ_0 is the initial bulk density at room temperature.

The porosity was calculated with the help of the experimentally determined bulk density and matrix density. The bulk density was obtained from the size and weight measurements of the cylindrical samples. The matrix density was measured by helium pycnometry (Pycnomatic ATC, Porotec).

The modulated force thermomechanical analysis (mf-TMA), which is based on the resonant vibration of the sample in the fundamental flexural mode,[19)] was used for the measurement of the resonant frequency. Young's modulus E may be calculated for a cylindrical sample with a uniform cross-section by a formula given in[20),21)] that can be rewritten for varying dimensions and mass

$$E = 1.6756 \frac{m_0 l_0^3}{d_0^4} \frac{1+\mu}{1+\varepsilon} f^2, \tag{2}$$

where f is the resonant frequency of the fundamental mode of the flexural vibration and other quantities are the same as for Eq. (1). Since the sample is not slender (its dimensions were ⌀12 × 130 mm), a correction coefficient $T = 1.0429$, which was calculated from a formula given in,[20)] was included into Eq. (2).

The mechanical strength was measured by the three-point-bending method.[22)] The sample of the size ⌀12 × 120 mm was subjected to a loading force, which increased with a rate of 2 N·s^{-1}. A set of 10 samples were broken at room temperature after its firing at the selected temperature from the interval (100, 1100°C).

Two types of measurements were performed in the present study. In type 1 we used the green clay samples that were studied from the room temperature up to a temperature 1050 or 1100°C under heating at a linear rate 5°C·min^{-1}. The maximum temperature was chosen as 1050°C for the measurement of the mass changes and in the DTA/TGA, and as 1100°C for TDA and mf-TMA. In type 2 we measured the samples at room temperature that were preheated with a heating rate of 5°C·min^{-1} on 100, 200, ..., 1100°C without a soaking at the highest temperature. The samples were cooled in the furnace down to room temperature. Temperature of 1100°C was chosen for both types of measurements because it is the presumptive highest firing temperature used in the industrial production of clay bricks and tiles. For the all measurements the ambient gas was air.

3. Results and discussion

The results of the XRD analysis were carried out at room temperature for green clay Radobica, and clay fired at 1000°C (see **Fig. 1**). Quantitative XRD analysis and thermal analyses DSC and TGA revealed that the green clay contained 48% of quartz, 37% of illite, 13% of Na-feldspar and 2% of calcite. Taking into account that a color of the fired samples was dark red, ferrous oxides are also present in the clay.

After firing at 1000°C, the main crystalline phases are 51% of quartz, 14% of Na-feldspar, 3% of hematite and 32% of

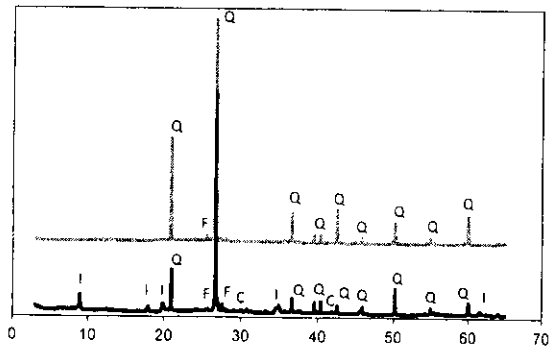

Fig. 1. XRD pattern of the green clay sample (black line) and clay sample fired at 1000°C (gray line) Q – quartz, I – illite, F – feldspar, C – calcite.

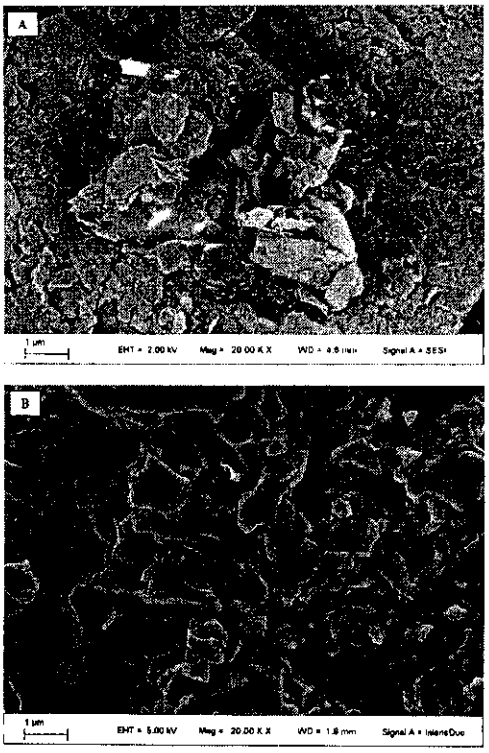

Fig. 2. SEM picture of the green clay sample (A) and clay sample fired at 1000°C (B).

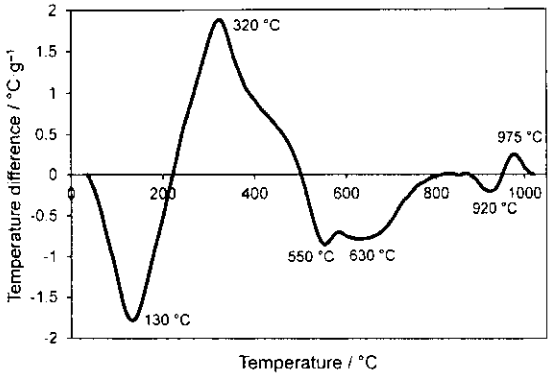

Fig. 3. DTA of the green clay sample.

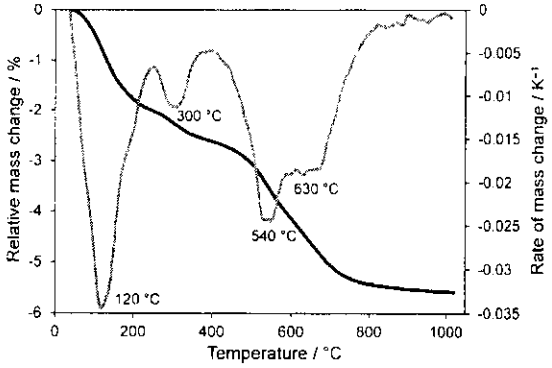

Fig. 4. Relative mass change (black line) and rate of mass change (gray line) of the green clay sample during heating up to 1050°C.

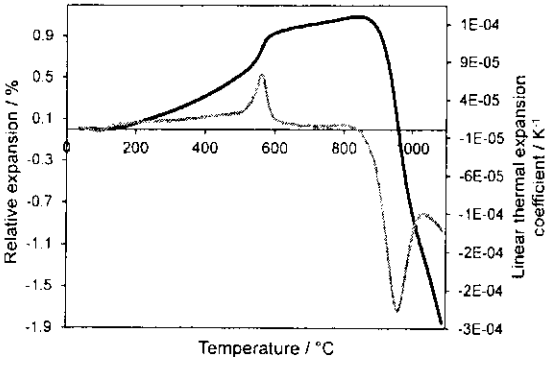

Fig. 5. Relative expansion (black line) and linear thermal expansion coefficient (gray line) of the green clay sample during heating up to 1100°C.

amorphous phase. From these data and from densities of these minerals (2.65 $g \cdot cm^{-3}$ for quartz, 2.70 $g \cdot cm^{-3}$ for illite, 2.56 $g \cdot cm^{-3}$ for feldspar, 5.26 $g \cdot cm^{-3}$ for hematite and 2.61 $g \cdot cm^{-3}$ for sodium glass) as well as from the bulk densities, which are 1.92 $g \cdot cm^{-3}$ for the green sample and 1.86 $g \cdot cm^{-3}$ for the fired sample, we can estimate their porosities. We obtain ~30% for the green sample and ~32% for the sample fired at 1000°C. These values are approximately the same as measured porosities (**Fig. 10**). This relatively high porosity is also visible in SEM picture of the fracture surface in **Figs. 2**(a) and 2(b).

3.1 Development of the elastic properties during heating

The composition and microstructure of clay change during heating. In general, results of the thermal analyses DTA, TGA and TDA reveal the processes which take place in the clay. Young's modulus is a function of the sample dimensions and mass. The temperature changes in these quantities must be taken into account, if a correct value of E should be obtained. All these influences as well as actual value of the resonant frequency must be considered in Eq. (2). Therefore, the values of Young's modulus are calculated from the results of TGA, TDA and mf-TMA.

The endothermic peak in the DTA curve (**Fig. 3**) in the temperature range from 25 to 220°C represents the release of the physically bound water from the pores and surfaces of the crystals in the clay. This process is reflected by a relatively large decrease in the sample mass by 2% (**Fig. 4**), and a small contraction registered in the TDA curve (**Fig. 5**). The small value of the contraction and significant mass loss lead to a decrease in the bulk density (**Fig. 6**). From the mechanical point of view, the release of the physically bound water makes the contacts between crystals stronger and Young's modulus increases ~36%. A very similar elastic behavior at these low temperatures was also found in ceramic mixtures based on kaolinite and illite.[6)–8),10)]

In the temperature range from 220 to 400°C a DTA exothermic peak is visible, which is related to a burning of organic impurities (Fig. 3). This process leads to a small decrease of the sample mass by 0.5% (Fig. 4). The mass loss and expansion of the sample (Fig. 5) causes a continuing decrease in the bulk density (Fig. 6). We can also expect a creation of the additional pores instead of the burned organic material. Since the Young's modulus depends directly on the bulk density and porosity, it decreases in this temperature region (**Fig. 7**).

The third process is dehydroxylation of illite which begins at 400°C and finishes at 800°C. It runs in two steps which reach the maximum rate at the temperatures 550 and 630°C being in accordance with the results given in.[23)] The dehydroxylation of illite is accompanied by mass loss as well as expansion of the

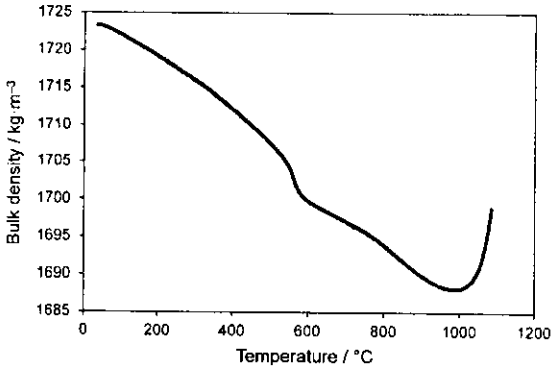

Fig. 6. Bulk density of the green clay sample during heating up to 1100°C.

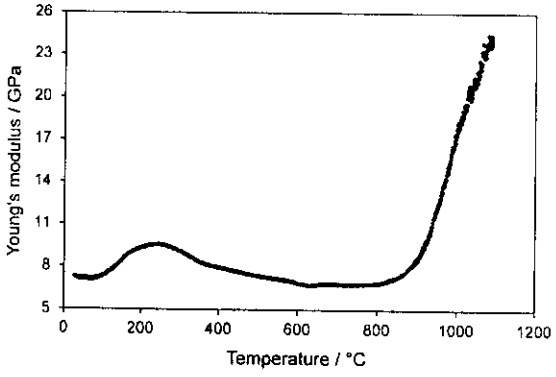

Fig. 7. Young's modulus of the green clay sample during heating up to 1100°C.

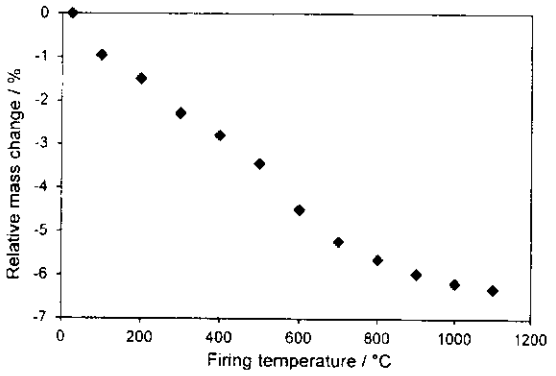

Fig. 8. Relative mass change of the clay in a dependence on the firing temperature.

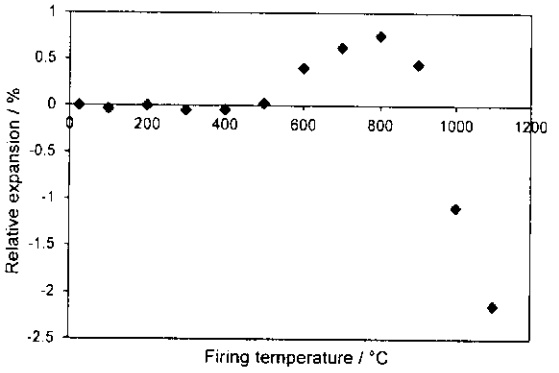

Fig. 9. Relative expansion of the clay sample in a dependence on the firing temperature.

samples.[8] A consequence of the expansion and mass loss of the sample is a decrease in the bulk density. The values of Young's modulus pass through very flat minimum between 400 and 800°C.

The sample has a relatively high amount of quartz that proves as a sharp minimum in the DTA curve and step in the TDA curve around 573°C as a consequence of the $\alpha \rightarrow \beta$ transformation of quartz. This transformation causes the additional decrease of the bulk density. In spite of that, the Young's modulus does not reflect the $\alpha \rightarrow \beta$ transformation of quartz through its decrease.

The last interval, which covers the temperature above 800°C, is connected with the high-temperature reactions in illite, sintering and vitrification. Above 800°C the mass change is very slow, i.e. the dehydroxylation is completed. There are two peaks in the DTA curve: one endothermic (at 920°C) and one exothermic peak (at 975°C), which are typical for illlite,[24] and are ascribed to a creation of the glassy phase and transformation of metaillite into spinel.[25] The shrinkage of the sample caused by sintering and changes in the metaillite lattice is steep and reaches ~2%. This contraction results in the increase of the bulk density. These high-temperature processes increase Young's modulus 3.2 times during heating from 800 to 1100°C.

3.2 Mechanical properties after firings at room temperature

We also measured mechanical properties of the studied clay in a dependence on the firing temperature from the interval (25, 1100°C). To explain the results of Young's modulus and mechanical strength, a mass change and a dimension change as well as porosity and bulk density were also measured. The measurements were performed at room temperature.

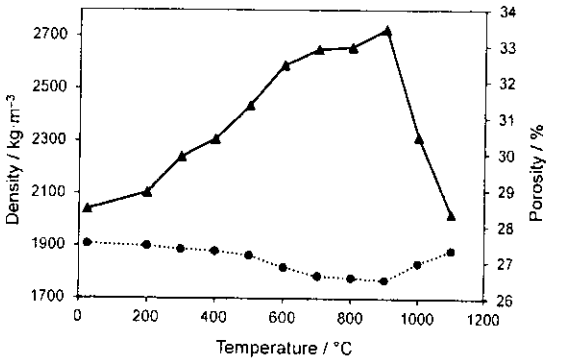

Fig. 10. Bulk density (dotted line) and porosity (solid line) of the clay in a dependence on the firing temperature.

The values of the relative mass loss are depicted in **Fig. 8**. The mass loss is registered at the low temperatures (up to 200°C), which is caused by a release of the physically bound water (the initial moisture of the samples was ~1.5 mass %). The similar results we obtained during heating (Fig. 4). The next contribution to the mass loss is a burning of the organic matter. An increased rate of the mass loss, observed above 500°C, is connected with dehydroxylation of illite. The irreversible volume change, which is depicted in **Fig. 9**, is negligible up to 500°C. Above this temperature, the sample expands due to dehydroxylation. Then we observe a contraction above 800°C when the high-temperature reactions in illite, creation of the glassy phase and sintering begin.

A density and porosity after partial firings are shown in

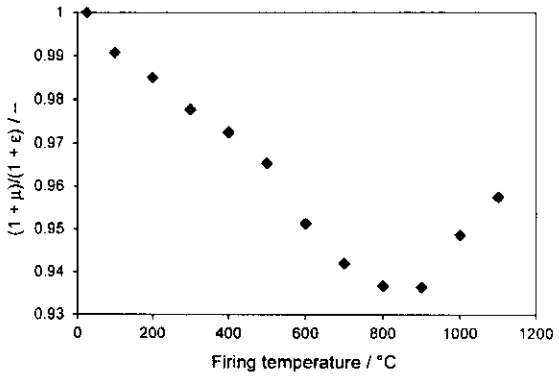

Fig. 11. Relationship between a ratio $(1 + \mu)/(1 + \varepsilon)$ and the firing temperature of clay sample.

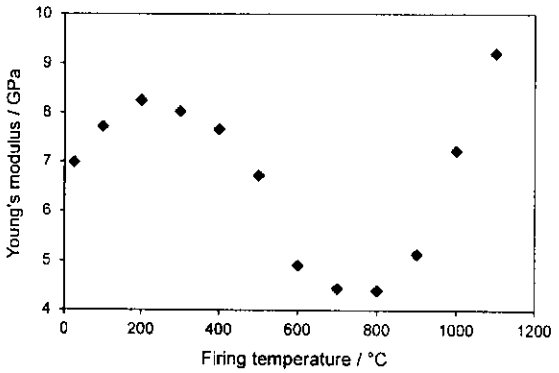

Fig. 12. Young's modulus of the clay sample in a dependence on the firing temperature.

Fig. 10. These properties are almost constant at low temperatures. Their first change occurs at ~300°C where a burning of the organics causes an increase of the porosity and decrease of the bulk density. Dehydroxylation of illite makes these changes more intensive. The sintering of the sample decreases the porosity and increases the bulk density.

The quantities $\mu = \Delta m/m_0$ and $\varepsilon = \Delta l/l_0 = \Delta d/d_0$ in Eq. (2) are relative mass loss and relative thermal expansion after the firing. Since $\mu < 0.06 \ll 1$ and $\varepsilon < 0.02 \ll 1$, the values of ratio $(1 + \mu)/(1 + \varepsilon) \approx 1$, see **Fig. 11**. Consequently, the changes of the volume and mass influence the Young's modulus only in a little degree. The main responsibility for changing the Young's modulus have internal processes in the sample such as creation of new phases and sintering which influence the resonant frequency in Eq. (2).

The values of Young's modulus are low for every firing temperature (**Fig. 12**) and are much lower than Young's moduli of the sample components (i.e. 94 GPa for quartz, 95 GPa for feldspar, 216 GPa for hematite and ~65 GPa for glass). The Young's modulus of the green sample, $E = 7$ GPa, is comparable with the Young's modulus of other green ceramics, see for example.[7),10)] The remove of the physically bound water after low-temperature firings increases Young's modulus. But dehydroxylation of illite decreases Young's modulus significantly. This is probably caused with an additional porosity which increases during dehydroxylation. Young's modulus raises its values above 800°C, which is connected with a sintering, but these values stay low. It can be explained with

1) the high porosity that varies between 28 and 33.5%,

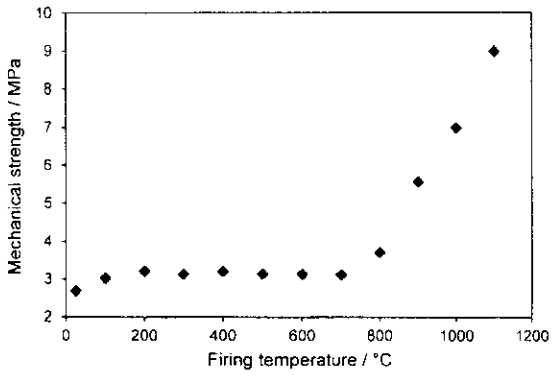

Fig. 13. The mechanical strength of the clay sample in a dependence on the firing temperature.

2) the relatively low firing temperature and short time of the firing. Both of them were not sufficient for mullitization and more intensive vitrification. A low degree of sintering and vitrification as well as the enduring of the pores is visible in Fig. 2(b).
3) the relatively low content of plastic constituent in the green sample. It does not allow create more glassy phase and mullite.

The next mechanical parameter, which we measured, was mechanical strength in dependence on the firing temperature (**Fig. 13**). The release of the physically bound water after low-temperature firings increases mechanical strength from 2.7 to 3.2 MPa. This trend is similar to a development of Young's modulus. On the other hand, the dehydroxylation of illite has no effect on mechanical strength. Its values are almost constant in the temperature interval from 200 to 700°C as was also confirmed for traditional ceramics.[26)] Above 700°C, the mechanical strength rapidly increases due to sintering and reaches 9 MPa at 1100°C. In spite of the theoretical proportionality between mechanical strength and Young's modulus, courses of these quantities seen in Figs. 12 and 13 are different. The mechanical flexural strength depends on sample surface defects and defect size while Young's modulus depends on conditions inside the sample. That is why Young's modulus reflected the dehydroxylation more sensitively than mechanical strength. The values of the mechanical strength as well as Young's modulus of the investigated fired clay are smaller that those obtained for traditional ceramics in.[26)]

3.3 Elastic properties of the fired ceramics during heating

Finally, we studied relative expansion, bulk density and Young's modulus of the sample fired at 1100°C during heating up to 1100°C. On the dilatometric curve (**Fig. 14**), we indicate quartz by a step of the thermal expansion around 573°C. The curve is bent down above 900°C that is caused by the press of the dilatometer's rod on the softened sample. This typical behavior of the push-rod dilatometer is an indirect confirmation of the presence of the glassy phase.

Because the mass of the fired sample is constant, the bulk density is only a function of the relative expansion. The bulk density slightly decreases from its initial value 1723 kg·m^3 at room temperature up to 1683 kg·m^{-3} at 1000°C. In this temperature interval we can indicate only $\alpha \rightarrow \beta$ transformation of quartz at 573°C as a small decrease of the bulk density.

Young's modulus of the fired clay sample during heating up to 1100°C is depicted in **Fig. 15**. There is well visible $\alpha \rightarrow \beta$

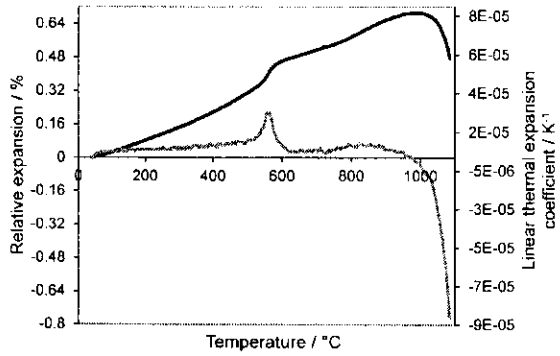

Fig. 14. The relative expansion (black line) and linear thermal expansion coefficient (gray line) of the clay sample fired at 1100°C during heating up to 1100°C.

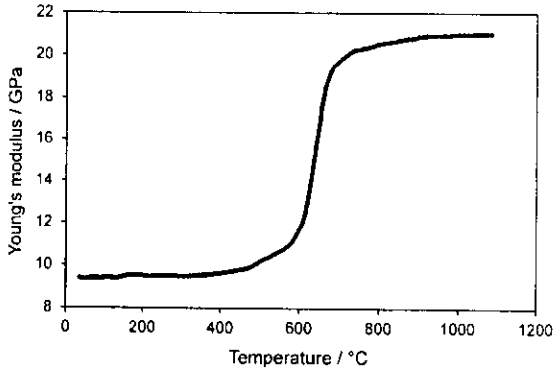

Fig. 15. Young's modulus of the clay sample fired at 1100°C during heating up to 1100°C.

transformation of quartz at 573°C when Young's modulus rapidly increases from 9.4 to 20.3 GPa. This S-curve is characteristic for every ceramics with some content of quartz. This increase is caused by closing the circumference cracks around the quartz grains.[11),27)]

4. Conclusions

Brick clay from a locality Radobica, Slovakia was investigated during heating up to 1100°C and also at room temperature after preheated at temperatures from 100 to 1100°C. The green clay contained 48% of quartz, 37% of illite, 13% of Na-feldspar and 2% of calcite. It was found:

- The mass loss increases almost linearly with the firing temperature and reaches 6% at 1100°C.
- The irreversible volume change after firings is negligible up to 500°C. Then we observe an increase in its values up to 800°C when the sintering begins. Above 800°C the intensive contraction due to sintering was observed.
- The relationship between Young's modulus and firing temperature is complex. After the small increase of Young's modulus after low-temperature firings, dehydroxylation lowers this mechanical parameter as long as the sintering takes place at and above 800°C. Then Young's modulus again increases.
- The values of Young's modulus and mechanical strength are low due to high porosity.
- The relatively low amount of illite, low firing temperature and short time of the firing were not sufficient for mullitization and more intensive vitrification.

Acknowledgements This research was supported by the grant VEGA 1/0162/15, VEGA 1/0869/13, project "PROMATECH" ITMS No: 26220220186, and by the Czech Science Foundation, Project No. P105/12/G059.

References

1) V. Das Kshama, B. V. Mohan, M. Lalithambika and C. G. R. Nair, *Ceram. Int.*, 18, 359–364 (1992).
2) J. Hlaváč, "Technology of silicates", SNTL, Praha (1981) [in Czech].
3) B. Čičel, I. Novák and I. Horváth, "Mineralogy and crystallochemistry of clays", SAV, Bratislava (1981) [in Slovak].
4) N. N. Kruglitsky, B. M. Datsenko and B. I. Moroz, *Ceram. Int.*, 18, 78–80 (1984).
5) C. M. F. Vieira, P. R. N. da Silva, F. T. da Silva, J. L. Capitaneo and S. N. Monteiro, *Revista Matéria*, 10, 526–536 (2005).
6) I. Štubňa, A. Trník, F. Chmelík and L. Vozár, "Advances in Ceramics characterization, raw materials, processing, properties, degradation and healing", InTech, Rijeka Croatia (2011) pp. 229–244.
7) A. Trník, I. Štubňa, G. Varga, P. Bačík and R. Podoba, *J. Ceram. Soc. Japan*, 119, 645–649 (2011).
8) T. Húlan, A. Trník, I. Štubňa, P. Bačík, T. Kaljuvee and L. Vozár, *Mater. Sci.-Medzg.*, in press. (2015).
9) S. Klumbach and F. R. Schilling, *Eur. J. Mineral.*, 26, 211–220 (2014).
10) I. Štubňa, A. Trnik, R. Podoba, R. Sokolář and P. Bačík, *J. Ceram. Soc. Japan*, 120, 351–354 (2012).
11) I. Štubňa, A. Trník and L. Vozár, *Ceram. Int.*, 33, 1287–1291 (2007).
12) C. Mahodaran, P. Sutharsan, S. Dhanapadian, R. Venkatachalapathy and R. M. Asanulla, *Appl. Clay Sci.*, 54, 20–25 (2011).
13) A. Haq, Y. Iqbal and M. RiazKahn, *J. Pak. Mater. Soc.*, 3, 77–90 (2009).
14) S. Ferrari and A. F. Gualtieri, *Appl. Clay Sci.*, 32, 73–81 (2006).
15) A. Aras, *Appl. Clay Sci.*, 24, 257–269 (2004).
16) P. M. Velasco, M. P. M. Ortíz, M. A. M. Giró and L. M. Velasco, *Constr. Build. Mater.*, 63, 97–107 (2014).
17) R. Podoba, Ľ. Podobník and A. Trník, *Építőanyag*, 64, 28–29 (2012).
18) I. Štubňa, A. Vážanová, G. Varga and D. Hrubý, Proc. Conf. "Research and teaching of physics on the context of university education", SPU Nitra (2007) pp. 69–74.
19) T. Húlan, A. Trník and I. Štubňa, *Bulletin of the Moscow State Regional University*, 2014, 21–29 (2014).
20) ASTM C 848-88: Standard test method for dynamic Young's modulus, shear modulus and Poisson's ratio for ceramic whiteware by sonic resonance. (published in 1999, Standard Documents, Philadelphia USA).
21) E. Schreiber, O. Anderson and N. Soga, "Elastic constants and their measurement", McGraw-Hill Book Co., New York (1973).
22) I. Štubňa, P. Šín, A. Trník and L. Vozár, *Meas. Sci. Rev.*, 14, 35–40 (2014).
23) A. F. Gualtieri and S. Ferrari, *Phys. Chem. Miner.*, 33, 490–501 (2006).
24) CSN 72 1083: Thermal analyses of ceramic raw materials. (published in 1973, Czechoslovak State Standard) [in Czech].
25) D. L. Carroll, T. F. Kemp, T. J. Bastow and M. E. Smith, *Solid State Nucl. Mag.*, 28, 31–43 (2005).
26) I. Štubňa, A. Trník, P. Šín, R. Sokolář and I. Medveď, *Mater. Tehnol.*, 45, 375–378 (2011).
27) A. Trník, I. Štubňa, G. Varga, M. Keppert and P. Bačík, *Mater. Sci.-Medzg.*, 19, 461–464 (2013).

PRÍLOHA č. 7

ISSN 1392–1320 MATERIALS SCIENCE (MEDŽIAGOTYRA). Vol. 21, No. 3. 2015

Development of Young's Modulus of Illitic Clay during Heating up to 1100 °C

Tomáš HÚLAN [1*], Anton TRNÍK [1,2], Igor ŠTUBŇA [1], Peter BAČÍK [3], Tiit KALJUVEE [4], Libor VOZÁR [1]

[1] *Department of Physics, Constantine the Philosopher University, 94974 Nitra, Slovakia*
[2] *Department of Materials Engineering and Chemistry, Czech Technical University, 16629 Prague, Czech Republic*
[3] *Department of Mineralogy and Petrology, Comenius University, 84215 Bratislava, Slovakia*
[4] *Laboratory of Inorganic Materials, Tallinn Technical University, 190 86 Tallinn, Estonia*

crossref http://dx.doi.org/10.5755/j01.ms.21.3.7152

Received 20 May 2015; accepted 24 July 2014

Young's modulus of green illite from Füzérradvány (Hungary) was measured in-situ in the temperature interval 20 °C – 1100 °C and auxiliary analyses DTA, TG and TDA, XRD and EGA, were also performed. It was found that a removal of the physically bound water (20 °C – 250 °C) sets illite crystals closer, which leads to a significant increase of Young's modulus from its initial value of 7 GPa to the maximum 12 GPa at 300 °C. Young's modulus slightly decreases in the temperature interval of dehydroxylation of illite (300 °C – 800 °C), and which then reaches up to 45 GPa at 1100 °C, increasing exponentially as a consequence of the sintering above 800 °C.
Keywords: illite; Young's modulus; physically bound water; dehydroxylation; sintering.

1. INTRODUCTION

Illite is a significant rock forming mineral that is a main component of illitic clay and soil. Its structure consists of the repetition of tetrahedron – octahedron – tetrahedron (T-O-T) sheets in one layer. The interlayer space is occupied mainly by potassium cations, which are responsible for the absence of swelling. Additionally the variable amounts of water molecules lie between the T-O-T layers [1 – 4].

Illitic clays, also called ball clays, are very often used in the manufacturing of traditional ceramics [5 – 9] and geopolymers [10]. Illite is usually mixed not only with other clays but also with microscopic crystals of carbonates, feldspars, micas and quartz and is very rarely found separately in nature.

Almost pure illite was found in the Füzérradvány location in North-Eastern Hungary [11, 12]. This illite was previously studied in [3 – 5, 11, 13, 14] and in other works. It was specified that this illite is of 1M polytype [3, 4]. According to [11] the illite contains 48.51 mass % of SiO_2, 31.26 mass % of Al_2O_3, 7.85 mass % of K_2O and ~ 4.3 mass % of Fe, Ti, Ca, Mg, Na and S oxides. Loss on ignition is ~ 6.9 mass %. The SEM images show individual grains with highly altered or damaged rim structures. In general, mostly hexagonal grains are separated by fractures with variable widths between 1 and 10 μm. The presence of a minor amount of quartz was seen in the CL images and was also confirmed by XRD [15].

Generally, during heating up to 1200 °C, illite goes through several changes. The first of which is a loss of physically bound water which takes place between room temperature and 300 °C [16, 17]. Because H_2O is bound to T-O-T clay minerals in different ways, the loss of the physically bound water occurs in overlapping temperature intervals. For illite, two DTA endothermic minima were observed in this temperature region [16].

The next process is dihydroxylation, which begins at ~ 450 °C [2, 13, 16 – 18] and is accompanied with mass loss of 5.2 – 5.6 mass % [17] and no shrinking [17 – 19]. It is still not possible to reach a unique definition because there are several possible models of the mechanism reaction of the illite dehydroxylation [13]. An Arrhenius plot showed two slopes which gave two values of the activation energy 697 kJ mol^{-1} (for higher temperatures) and 231 kJ mol^{-1} (for lower temperatures) [13].

Illite peaks in XRD pattern are present during heating up to ~ 950 °C when begin to diminish and disappear at ~ 1050 °C [9, 14, 18]. The high-temperature reactions are accompanied with steep contraction [14, 19] and new phases are formed. A quantitative XRD analysis gave a mineralogical composition of the Füzérradvány body fired at 1080 °C: quartz (1.9 – 7.9 %), Ca-plagioclase (1.2 %), γ-alumina (9.8 – 11.9 %), mullite (4.5 – 5.8 %), K-feldspar (1.2 – 2.1 %), and amorphous phase (75.4 – 77.1 %) [14].

Elastic properties of illite determined by some authors are listed in Table 1 compiled from data given in [20 – 24]. All data in Table 1 were measured at room temperature using green illite samples. The values, with the exception of [23, 24], are calculated for illite without pores.

From the ceramic point of view, some part of illite in the kaolin-based ceramic mixture increases a content of the glassy phase as a consequence of the fluxing action of K_2O [5, 6] and decreases the firing temperature [25]. Increasing content of illite in such mixtures results in a decrease of mullite, cristobalite and quartz in the fired products [5]. Illite continues to expand up to the sintering and the shrinkage starts at the same time as vitrification. In this temperature range, the mechanical strength rapidly increases and the material becomes plastic. This is a reason why illite (or illitic clay) is preferred for a fast firing [19].

* Corresponding author. Tel.: +421-37-6408623; fax: +421-37-6408556.
E-mail address: *tomas.hulan@ukf.sk* (T. Hulan)

Table 1. Isotropic elastic modulus [GPa] and Poisson's ratio of illite

	Bulk modulus (K)	Shear modulus (G)	Young's modulus (E)	Poisson's ratio (μ)
[20]	60.1	25.3	66.6 [1]	0.316 [2]
[21]	60.2	25.4	66.8 [2]	0.315 [2]
[22]	62.2	25.7	67.8 [1]	0.319 [2]
[23]	6-12 [3]	4-6 [3]	10-15 [1]	-
[24]	-	-	10-15 [1]	-

[1] calculated from K and G as $E = 9KG/(3K+G)$,

[2] calculated from G and E as $\mu = (E/2G) - 1$,

[3] for clay generally.

As follows from the references [1–4, 13, 18], the main focus of the previous research was the structure of illite, its reactions to dehydroxylation and high temperature. The mechanical properties of illite during heating remain unknown. The aim of this work is experimental study of the elastic properties of illite measured in-situ during heating.

2. EXPERIMENTAL

Samples

Samples made from raw illite, supplied from the mine in Füzérradvány, were used for thermal analyses DTA, TG, TDA and mf-TMA (modulated-force thermomechanical analysis) during heating. The composition of illitic clay, as given by a supplier [25], is shown in Table 2.

Table 2. The chemical composition of illite from Füzérradvány, Hungary (in mass %)

SiO_2	Al_2O_3	Fe_2O_3	TiO_2	CaO	MgO	K_2O	Na_2O	L.O.I.
58.0	24.0	0.6	0.05	0.38	1.70	7.85	0.10	7.3

The raw illite, which was in pieces of 0.2–3 cm, was firstly crushed and then sieved to obtain a powder with particles not larger than 0.1 mm. Then 750 g of the powder were mixed with 250 g of the distilled water to obtain a plastic mass. Cylindrical samples were made from this mass with a laboratory extruder. After open air free drying, the samples contained ~ 3 mass % of the physically bound water and their diameter was ~ 11 mm.

A heating rate (5 °C min^{-1}) was the same for all thermal analyses. The green samples were heated in the air from room temperature up to 1100 °C, which is the presumptive highest firing temperature used in industries for building clay ceramics.

Modulated-force thermomechanical analysis (mf-TMA)

Modulated-force thermomechanical analysis, based on free vibration of the sample in a fundamental flexural mode, was used for a measurement of Young's modulus on the cylindrical samples with initial dimensions ∅ 11 × 120 mm during heating from 20 °C to 1100 °C with a rate of 5 °C min^{-1}. The vibrations were excited with an electromagnetic impactor and detected with a microphone. A resonant frequency of the vibrations was obtained using the fast Fourier transformation. The resonant frequency f, the length l, diameter d, and the mass m of the sample were used for calculating E according to [26, 27]. Since the ratio length/diameter = 10.9 < 20, the value of E must be multiplied with a correction coefficient T_{1c} = 1.04402 (calculated for a circular cross-section and Poisson's ratio μ = 0.3). Young's modulus at the temperature t is

$$E = 1.6774 \frac{m_0 l_0^3}{d_0^4} \frac{[1 + \Delta m(t)/m_0]}{[1 + \Delta l(t)/l_0]} f^2(t), \qquad (1)$$

where $\Delta l(t)/l_0$, $\Delta m(t)/m_0$, are relative linear thermal expansion and relative mass change of the sample measured by dilatometer and TG analyzer respectively. Deriving Eq. (1), the equal relative expansion of the sample in both directions, axial and radial, was presumed. The values l_0, d_0, m_0 are the initial length, diameter, and mass of the sample at room temperature, respectively, and $f(t)$ is the resonant frequency at the temperature t.

Differential thermal analysis (DTA), thermogravimetry (TG) and thermodilatometric analysis (TDA)

As follows from Eq. (1), the determination of E requires measuring the actual dimensions and mass of the sample during heating. This task is done by TD and TG analyses. Given the relative expansion $\Delta l(t)/l_0$, as measured by the dilatometer, and the initial dimensions l_0, d_0, the true length $l(t)$ and diameter $d(t)$ of the sample were calculated. Similarly, the true mass $m(t)$ was determined from the relative mass change $\Delta m(t)/m_0$ measured with TGA/DTA analyzer Derivatograph 1000 [28].

To reduce the temperature shift between TG, DTA, TDA and mf-TMA curves, the samples for these analyses had the same cross-section. The sample dimensions were ∅ 11 × 40 mm for TDA and ∅ 11 × 20 mm for TG and DTA. A reference compact sample for DTA had the dimensions of ∅ 11 × 20 mm and was made from pressed Al_2O_3 powder.

X-ray diffractometry (XRD) analysis

The XRD analysis of the powder samples was performed with the diffractometer BRUKER D8 Advance with Cu anticathode ($\lambda\alpha_1$ = 1.5406 Å), accelerating voltage 40 kV and beam current 40 mA. Data was obtained with the BRUKER LynxEye detector. The Rietveld method was used for a quantitative XRD analysis.

Evolved gas analysis (EGA)

The evolved gas analysis was performed on a powder sample (50 mg) using Setaram LabSys 1600 thermoanalyzer coupled with Pfeiffer Omnistar Mass Spectrometer in the atmosphere 79 % of Ar + 21 % of O_2 with flow rate of 60 ml min^{-1}.

Porosity

The porosity was calculated with the help of experimentally determined bulk density and matrix density. The bulk density was obtained by means of size and weight measurements of cylindrical samples. The matrix density was measured by the helium pycnometry (Pycnomatic ATC, Porotec).

3. RESULTS AND DISCUSSION

The results of the quantitative XRD analysis conducted at room temperature for the green sample and the samples fired at the temperatures 650 °C, 750 °C and 1100 °C are given in Table 3. The green sample contains illite as a main phase with an addition of 12 mass % of quartz and small amounts of montmorillonite and K-feldspar orthoclase. As the firing temperature increases, the amount of illite decreases, while the amount of muscovite and amorphous phase increases. In the sample fired at 1100 °C, no phyllosilicates are observed. The sum of parts of illite, muscovite and amorphous phase is approximately constant (80 mass % for the green sample, 80 mass % for the sample fired at 650 °C, 82 mass % for the sample fired at 750 °C and 79 mass % for the sample fired at 1100 °C). The transformation of illite at higher temperatures can be a source of muscovite [29]. The cause of the amorphous phase in the samples fired at 650 °C and 750 °C is probably also due to thermal changes of illite/muscovite. The amorphous phase in the sample fired at 1100 °C is a glassy phase. K-feldspar (orthoclase and sanidine) withstands thermal treatment and does not create the glassy phase. Mullite is also created at the highest firing temperature.

Table 3. Mineral composition of the samples in mass %

	green	650 °C	750 °C	1100 °C
Illite	80	69	34	0
Montmorillonite	4	3	4	0
Muscovite	0	7	35	0
Quartz	12	12	11	11
Orthoclase	4	5	4	2
Sanidine	0	0	0	4
Mullite	0	0	0	4
Amorphous	0	4	13	79

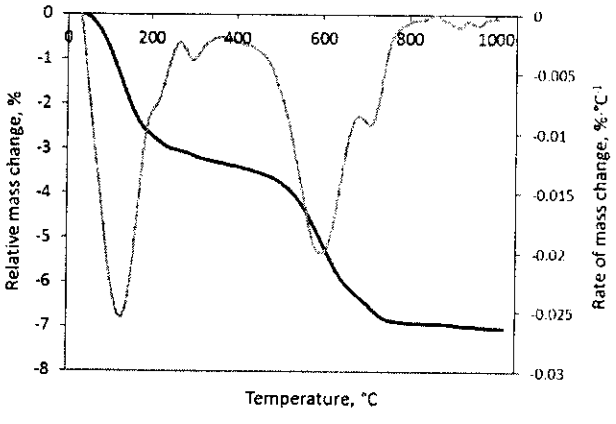

Fig. 1. Thermogravimetry of illite, TG (black line) and DTG (gray line)

The results of thermogravimetric analysis (Fig. 1.) show three steps of the decrease of the sample mass. The first step is a result of the physically bound H_2O escaping (between 20 °C and 300 °C) which occurs in two overlapping processes. The escaping of the physically bound water occurs in two overlaying processes. The first of them, which is more intensive, reaches the maximum rate at ~ 120 °C and the second one at ~ 215 °C. According to [2], a mass loss with small minimum at ~ 300 °C in the DTG curve is related to dehydration when H_2O molecules located in K-free sites of the illite interlayers are removed.

The second step is a release of the constituent water (between 400 °C and 800 °C). A dehydroxylation of illite runs in two steps which reach the maximum rate at the temperatures ~ 600 °C and ~ 700 °C being in accordance with the results showed in [13].

The results of TG are supported with the mass spectrometry (EGA) where an emission of H_2O and CO_2 were measured, see Fig. 2. EGA showed that H_2O is emitted at three clearly separate temperature intervals. The first two, which are connected with the physically bound water, are also registered in DTG and DTA curve where two overlaid processes are expressed with one intensive minimum at ~ 150 °C and one shoulder at ~ 230 °C. The dehydroxylation of illite is registered by EGA between 350 °C and 700 °C as a two-step process which is an agreement with results of TG and DTA. According to EGA, the emission of the small amount of CO_2 is also present and is caused by the burning of the organic matter in illite clay.

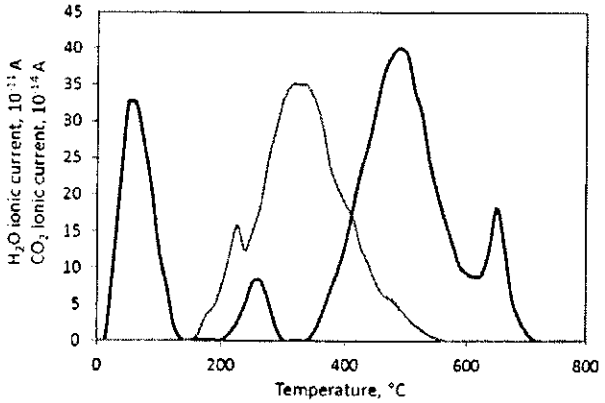

Fig. 2. Mass spectrometric results for escaping gases H_2O (black line) and CO_2 (gray line)

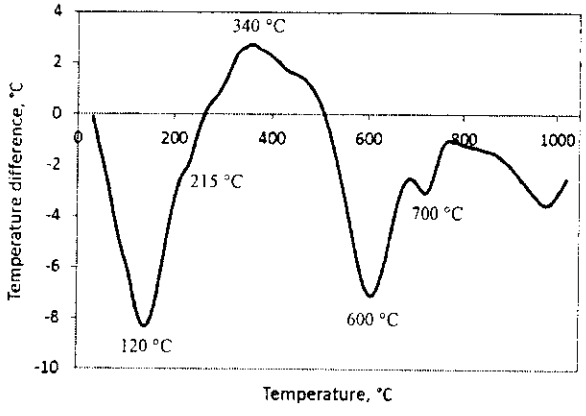

Fig. 3. DTA curve of illite

Since these processes are linked with the absorption of heat, they are represented three clear endotherms in the DTA curve with minima at 120 °C, 600 °C and 700 °C and two shoulders at ~ 215 °C and ~ 300 °C, see Fig. 3. Besides that, there is an absorption of heat above 800 °C which results in a change of metaillite into a disordered

structure and also a vitrification of the sample. An exotherm with maxima at ~ 340 °C in DTA curve is caused by the thermooxidation of organic matter.

The results of TDA in the temperature interval between 20 °C and 1100 °C are depicted in Fig. 4, where the interval between 20 °C and 400 °C is enlarged. The sample slightly expands its volume from room temperature up to ~ 500 °C (coefficient of the linear thermal expansion CLTE is ~ 1×10^{-5} K^{-1}) where the dehydroxylation starts. During the dehydroxylation, the expansion becomes faster and after its completion, the expanding continues with CLTE ~ 1×10^{-5} K^{-1} up to the temperature of 900 °C. TDA also confirms two-step dehydroxylation of illite via two maxima of the CLTE, the first of them is at ~ 600 °C and the second is at ~ 700 °C. This correlates with TG and DTA. Above 900 °C, the TDA curve begins to bend downwards as a result of the sintering and vitrification [19]. Besides that, above 800 °C metaillite began to change into a disorder structure. At ~ 1100 °C, the layer structure of metaillite had been destroyed, and amorphous SiO_2 and mullite crystallite appeared [18]. These structural changes also led to the contraction of the sample. The TDA curve of the fired sample, Fig. 4, confirms a small amount of quartz via small step around 570 °C. The presence of the glassy phase exhibits itself as a contraction above 1000 °C caused by the press of the dilatometer's push-rod on the softened sample.

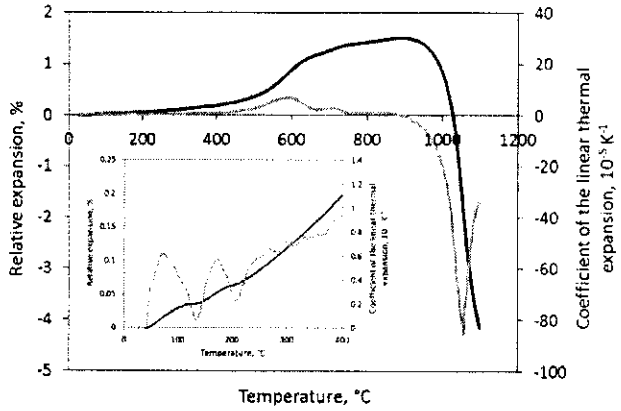

Fig. 4. Relative expansion (black line) and coefficient of the linear thermal expansion (gray line) of illite. The inset shows the interval 20 – 400 °C in greater details

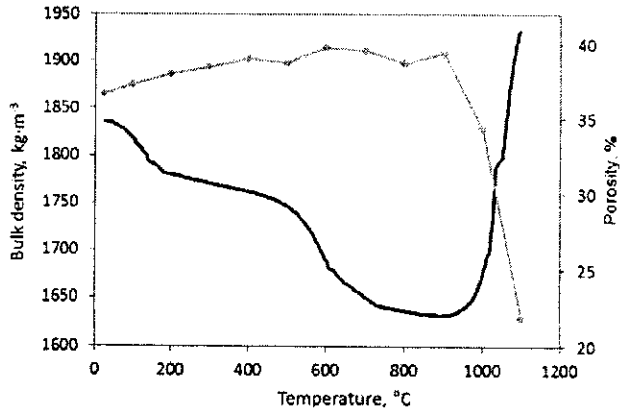

Fig. 5. Bulk density (black line) and porosity of illite (gray line)

Since E is proportional to a bulk density, which follows from Eq. (1), we derived this quantity from results of TG and TDA (Fig. 5.). The bulk density is determined with the mass loss up to 700 °C, which reaches ~ 7 mass % while the thermal expansion is only 1.4 %. Above 700 °C, the sample mass becomes constant and the bulk density is determined through the thermal contraction only. The contraction is caused by the sintering as noted above.

We also measured the porosity. The obtained results in Fig. 5 show that the porosity of the samples increases up to the firing temperature of 600 °C. Then a mild decrease of the porosity occurs for the samples fired at 700 °C and 800 °C followed by steep decrease of the porosity of samples fired at 1000 °C and 1100 °C, the decrease in the porosity being 17 %.

The relationship between E, which was calculated by Eq. (1), and the temperature t is depicted in Fig. 6. The first interval, which characterizes a dehydratation at low temperatures up to ~ 300 °C, is typical for samples made from clay materials. We obtained similar pictures for samples made from green electroporcelain mixtures, as well as from kaolin and illitic brick clays [30 – 32]. E of the samples, which had an equilibrium moisture 1 – 2 mass% after drying for a long time in the open air, is very sensitive to the loss of this water when the H_2O molecules escape from faces of the illite crystals. This process makes contacts between the crystals tighter which leads to an improvement of the elastic properties. The crystals are held together by ionic forces which are stronger when the crystals are drawn into intimate contact by the departing water films [33]. When we compare the results of mf-TMA and TDA in this low-temperature interval, we find that E of the sample increases while its volume also increases contrary to theoretical expectation which states that E is inversely proportional to the thermal expansion. We can conclude that the elastic behavior is much more influenced by properties of the boundaries between crystals than their interiors.

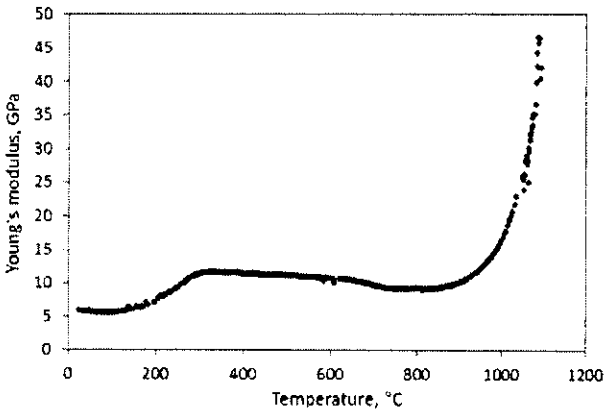

Fig. 6. Young's modulus of illite

No phase change takes place between the end of dehydration and the start of dehydroxylation. The linear decrease of E is caused by the weakening of the interatomic forces because the temperatures are too low for sintering. There is a good correlation with TDA results in the same temperature interval.

Above 500 °C, the dehydroxylation of illite that begins is accompanied with mass change (Fig. 1.) and thermal expansion (Fig. 4.). Dehydroxylation is reflected in E as a decrease of its values (Fig. 6.). It can be caused by the microporosity which results from simultaneous

increase of the volume of the sample and a decrease of its mass. It also leads to lesser values of the bulk density above 500 °C (Fig. 5.). But E does not decrease as dramatically as the bulk density does between 500 °C and 700 °C. In spite of the expected weakening of the metaillite crystals, E decreases only slightly. It also refers to a main role of the contacts between crystals which seems to be more important than mechanical properties of the crystals. And, finally, E exponentially increases due to sintering above 800 °C. This fact is also confirmed with TDA results.

4. CONCLUSIONS

Young's modulus of green illite from Füzérradvány (Hungary) was measured in the temperature interval 20 °C – 1100 °C and auxiliary analyses DTA, TG and TDA, XRD and EGA, were also performed. We found that:

- A removal of the physically bound water (20 °C – 250 °C) sets illite crystals closer, which leads to a significant increase of Young's modulus.
- In the next section, between the end of the escape of the physically bound water and the start of the intensive sintering (300 °C – 800 °C), the Young's modulus slightly decreases. Dehydroxylation does not significantly influence the development of Young's modulus.
- Young's modulus exponentially increases above 800 °C as a consequence of the sintering.

Acknowledgement

This work was supported by the grant VEGA 1/0646/12 from the Ministry of Education of the Slovak Republic and by the Czech Science Foundation under the project No. P105/12/G059. The authors are indebted to J. Biber from Inter-ILI Engineering Office (Hungary) for a supply of illite.

REFERENCES

1. **Stixrude, L., Peacor, D. R.** First-Principles Study of Illite-Smectite and Implications for Clay Mineral Systems *Nature* 420 2002: pp. 165 – 168.
2. **Drits, V. A., McCarty, D. K.** The Nature of Structure-Bonded H_2O in Illite and Leucophyllite from Dehydration and Dehydroxylation Experiments *Clay and Clay Minerals* 55 (1) 2007: pp. 45 – 58.
3. **Ferrari, S., Gualtieri, A. ., Grathoff, G.H., Leoni, M.** Model of Structure Disorder of Illite: Preliminary Results *Zeitschrift für Kristallographie Supplements* 23 (1) 2006: pp. 493 – 498
4. **Gualtieri, A. F., Ferrari, S., Leoni, M., Grathoff, G. H., Hugo, R., Shatnawi, M. T. M., Paglia, G., Billinge, S.J. L.** Structural Characterization of the Clay Mineral Illite-1M *Journal of Applied Crystallography* 41 2008: pp. 402 – 415. http://dx.doi.org/10.1107/S0021889808004202
5. **Ferrari, S., Gualtieri, A. F.** The Use of Illitic Clays in the Production of Stoneware Tile Ceramics *Applied Clay Science* 32 (1-2) 2006: pp. 73 – 81.
6. **Wattanasiriwech, D., Wattanasiriwech, S.** Fluxing Action of Illite and Microcline in a Triaxial Porcelain Body *Journal of the European Ceramic Society* 31 (8) 2011: pp. 1371 – 1376.
7. **Aras, A.** The Change of Phase Composition in Kaolinite- and Illite-Rich Clay-Based Ceramic Bodies *Applied Clay Science* 24 (3-4) 2004: pp. 257 – 269. http://dx.doi.org/10.1016/j.clay.2003.08.012
8. **Sedmale, G., Korovkins, A., Seglins, V., Lindina, L.** Application of Chemically Treated Illite Clay for Development of Ceramic Products *2nd International Conference on Competitive Materials and Technological Processes IOP Conf. series: Materials Science and Engineering* 47 2013: 012056.
9. **Escalera, E., Antti, M.L., Odén, M.** Thermal Treatment and Phase Formation in Kaolinite and Illite Based Clays from Tropical Regions of Bolivia *6th EEIGM International Conference on Advanced Materials Research IOP Conf. Series: Materials Science and Engineering* 31 2012: 012017.
10. **Buchwald, A., Hohmann, M., Posern, K., Brendler, E.** The Suitability of Thermally Activated Illite/Smectite Clay as Raw Material for Geopolymer Binders *Applied Clay Science* 46 (3) 2009: pp. 300 – 304.
11. **Pécskay, Z., Molnár, F., Itaya, T., Zelenka, T.** Geology and K-Ar Geochronology of Illite from the Clay Deposit at Füzérradvány, Tokaj mts., Hungary *Acta Mineralogica-Petrographica* 46 2005: pp. 1 – 7.
12. **Viczian, I.** Hungarian Investigation on the "Zempleni" Illite *Clays and Clay Minerals* 45 (1) 1997: pp. 114 – 115. http://dx.doi.org/10.1346/CCMN.1997.0450114
13. **Gualtieri, A. F., Ferrari, S.** Kinetics of Illite Dehydroxylation *Physics and Chemistry of Minerals* 33 (7) 2006: pp. 490 – 501. http://dx.doi.org/10.1007/s00269-006-0092-z
14. **Ori, R.** The Mineralogical and Technological Characterization of Illite from Füzérradvány (Hungary) as a Raw Material for Traditional Ceramics *PhD thesis, University of Modena and Emilia Region, Modena* 2003 (in Italian).
15. **Gucsik, A., Ninagawa, K., Nishido, H., Okumura, T., Bidló, A., Kovács, G., Heil, B., Patocskai, Z.** Cathodoluminiscence Microcharacterization of Illite from Füzérradvány, NE Hungary *Acta Mineralogica-Petrographica, Abstract series* 5 2006: p. 36.
16. Czechoslovak State Standard CSN 72 1083: *Thermal Analyses of Ceramic Raw Materials.*
17. **Schomburg, J., Zwar, H.** Thermal Differential Diagnosis of Mica Mineral Group *Journal of Thermal Analysis* 48 (1) 1997: pp. 135 – 139.
18. **Liu, X., Li, H., Hu, Y., Yi, D., Wang, J.** Phase Changes During Heating of Illite *TMS Annual Meeting*, San Antonio, Texas, USA 2006: pp. 309 – 316.
19. **Venturelli, C., Paganelli, M.** Sintering Behaviour of Clays for the Production of Ceramics *Ceramic Forum International Ber. DKG* 84 (5) 2007: pp. E1 – E3.
20. **Wang. Z., Wang, H., Cates, M.** Effective Elastic Properties of Solid Clays *Geophysics* 66 (2) 2001: pp. 428 – 440.
21. **Bayuk, I. O., Ammerman, M., Chesnokov, E. M.** Elastic Moduli of Anisotropic Clay *Geophysics* 72 (5) 2007: pp. D107 – D117.
22. **Katahara, K. W.** Clay Mineral Elastic Properties *66th SEG Annual International Meeting* Expanded Abstracts, Denver, Colorado, USA 1996: pp. 1691 – 1694.
23. **Vanorio, T., Prasad, M., Nur, A.** Elastic Properties of Dry Clay Mineral Aggregates, Suspensions and

Sandstones *Geophysical Journal International* 155 (1) 2003: pp. 319–326. http://dx.doi.org/10.1046/j.1365-246X.2003.02046.x

24. **Prasad, M., Kopycinska, M., Rabe, U., Arnold, W.** Measurement of Young's Modulus of Clay Minerals Using Atomic Force Acoustic Microscopy *Geophysical Research Letters* 29 (8) 2002: pp. 13-1 – 13-4.
25. *A Short Description of the Mining of Illite in Hungary.* Inter-ILI Mérnöki Iroda, Kosd, Hungary, 2012.
26. ASTM E1876-09: *Standard Test Method for Dynamic Young's Modulus, Shear Modulus and Poisson's Ratio by Impulse Excitation of Vibration*, ASTM International, West Conshohocken, PA, 2009.
27. ASTM C848-88: *Standard Test Method for Dynamic Young's Modulus, Shear Modulus and Poisson's Ratio for Ceramic Whiteware by Sonic Resonance*, ASTM International, West Conshohocken, PA, 2011.
28. **Podoba, R., Trník, A., Podobník, Ľ.** Upgrating of TGA/DTA Analyzer Derivatograph *Építőanyag* 64 (1-2) 2012: pp. 28–29.
29. **Gharrabi, M., Velde, B., Sagon, J. P.** The Transformation of Illite to Muscovite in Pelitic Rocks: Constraints from X-Ray Diffraction *Clays and Clay Minerals* 46 (1) 1998: pp. 79–88. http://dx.doi.org/10.1346/CCMN.1998.0460109
30. **Štubňa, I., Trník, A., Vozár, L.** Thermomechanical and Thermodilatometric Analysis of Green Alumina Porcelain *Ceramics International* 35 (3) 2009: pp. 1181–1185.
31. **Štubňa, I., Šín, P., Trník, A., Veinthal, R.** Mechanical Properties of Kaolin During Heating *Key Engineering Materials* 527 2013: pp. 14–19. http://dx.doi.org/10.4028/www.scientific.net/KEM.527.14
32. **Štubňa, I., Trník, A., Podoba, R., Sokolář, R., Bačík, P.** Elastic Propertis of Waste Calcite-Clay Ceramics During Firing *Journal of the Ceramic Society of Japan* 120 (1) 2012: pp. 351–354.
33. **McPhee, K. H.** An Introduction to Inorganic Dielectrics *IRE Transact. Component Parts* 6 (1) 1959: pp. 3–33. http://dx.doi.org/10.1109/TCP.1959.1136271

Advanced Materials Research Vol. 1126 (2015) pp 53-58
© (2015) Trans Tech Publications, Switzerland
doi:10.4028/www.scientific.net/AMR.1126.53

Submitted: 2015-03-21
Accepted: 2015-04-22

PRÍLOHA č. 8

The Influence of Texture and Firing on Thermal and Elastic Properties of Illite-Based Ceramics

Daniel Antal[1, a], Tomáš Húlan[1, b *], Anton Trník[1, 2, c], Igor Štubňa[1, d], and Ján Ondruška[1, e]

[1]Department of Physics, Faculty of Natural Science, Constantine the Philosopher University, A. Hlinku 1, 94974 Nitra, Slovakia

[2]Department of Materials Engineering and Chemistry, Faculty of Civil Engineering, Czech Technical University, Thakurova 7, 16629 Prague, Czech Republic

[a]antal@fnnitra.sk, [b]tomas.hulan@ukf.sk, [c]atrnik@ukf.sk, [d]istubna@ukf.sk, [e]jondruska@ukf.sk

*corresponding author

Keywords: illite, texture, dimension changes, Young modulus, thermal diffusivity, firing, ceramics.

Abstract. The texture in illite-based ceramics was introduced by spreading a large number of thin layers of a wet plastic mass one on top of the other. The basal planes of the plate-like illite crystals are predominantly oriented parallelly with the direction of spreading. The samples were fired at different temperatures ranging from room temperature up to 1100 °C with a heating rate of 5 °C/min, then freely cooled and measured at room temperature. We determined Young modulus (E), thermal diffusivity (a) and relative dimension changes ($\Delta l/l_0$) in two directions: parallelly to the basal planes (a subscript ||) of the illite crystals and perpendicularly to these planes (a subscript ⊥). It was found that the ratio $E_{||} / E_{\perp} \approx 2.9$ and $a_{||} / a_{\perp} \approx 2.0$ up to 900 °C. Above 900 °C, the values of E and a increase due to sintering, and the differences between the values measured in the two directions decrease. In the case of the thermal diffusivity these differences do not disappear even after firing at the temperature of 1200 °C.

Introduction

Various clay minerals which are the main components of traditional ceramics (such as kaolinite, illite, montmorillonite, and chlorite) have a layered structure and their crystals have a plate-like shape with anisotropic properties. If a clay body is formed under certain conditions, such as sedimentation and consolidation, the clay body becomes anisotropic [1]. Clay crystals rotate normal to an axial load. This results in the development of anisotropic physical properties [2].

The texture is found in clay ceramics prepared from a wet plastic mass using a potter wheel [3]. It can be also created by friction forces during manufacturing electroporcelain blanks in a vacuum extruder. A well-developed textured layer with the thickness of 2 – 4 mm is located on the surface of the blank [4-6]. The modulus of elasticity and mechanical strength of these samples were described in [7]. It was also found that the texture rotates the polarization plane of an electromagnetic wave [8, 9]. The investigation of mechanical properties of quartz porcelain showed that Young modulus and the mechanical strength retain their difference in the two directions during firing and even after firing at 1320 °C [7].

As follows from [4-10], the texture and its impact on different physical properties have been studied mainly on kaolin and kaolin-based ceramics. It seems that similar research has not been conducted on illitic samples, or it is very rare. The goal of this study is an investigation of the texture in illit-based ceramic samples by observing the anisotropy of their thermophysical and mechanical properties as a function of the firing temperature.

Experimental

Textured samples were made from raw illite supplied from the mine in Füzérradvány, Hungary. The chemical composition of illitic clay, as given by the supplier, is shown in Table 1.

Table 1: The chemical composition (in wt.%) of illite from Füzérradvány, Hungary

SiO_2	Al_2O_3	Fe_2O_3	TiO_2	CaO	MgO	K_2O	Na_2O	L.O.I.
58.0	24.0	0.6	0.05	0.38	1.70	7.85	0.10	7.3

The raw illite, which was in pieces of 0.2 – 3 cm, was crushed, milled and then sieved to obtain a powder with particles not larger than 0.1 mm (see the granulometric distribution in Fig. 1). The texture occurs especially due to the part of the material with particle sizes below 2 μm composed of plate-like illite crystals. To obtain a plastic mass, 750 g of the powder was mixed with 250 g of distilled water. Thin layers of the plastic mass were repeatedly spread one on the other with a metal sheet to get textured body of the total thickness 12 cm (see Fig. 2). The friction between the metal sheet and wet plastic mass makes the *c*-axes of the plate-like illite crystals to lie perpendicularly to the direction of the spreading. The technique which includes friction creates the texture that can be confirmed by XRD [4]. The samples were cut from the body, then dried and the surfaces of the dry samples were abraded.

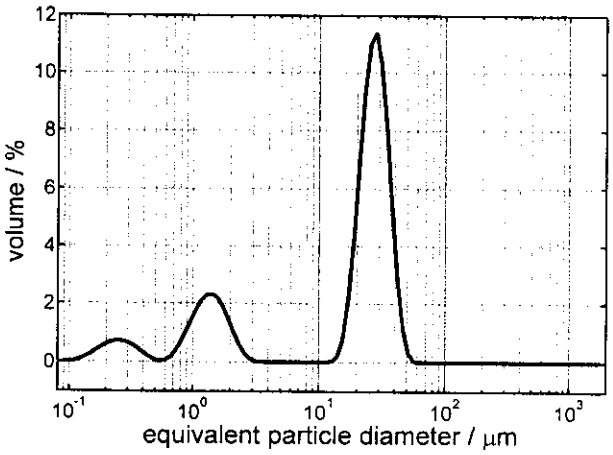

Fig. 1: The granulometric distribution of illite powder

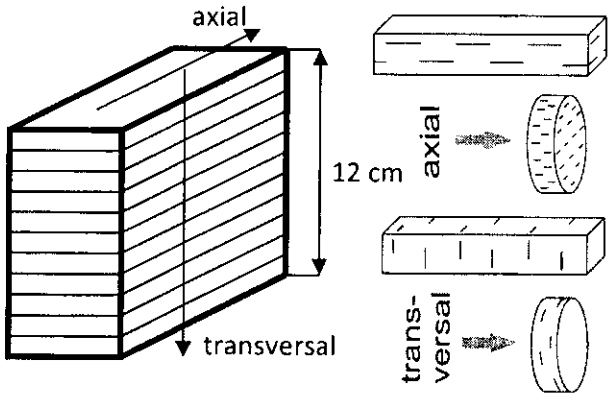

Fig. 2: Textured body made from layers (~1.6 mm thick) and samples used for analyses

To determine the Young modulus E and the relative expansion after firing, we used samples with the initial dimensions ~10×10×120 mm. These samples were cut out from a textured body in two ways as follows. First, long edges of the samples were parallel to the *axial* direction – the texture of these samples is referred to as axial and the corresponding measured quantities have a subscript "$\parallel$". Second, long edges of the samples were parallel to the *transversal* direction – the texture of these samples is referred to as transversal and the corresponding measured quantities have a subscript "$\perp$". To determine the thermal diffusivity, we prepared disc samples (∅12.5×2.5 mm) in axial and transversal direction (see Fig. 2). For each measurement we used five samples with the same texture orientation.

The samples were fired at the temperatures between 100 °C and 1200 °C with a 5 min soaking at the selected temperature. Heating and cooling rate were the same, 5 °C/min. After cooling, the relative expansion, Young modulus and the thermal diffusivity were determined from the measurements at room temperature.

Illite changes its composition and structure when it is heated. To know the processes induced by heat and their temperature intervals, thermal analyses TG and DTA were performed using TG/DTA analyzer Derivatograph 1000 [11].

The relative linear expansion after firings at selected temperatures was determined as $(l - l_0)/l_0$ where l is the length of the sample after firing and l_0 is the length of the green sample.

We used an impulse excitation technique to determine the resonant frequency of longitudinal vibrations [12]. The resonant frequency f, length of the sample l and bulk density ρ (determined from dimensions and mass) were used to calculate Young modulus E as

$$E = 4l^2 f^2 \rho . \quad (1)$$

The thermal diffusivity was measured by the flash method on an apparatus Netzsch LFA 427 Laserflash in a static air atmosphere. A radiation model with pulse correction was used for the signal analysis [13]. Before each measurement the samples were coated with a graphite spray.

The standard deviation of the ratio of the axial vs. transversal quantity X was calculated as $\sqrt{\Delta X_{\parallel}^2 / X_{\perp}^2 - (X_{\parallel}^2 . \Delta X_{\perp}^2) / X_{\perp}^4}$, where $\Delta X_{\parallel}$ and $\Delta X_{\perp}$ are the standard deviations of the quantity measured in axial and transversal direction, respectively.

Results and discussion

According to XRD, the green sample contains 80% of illite, 12% of quartz, 4% of montmorillonite and 4% of orthoclase. As the firing temperature increases, the content of illite decreases, while the contents of muscovite and amorphous phase increase. In the sample fired at 1100 °C, 79% of the amorphous phase, 6% of feldspar and 4% of mullite are observed [14].

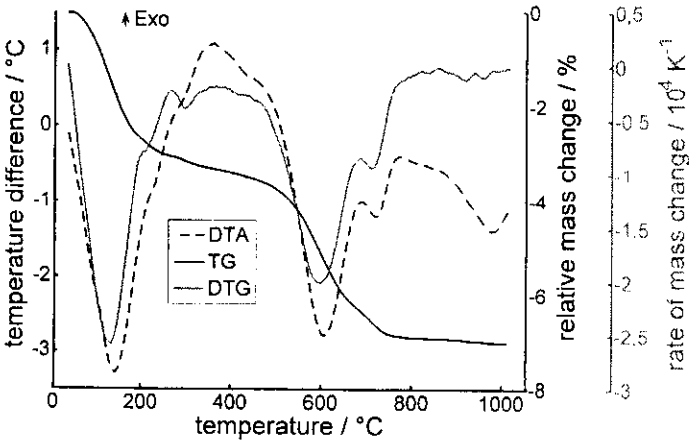

Fig. 3: The thermal analyses of illite; TG (black line), DTG (gray line) and DTA (dashed line)

The results of TG, DTG and DTA (see Fig. 3) show several steps in a decrease of the sample mass due to removing of physically and chemically (constituent) bound water. Removing of physically bound water occurs in two overlaying processes. The first one is more intensive and reaches a maximal rate at ~120 °C, while the second one at ~215 °C. A small minimum at ~300 °C is visible on the DTG curve. According to [15], this weight loss is related to dehydration when H_2O molecules located in the illite interlayers are removed. Further mass loss is a consequence of releasing of the constituent water (between 400 and 800 °C), called dehydroxylation. The dehydroxylation of illite runs in two steps that reach a maximal rate at the temperatures ~600 °C and ~700 °C, respectively.

Besides removing of water, escape of a small amount of CO_2 is also present. It is caused by burning of organic compound in illite clay [14].

Since these processes are connected with consumption of heat, they are represented in the DTA curve as three clear minima (at 120 °C, 600 °C and 700 °C) and two small minima at ~215 °C and ~300 °C. Besides these processes, there is consumption of heat above 800 °C corresponding to vitrification of the sample. In this temperature range there is also a change of metaillite (illite after dehydroxylation) into a disordered structure and the creation of new phases.

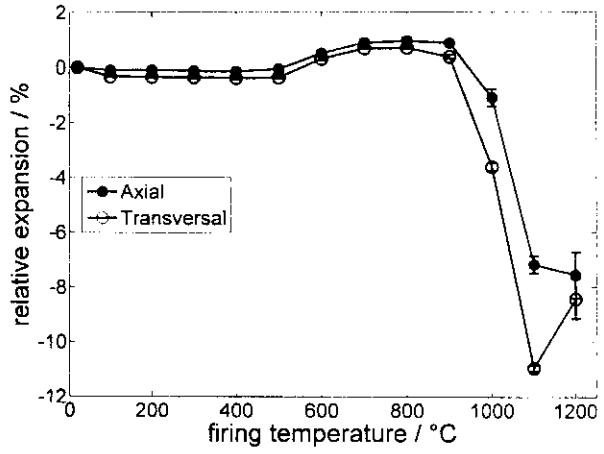

Fig. 4: Relationship between relative expansion and firing temperature for the sample along the axial direction (•) and transversal direction (o)

The results of the relative expansion as a function of the firing temperature are given in Fig. 4. After drying of the samples (temperature >200 °C), we observe a small difference (~0.2%) between the relative expansions of the textured bodies in the axial and transversal directions.

This small difference is probably caused by a presence of water absorbed in the interlayer spaces of illite lattice before drying. Consequently, we may expect more intensive contraction in the transversal direction after the removing of water molecules during drying of the sample. Thermal treatment of illite samples in the dehydroxylation region (500 – 800 °C) changes the structure of illite irreversibly, which at room temperature results also in changes of dimensions. Nevertheless, the difference between the relative expansions in different directions stays approximately the same. From this result we can conclude that under the influence of dehydroxylation the crystals of illite are expanded equally to all directions. The relative contraction of the samples measured along the transversal direction becomes larger than the contraction in the axial direction above 800 °C when sintering and vitrification influence the structure significantly. Dehydroxylation disrupts octahedral layer, and therefore the shrinkage in the transversal direction is more intensive above 800 °C. A significant difference between behaviors of these two samples is observed at the highest temperatures. The shrinkage in the axial direction continues to increase, while the shrinkage in the transversal direction turns into expansion. Such behavior, i.e., the change of the contraction into expansion at high temperatures, is explained by a creation of the closed pores filled with a gas in the original material [16]. This explanation, in our case, requires an assumption of the creation of elongated pores parallel to the transversal direction.

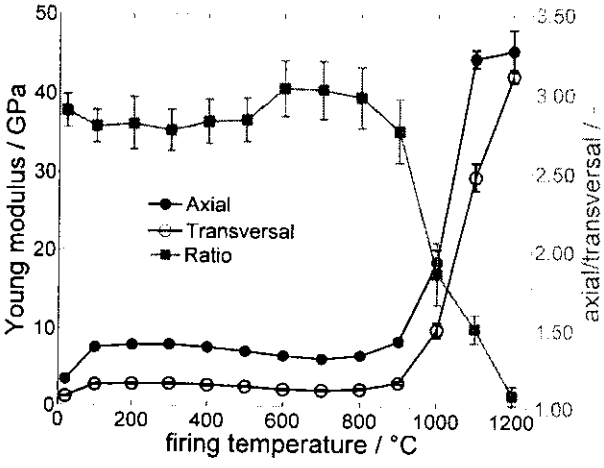

Fig. 5: Relationship between Young modulus and firing temperature for the sample measured along the axial direction (•) and transversal direction (o)

Young modulus (see Fig. 5) shows a clear difference between its values in two directions: (1) along the axial direction (i.e., parallely with the basal planes of the illite crystals) and (2) along the transversal direction (i.e., perpendicularly to the basal planes of the illite crystals). We get $E_{\parallel} \approx 2.6E_{\perp}$ at the temperatures up to 900 °C. The dehydroxylation causes a decrease of Young modulus. We can also observe that the decrease of E is more significant in the transversal direction. At the temperatures above 900 °C an intensive increase of E is observed. The reason is solid state sintering followed by liquid phase sintering. The investigated samples contain ~80 % of the amorphous (glassy) phase after firing at 1100 °C. The values E in Fig. 5 are close to those for glass.

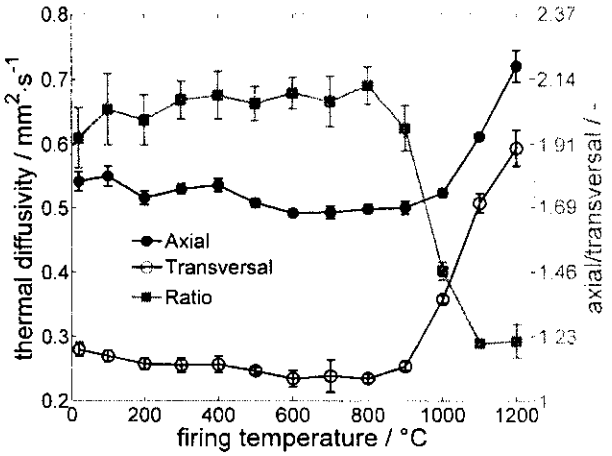

Fig. 6: Relationship between thermal diffusivity and firing temperature for the sample measured along the axial direction (•) and transversal direction (o)

The thermal diffusivity (see Fig. 6) was also measured in the two directions with respect to texture orientation. Thermal flow passed parallelly to the basal planes of illite crystals or perpendicularly to the basal planes. The plot of the relationship between the thermal diffusivity and firing temperature is quite similar to Fig. 5. The thermal diffusivity keeps low values up to firing at the temperature 800 °C, and we have $a_{\parallel} \approx 2a_{\perp}$. Then, these values increase due to sintering and the difference between them in axial and transversal direction decreases.

Conclusions

Illite-based samples with texture were fired at different temperatures ranged from room temperature up to 1200 °C and were then cooled to room temperature and measured. We determined Young modulus (E), the thermal diffusivity (a) and the relative dimension changes ($\Delta l/l_0$) in two directions: parallel to the basal planes of the illite crystals and perpendicular to these planes. It was found that $E_{\parallel} / E_{\perp} \approx 2.9$ and $a_{\parallel} / a_{\perp} \approx 2.0$ up to 900 °C. Above 900 °C, the values of E and a increase as the consequence of the sintering and the differences between values measured in the two directions decrease. When the relationships between Young modulus and thermal diffusivity are compared, some common features are observed. These quantities, which characterize transfer of energy (mechanical and heat) indirectly, show that this transfer is more intensive in the axial direction, where the basal planes of the illite crystals are predominantly oriented parallely to the axial direction. It means that the transfer of mechanical energy and heat is more intensive along the SiO_4 sheets in the illite lattice where stronger bonds are assumed. This is also in agreement with the results of the relative changes of the samples dimensions that are larger in the transversal direction due to weaker bonds.

Acknowledgements

This work was supported by the grant VEGA 1/0162/15 from the Ministry of Education of Slovak Republic and by the Czech Science Foundation, Project No. P105/12/G059. The authors are indebted to J. Biber from Inter-ILI Engineering Office (Hungary) for a supply of illite.

References

[1] T. Vanorio, M. Prasad, A. Nur, Elastic properties of dry clay mineral aggregates, suspensions and sandstones, Geophysical Journal International, 155 (2003) 319-326.

[2] M.B. Clennell, D.N. Dewhurst, K.M. Brown, G.K. Westbrook, Permeability of consolidated clays, Geological Society, Special Publications, 158 (1999) 79-96.

[3] J. Barrios Neira, J.C. Martín de la Cruz, Y.M. Montealegre Contreras, Study of the raw materials used in the manufacture of ceramic in Fran Ali (Oued Lau. Marruecos), Boletin de la Societad Espanola de Ceramica y Vidrio, 51 (2012) 222-230.

[4] V. Trnovcová, I. Furár, F. Hanic, Influence of technological texture on electrical properties of industrial ceramics, Physics and Chemistry of Solids, 68 (2007) 1135-1139.

[5] I. Štubňa, Š. Valovič, Thermal expansion of textured electroceramics, Industrial Ceramics, 24 (2004) 121-124.

[6] I. Štubňa, V. Trnovcová, The effect of texture on thermal expansion of extruded ceramics, Ceramics – Silikáty, 42 (1998) 21-24.

[7] I. Štubňa, A. Lintnerová, L. Vozár, Anisotropic mechanical properties of textured quartz porcelain, Ceramics – Silíkáty, 52 (2008) 90-94.

[8] A.N. Beljanin, V.N. Rudakov, Radiodefectoscopy of the ordered inhomogeneous dielectrics, Izvestia Vuzov – Defektoskopia, 4 (1968) 1-4 (in Russian).

[9] I. Štubňa, M. Kalužná, V. Trnovcová, Mapping the texture of electroporcelain blank by radiointroscopy, Industrial Ceramics, 30 (2010) 17-20.

[10] K. Boussois, S. Deniel, N. Tessier-Doyen, D. Chateigner, C. Dublanche-Tixier, P. Blanchart, Characterization of textured ceramics containing mullite from phyllosilicates, Ceramics International, 39 (2013) 5327-5333.

[11] R. Podoba, Ľ. Podobník, A. Trník, Upgrading of TGA/DTA analyzer derivatograph, Építőanyag 64 (2012) 28-29.

[12] T. Húlan, A. Trník, I. Štubňa, The apparatus form measurement of Young modulus of ceramics at elevated temperatures, Vestnik MGOU, seria fizika – matematika (2014) 21-29.

[13] H. Mehling, G. Hautzinger, O. Nilsson, J. Fricke, R. Hofmann, O. Hahn, Thermal diffusivity of semitransparent materials determined by the laser-flash method applying a new analytical model, International Journal of Thermophysics, 19(3) (1998) 941-949.

[14] T. Húlan, I. Štubňa, A. Trník, P. Bačík, T. Kaljuvee, L. Vozár, Thermomechanical analysis of illite from Fuzérradvány, Materials Science (Medžiagotyra), accepted manuscript

[15] V.A. Drits, D. McCarty, The nature of structure-bonded H_2O in illite and leucophyllite from dehydratation and dehydroxylation experiments, Clay and Clay Minerals, 55 (2007) 45-58.

[16] C. Venturelli, M. Paganelli, Sintering behaviour of clays for the production of ceramics, Ceramic Forum International Ber. DKG, 84 (2007) E1-E3.

Publikácie doktorandov a pracovníkov TFL KF, ktorí využívali prístroje zakúpené z projektu (guľový mlyn PM 100 RETSCH a sitovací stroj AS 200 Control RETSCH), pričom neboli riešiteľmi projektu:

PRÍLOHA č. 9

Vedecký recenzovaný zborník
Peer-reviewed Proceedings

Nové trendy akustického spektra
New Trends of Acoustic Spectrum

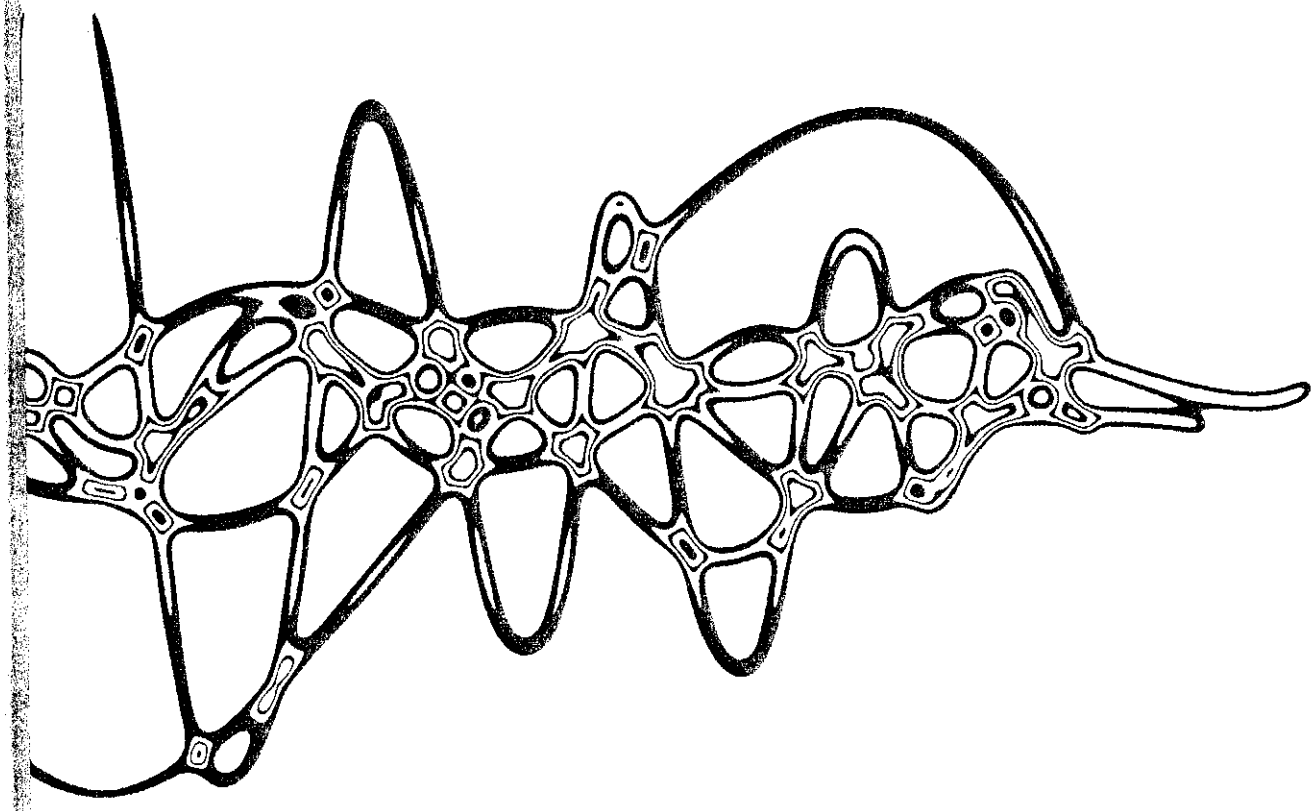

Martin Čulík – Anna Danihelová

2015

Technická univerzita vo Zvolene
Drevárska fakulta

Editori / Editors:
Martin Čulík, Anna Danihelová

NOVÉ TRENDY AKUSTICKÉHO SPEKTRA

Vedecký recenzovaný zborník

NEW TRENDS OF ACOUSTIC SPECTRUM

Peer-reviewed Proceedings

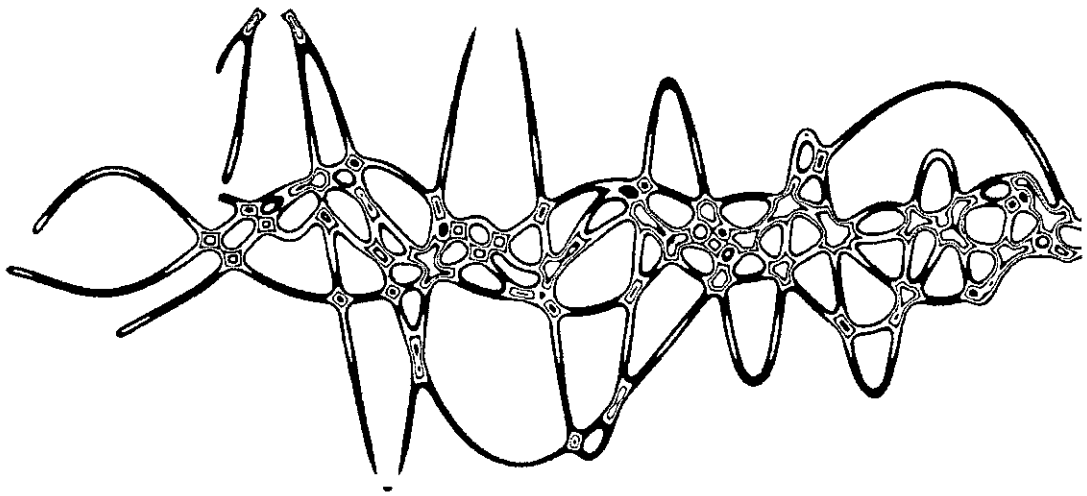

2015

Poďakovanie:
Vedecký recenzovaný zborník vznikol s podporou výskumu v grantovom projekte VEGA č. 2/0097/15 „Zvukové vlastnosti historických organov na Slovensku", riešeného na Ústave hudobnej vedy SAV v Bratislave.

Editori / Editors: Martin Čulík, Anna Danihelová

NOVÉ TRENDY AKUSTICKÉHO SPEKTRA
Vedecký recenzovaný zborník

NEW TRENDS OF ACOUSTIC SPECTRUM
Peer-reviewed Proceedings

I. vydanie
Rok vydania 2015
Počet strán 151, náklad 50 výtlačkov
Vydavateľ: Technická univerzita vo Zvolene
Za odbornú a jazykovú úroveň textu sú zodpovední autori jednotlivých príspevkov.
V zborníku sú publikované pôvodné vedecké práce. Príspevky boli recenzované.
Tlač Vydavateľstvo Technickej univerzity vo Zvolene
Technický redaktor Martin Čulík | Grafický návrh obálky Miroslav Chovan

ISBN 978-80-228-2759-1

THE SOUND VELOCITY OF TEXTURED KAOLIN SAMPLES MEASURED USING FLEXURAL AND LONGITUDINAL VIBRATIONS

Daniel Antal, Igor Štubňa, Tomáš Húlan

1 Introduction

Elastic properties of clay minerals are almost unknown, mainly because of the difficulty presented by the intrinsic properties. So far the effective elastic properties of clays have been derived either by theoretical computation, by a combination of theoretical and experimental investigations. These derived values of clay moduli show little agreement.

A well-developed texture of the clay bodies can be created by an artificial way when clay bodies are prepared from a wet plastic mass using a potter wheel or extruder. In this case, the base planes of the plate-like crystals of clay minerals are oriented parallely with the direction of the friction forces which is observed in a production of the high-voltage insulators and tiles. The presence of the texture causes the anisotropy of their mechanical, thermophysical and electrical properties [1-3].

Elastic properties of the textured kaolin-based ceramic samples were experimentally studied in our previous works [4, 5] using impulse ultrasound method [4] as well as sonic resonant method [5]. In the both experiments, the samples were cut from a large blank (Ø300 mm) prepared with extrusion. The texture in such blank is not homogenous – is well developed on the surface and becomes chaotic in deeper layers. To avoid an uncertainty of the texture in the sample volume, we prepared new samples in which the texture should be more homogenous.

The goal of this article is an investigation of the sound velocity in these samples related the texture and firing temperature and comparing the sound velocities measured using flexural and longitudinal vibrations.

2 Experimental

Sedlec kaolin Ia was used for preparing the textured samples. Its chemical composition is given in Table 1. The producer guaranties kaolinite content higher than 90 wt.%.

Table 1. The chemical composition of kaolin (wt.%).

SiO_2	Al_2O_3	Fe_2O_3	TiO_2	CaO	MgO	K_2O	Na_2O	L.O.I.
45.80	37.51	0.98	0.17	0.58	0.46	1.17	0.58	12.95

Thin layers of the plastic mass (750 g of kaolin + 270 g of water) were repeatedly spread one on top of the other with a metal sheet to get a textured body (see Fig. 1). The friction between the metal sheet and wet plastic mass causes the *c*-axes of the plate-like crystals of kaolinite to lie perpendicularly to the direction of the spreading, i.e. the basal planes of the kaolinite crystals are predominantly located in the XZ plane in Fig. 1.

After the drying the samples were cut out from a textured body using a rotatory saw in two ways as visible in Fig. 1: a) long edges of the samples were parallel to the axial direction – the texture of these samples is referred to as axial (see Fig. 1) and the corresponding measured quantities have a subscript "$\parallel$"; b) long edges of the samples were parallel to the transversal direction – the texture of these samples is referred to as transversal (see Fig. 1) and the

corresponding measured quantities have a subscript "$\perp$". The surface of these samples was abraded by a fine sand paper to obtain smooth planparallel faces.

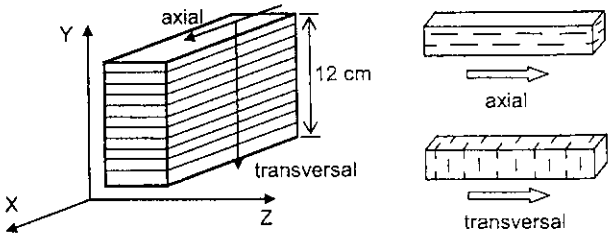

Figure 1. Textured body (30×120×120 mm) made from layers (~1.5 mm thick) and samples used for analyses.

An impulse excitation technique (IET) was used for excitation of the free flexural or longitudinal vibrations in the sample [6]. The time dependence of the amplitude of the vibration was transformed into frequency spectrum via fast Fourier transformation in the apparatus described in [7]. The direction of the mechanical impulse is pictured as thick arrow in Fig. 2.

The resonant frequency of the fundamental mode f_L and length of the sample l were used to calculate the sound velocity from the longitudinal vibrations as

$$c_L = 2lf_L. \tag{1}$$

If the longitudinal wave propagates along the X axis (i.e. along the basal planes of the kaolinite crystals), we obtain "axial" sound velocity $c_{L\parallel}$ (arrow $c_{L\parallel}$). If the longitudinal wave propagates perpendicularly to the basal planes, we obtain the "transversal" sound velocity $c_{L\perp}$ (arrow $c_{L\perp}$).

The sound velocity can be also determined from the flexural vibration. For the prismatic sample of the length l and cross-section $a \times a$ the sound velocity is

$$c_F = 0.97286\frac{l^2 f_F}{a}, \tag{2}$$

where c_F is the resonant frequency of the fundamental mode of the flexural vibration of the free-free sample [6]. To determine $c_{F\parallel}$, we must excite the sample along the arrow $c^{YX}{}_{F\parallel}$ or $c^{ZX}{}_{F\parallel}$ (Fig. 2). To determine $c_{F\perp}$, we must excite the sample along the arrow $c_{F\perp}$.

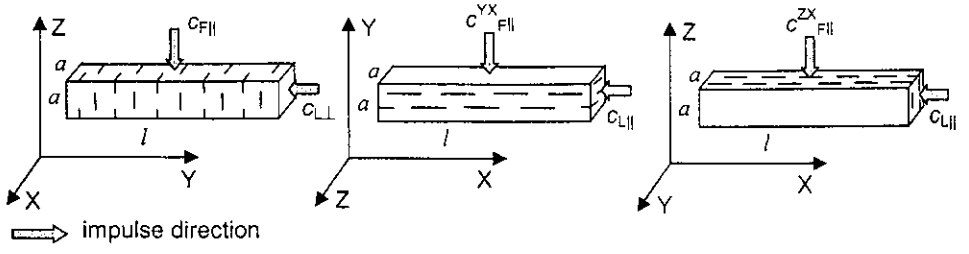

Figure 2. Impulse direction to excite the vibrations of textured samples and corresponding quantity that was determined using the particular resonant frequency.

The Eq. (1) and Eq. (2) are valid for isotropic sample. The sample, which is visible in Fig. 1, is layered and anisotropic. The complex sixth order differential equation describes the flexural vibrations of such sample [8]. In our case, the layers are not clearly developed and are not separated with sharp boundaries, so we use the simple formulae (1) and (2).

3 Results and discussion

The results of the measurement of the sound velocity are shown in Fig. 3 and Fig. 4.

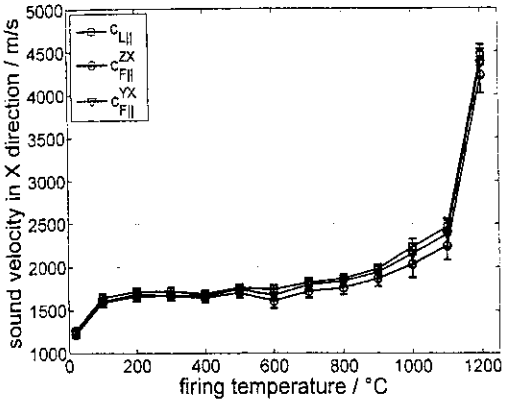

Figure 3. The sound velocity in the axial direction for the samples after their selected firings.

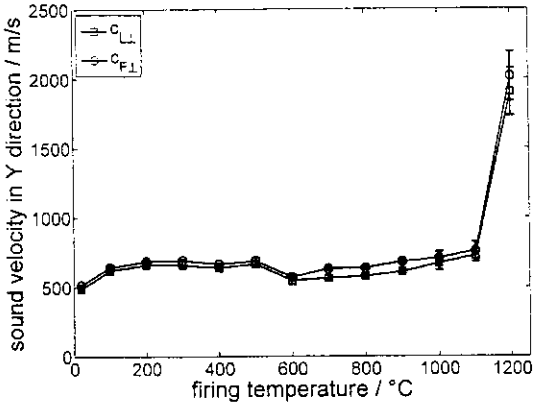

Figure 4. The sound velocity in the transversal direction for the samples after their selected firings.

The first, obvious, observation shows that both methods – based on the longitudinal and flexural vibrations – are equivalent. We also obtained the same results if the sample vibrates flexurally in the plane XY or XZ. During the resonant vibrations, the standing wave propagates along X-axis of the sample in both cases, i.e. the direction of the propagation of the both waves, longitudinal and flexural, is parallel with axial direction (which is valid for Fig. 3) or parallel with transversal direction (which is valid for Fig. 4). Or, in other words, parallel with the basal planes of the kaolinite crystals or perpendicular to them.

Kaolinite crystal is composed from repeating two-sheet layers. The layer consists of one aluminum tetrahedral sheet and one silicon octahedral sheet. Interlayer hydroxyl groups extend from the octahedral sheet into the interlayer region where they form hydrogen bonds to basal oxygen atoms of the opposing tetrahedral silicate sheet. Between tetrahedrons, the stronger covalent bonds take places [9]. We can assume easier path for mechanical wave in the tetrahedron sheet. Therefore the sound velocity is higher when the mechanical wave (longitudinal or flexural) propagates parallelly with the basal planes of the kaolinite crystals. In addition to that, this propagation is weakly influenced by dehydroxylation.

On the other side, the bonds in the tetrahedron sheet are weaker and they are partially destroyed during dehydroxylation that runs at the temperatures above 400 °C. Consequently, conditions for a transport of the mechanical energy by means of the mechanical wave are less favorable. We can expect lower values of the sound velocity. This assumption is confirmed with experimental results given in Fig. 3 and Fig. 4. The decrease of the sound velocity in the transversal direction around the temperature 500 °C is a result of the dehydroxylation.

The next process, which takes place at the temperatures above 800 °C is a sintering. The influence of the sintering on the samples is different with axial and transversal texture. We observe gradual increase of the sound velocity for the axial texture above 900 °C and steep increase above 1100 °C (see Fig. 3). We can assume that high-temperature processes (collapse of the metakaolinite structure and creation of Al-Si spinel around 960 °C) influence the propagation of the mechanical waves in a less measure, i.e. the tetrahedral sheet is responsible for it.

If the sound velocity is measured in the transversal direction, we observe very gradual increase of the sound velocity up to 1100 °C and then steep increase of its values (Fig. 4). The temperatures around 1100 °C are considered as region of the creation of mullite and start of the intensive contraction due to sintering.

4 Conclusions

The textured samples, prepared from kaolin Sedlec, were fired at selected temperatures from 100 °C up to 1200 °C. The sound velocity was measured: a) along the basal planes of the kaolinite crystals (axial direction), and b) along their c-axis (transversal direction). It was found that:

- Texture does not influence the values of the sound velocity obtained by impulse excitation technique using flexural or longitudinal vibrations.
- The sound velocity in the axial direction reached significantly higher values than those in the transversal direction.
- Dehydroxylation, as well as high-temperature transformations, influenced the sound velocity mainly in transversal direction.

Acknowledgements

This work has been supported by the grant VEGA 1/0464/12.

References

[1] Trnovcová V., Furár I., Hanic F.: *Physics and Chemistry of Solids* **68** (2007) 1135-1139
[2] Štubňa I., Valovič Š.: *Industrial Ceramics*, **24** (2004) 121-124
[3] Štubňa, I. - Trnovcová, V.: *Ceramics - Silikáty*, **42** (1998) 21-24
[4] Štubňa, I. – Lintnerová, A. – Vozár, L.: *Ceramics – Silikáty*, **52** (2008) 90-94
[5] Štubňa, I. – Lintnerová, A. – Trník, A.: *Industrial Ceramics*, **29** (2009) 39-42
[6] ASTM E 1876-09: Standard test method for dynamic Young's modulus, shear modulus and Poisson's ratio by impulse excitation of vibration
[7] Húlan T. – Trník, A.: *Vestnik MGOU, seria fizika – matematika*, 2014, N2, 21-29
[8] Mead, D.J.: *Journal of Sound and Vibration*, **83** (1982) 363-377
[9] Chakraborty, A.K.: *Phase transformation of kaolinite clay*. Springer, New Delhi 2014

Summary

The determination of the sound velocity in kaolin textured samples is presented. We compared sound velocities obtained from a) longitudinal and b) flexural vibration. It was confirmed that both methods are equivalent for determining the sound velocity and the differences in results are within uncertainty of measurement. Thermally induced processes as dehydroxylation or sintering influence mainly sound velocity measured parallely to the basal planes of the kaolinite crystals.

Contact address

Daniel Antal[1], Igor Štubňa[2], Tomáš Húlan[3]
Faculty of Natural Sciences, Constantine the Philosopher University in Nitra
Tr. A. Hlinku 1, 949 74 Nitra, Slovakia
[1]antal@fnnitra.sk, [2]istubna@ukf.sk, [3]tomas.hulan@ukf.sk

Publikácie doktorandov a pracovníkov TFL KF, ktorí využívali prístroje zakúpené z projektu (guľový mlyn PM 100 RETSCH a sitovací stroj AS 200 Control RETSCH), pričom neboli riešiteľmi projektu:

PRÍLOHA č. 10

TECHNICAL UNIVERSITY OF KOŠICE
FACULTY OF METALLURGY

PREPARATION OF CERAMIC MATERIALS

PROCEEDINGS OF EDITED CONTRIBUTIONS

Slovak Silicate Society
Slovak Glass Society

9th – 11th June 2015 Herľany, Slovakia

TECHNICAL UNIVERSITY OF KOSICE
FACULTY OF METALLURGY,
DEPARTMENT OF CERAMICS

Institute of Geotechnics – Slovak Academy of Sciences, Kosice
Slovak Silicate Society
Slovak Glass Society

PREPARATION OF CERAMIC MATERIALS

Proceedings of the XI. International Conference

Herl'any

June 9th – 11th, 2015

Internet: Full text available online at http://web.tuke.sk/seminar_PKM/

Proceedings - XIth International Conference
PREPARATION OF CERAMIC MATERIALS
Herľany, June 9th – 11th, 2015
Editor: Organizing Committee of International Conference
PREPARATION OF CERAMIC MATERIALS 2015
Faculty of Metallurgy, Department of Ceramics

June 2015.
I. edition .
Number of Copies – 101.
Number of Pages – 153

The publication of proceedings was supported by
SLOVAK SILICATE SOCIETY- ASSTS
SLOVAK GLASS SOCIETY
TECHNICAL UNIVERSITY OF KOSICE, FACULTY OF METALLUGY

Edited by:
Assoc. Prof. RNDr. František Lofaj, DrSc.,
Assoc. Prof. Ing. Miroslav Hnatko, Ph.D.,
Assoc. Prof. Ing. Beatrice Plešingerová, CSc.,
Assoc. Prof. Ing. Gabriel Sučik, Ph.D.,
Ing. Diana Horkavcová, Ph.D.,
RNDr. Martin Fabián, Ph.D.,

ISBN: 978-80-553-2122-6

INFLUENCE OF MILLING ON DC CONDUCTIVITY OF ILLITE

Štefan Csáki[1,2], Viera Trnovcová[1], Ján Ondruška[1], Igor Štubňa[1]

[1]Department of Physics, Constantine the Philosopher University, A. Hlinku 1, 949 74 Nitra, Slovakia
[2]Department of Physics of Materials, Charles University in Prague, Ke Karlovu 5, 121 16 Praha 2, Czech Republic

e-mail stefan.csaki@ukf.sk

The illitic clay (80 % illite, 4 % montmorillonite, 4 % orthoclase and 12 % quartz) was milled in a ball mill for 0, 30, 60, 90, 120 and 180 min. From the milled clay, samples for thermoelectrometry, TGA and DSC were prepared. It was found the dehydroxylation of illite is a 2-step process, and it is shifted to lower temperatures with increasing time of milling. The thermogravimetry measurements showed the dehydroxylation mass loss does not depend on the milling time. The dependence of DC conductivity of green samples varies with different milling time. Up to ~250 °C, H^+ and OH^- ions are dominant charge carriers. When physically bound water is removed, the concentration of the H^+ and OH^- ions decreases and dominant charge carriers become mainly K^+ and Na^+.

Keywords: *illite, milling, thermoelectrometry, DC conductivity*

Introduction

The processing of raw materials in ceramic products requires a preparation of ceramic powders. The shape and size of the crystals of phyllosilicates influence properties of ceramic materials significantly during preparing the green ceramic body as well as during firing. The size of crystals of kaolinite, illite and other clay minerals determines plastic qualities, shrinkage rate, forming potential and drying characteristics. A larger part of bigger crystals in clay results in a less plasticity, less shrinkage and faster drying. A larger part of smaller crystals shifts phase transformations to lower temperatures. Therefore, the milling of hard minerals (such as quartz, feldspar and others) as well as crushing of phyllosilicate clumps (mainly from kaolinite and illite), are necessary technological steps in a manufacturing traditional ceramics [1-3]. A reasonable milling time leads to an increase of the specific surface area. After a long milling, changes in some clay mineral components (e.g. muscovite) can be observed because of its transformation into illite-1M, quartz, albite and others [4]. The dry milling of kaolinite is also a possible way how to obtain a nanomaterial [5, 6].

A firing process and sintering are significantly influenced by crystallinity of the phyllosilicates. The low crystallinity and small size of crystals help to decrease the maximum firing temperature [7-10] as well as the temperature of phase transformations [11]. It is important to know how the milling influences a firing process and physical properties of the ceramic samples. Influence of a milling time on XRD, TGA and DTA was studied for kaolin in [5, 6, 12, 13]. It was found that the DTA effects of dehydroxylation shifted to lower temperatures, decreased in intensity

with increasing milling time. They disappeared completely after 120 min of milling [5]. The activation energy of dehydroxylation became lower with the increase of the milling time [12,14]. The temperature of the first exothermic effect, which is characteristic for a release of the physically bound water (PBW), shifted slightly to lower temperatures after milling [5,13]. It was also found that milling increased a quantity of the mullite in porcelain [15] and mullite was transformed from kaolinite at lower temperature [16]. The influence of milling on firing is relatively well known for system kaolinite – quartz/alumina – feldspar that is connected with manufacturing of porcelain. This influence was less studied for ceramic mixtures with illite. In this contribution, the influence of milling on results of the TGA, DSC, and DC conductivity of illitic clay are shown and discussed.

Experimental

Samples were made from the illitic clay supplied from the mine in Füzérradvány, Hungary (**Table 1**). This clay is composed of 80 % illite, 4 % montmorillonite, 4 % orthoclase and 12 % quartz.

Table 1: The chemical composition (in wt. %) of illite from Füzérradvány, Hungary

SiO_2	Al_2O_3	Fe_2O_3	TiO_2	CaO	MgO	K_2O	Na_2O	L.O.I.
58.0	24.0	0.6	0.05	0.38	1.70	7.85	0.10	7.3

To obtain a powder with small particles, the clay was crushed and dried at 120 °C for 1 hour and then milled. In our experiments we used a mill RETSCH PM 100 with alumina balls and vessel in which the crushed illitic clay was milled for different time periods 0, 30, 60, 90, 120, and 180 min (samples are called as M0, M30, M60, M90, M120, and M180, respectively). A possible way how to obtain a relatively homogeneous batch of the milled clay is a sieving. Our experience [17] showed that the coarser screen was used, the more quartz and feldspar was present on the screen. To prevent differences between mineral compositions of the samples after different milling times, we did not sieve the milled clay.

Samples for electrical conductivity were prepared from wet plastic mass as prisms with dimensions of 10×10×20 mm with inserted parallel platinum wire electrodes. The sample arrangement gave a good electrical contact between the measured material and platinum electrodes during the whole measurement cycle as experienced in [18, 19].

The measuring circuit was fed from the stabilized voltage source Tesla BS 525 with 10 V. The voltage was recorded by the multimeter Agilent 34972A and the current was recorded by electrometer Keithley 6514 [19]. Measurements were performed up to 1100 °C with heating rate 5 °C/min in the air: 1) the first run on the green samples, 2) the second run on the samples used in the first run, it means that they were previously heated to 1100 °C. To reach identical initial conditions for DC conductivity measurements, the samples were placed into a measuring cell and

heated up to 120 °C for 2 h. Then the heating was switched off and temperature dependence of the DC conductivity was measured from the temperature 40 °C up to 1100 °C.
We used powder samples for TGA and DSC that were performed up to 1100 °C with a heating rate 5 °C/min using analysers Mettler Toledo TGA/SDTA 851 and Netzsch DSC 404.

Results and discussion

The results of DTG obtained on powder samples of the mass ~50 mg are visible in Fig. 1. In spite of expectation, the sample M180 contains the smallest amount of the (PBW). When we look at the mass loss at the temperature 200 °C (i.e. when most PBW is removed), no regular dependence on the milling time is observed:
$\Delta m/m_0$ = 2.65 % for M120, $\Delta m/m_0$ = 2.25 % for M0, $\Delta m/m_0$ = 2.05 % for M60 and $\Delta m/m_0$ = 1.85 % for M180. We observe 3 steps of the remove of PBW which are represent with minima at ~80 °C, 160 °C (which survives only for M0 and M60) and 260 °C.

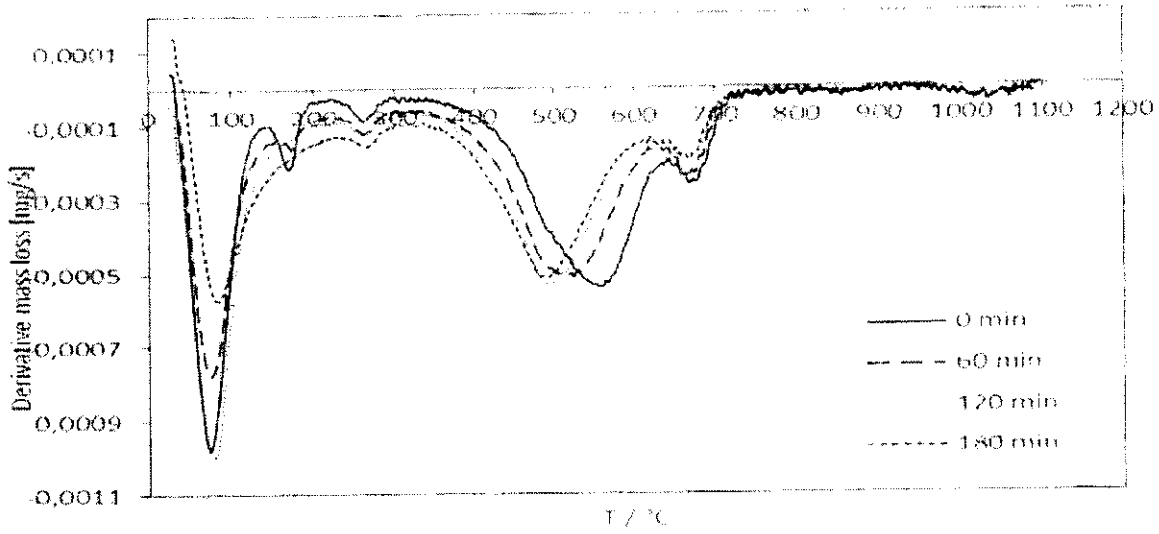

Fig. 1: Thermogravimetric results (DTG) for samples M0, M60, M120 and M180

Dehydroxylation of illite is a typically 2-step process with 2 endothermic minima [20, 21]. The mean peak is shifted to lower temperatures with an increasing milling time. We also observe that the longer milling the lower temperature of the start of dehydroxylation. We suppose, in analogy with kaolinite, that the milling increases the concentration of defects in illite and reduces the crystalline size. Both of them decrease the activation energy of dehydroxylation as found for kaolinite [12, 14], we can assume the same for illite. It shifts the dehydroxylation to lower temperatures. In the cases the mass loss is ~4 % due to dehydroxylation. Contrary to kaolinite [5], our results do not show a clear decrease of the dehydroxylation mass loss with increasing milling time. It can be explained by differences between illite and kaolinite. The illite crystals are smaller than kaolinite ones and they often have

irregular form and probably many defects [22]. Such crystals are less affected by the milling than relatively well developed kaolinite crystals.

Qualitatively DSC curves (Fig. 2), which describe removing PBW and dehydroxylation, are in an agreement with DTG: they also confirm the shift of dehydroxylation to lower temperatures with increasing time of the milling, but the lower-temperature peak's temperatures and their shifts registered by these two different methods are not the same, see Tab. 2.

In addition to endothermic minima in Fig. 2, which belong to removing PBW and dehydroxylation, the another endothermic process is characterized by the minimum between 750 °C and 1100 °C. Actually, sintering, vitrification and high-temperature reactions (creation of Al-Si spinel and mullite) take place here [21, 23].

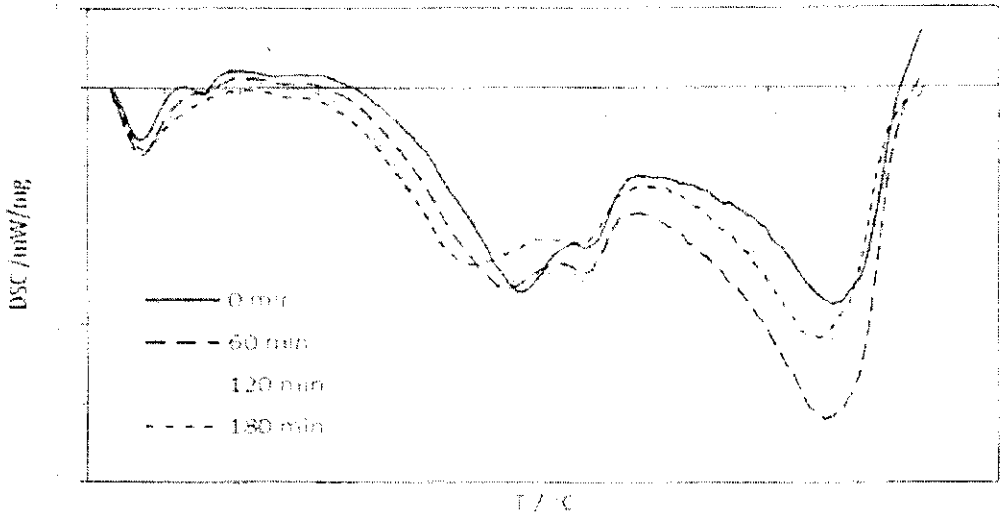

Fig. 2: DSC results for samples M0, M60, M120 and M180

Table 2: DSC and DTG peak temperatures in a dehydroxylation region

Milling time [min]	DSC peak temperature [°C]	Shift of DSC peak [°C]	DTG peak temperature [°C]	Shift of DTG peak [°C]
0	571	0	557	0
60	552	19	514	43
120	527	44	493	64
180	502	69	489	68

The results of the thermoelectrometry of the green illite samples are shown in Fig. 3. Up to ~250 °C, the DC conductivity is significantly influenced by PBW. In this temperature range, H^+ and OH^- ions are dominant charge carriers. When PBW is removed by heating, a concentration of the H^+ and OH^- ions decreases and dominant charge carriers become mainly K^+ and Na^+ [18]. The presence of these ions is confirmed by chemical analysis (Tab. 1). We suppose that the most important charge carriers are K^+ ions because potassium is a component of illite.

It follows from the temperature dependencies of DC conductivity that the DC conductivity increases with increasing time of milling. The conduction activation energy in this temperature region (250 °C – 440 °C) is 0.85 eV which is typical for movement of alkali ions in silicate materials. We can suppose that the milling looses the tightly bound alkali ions, not only from illite but also from feldspar, to sites where these ions are only loosely bound and are prepared to participate in the conduction process. The longer is the milling time the higher is concentration of these "free" alkali ions, and, consequently, the higher is the DC conductivity. An anomaly in the dependencies around 450 °C can be connected with beginning of dehydroxylation. Above 900 °C, an influence of the milling on DC conductivity is negligible.
After heating up to 1100 °C, temperature dependencies of the DC conductivity, measured in the temperature range 40 – 1100 °C, show a more simple character (Fig.4).

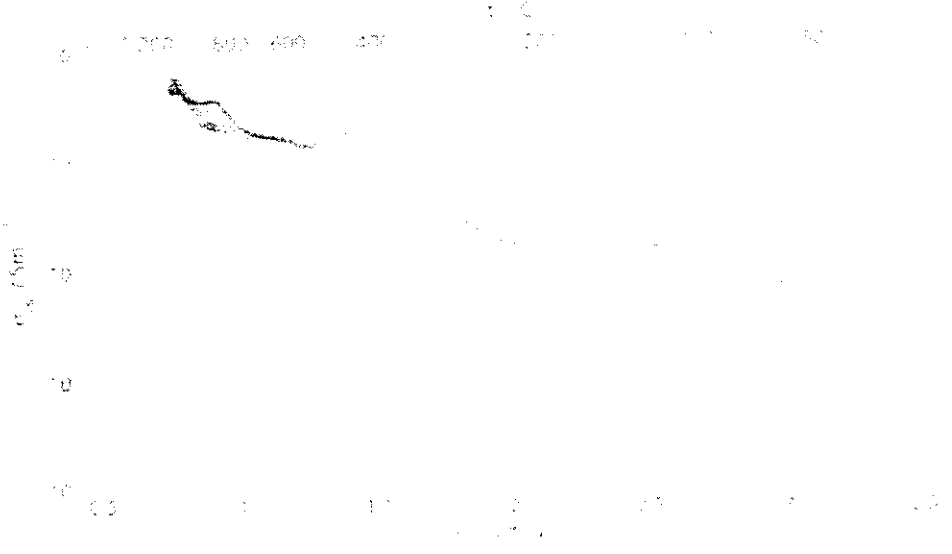

Fig. 3: Temperature dependences of the DC conductivity, in the 1st run, for samples: M30 (○), M60 (□), M90 (◇), and M180 (✳)

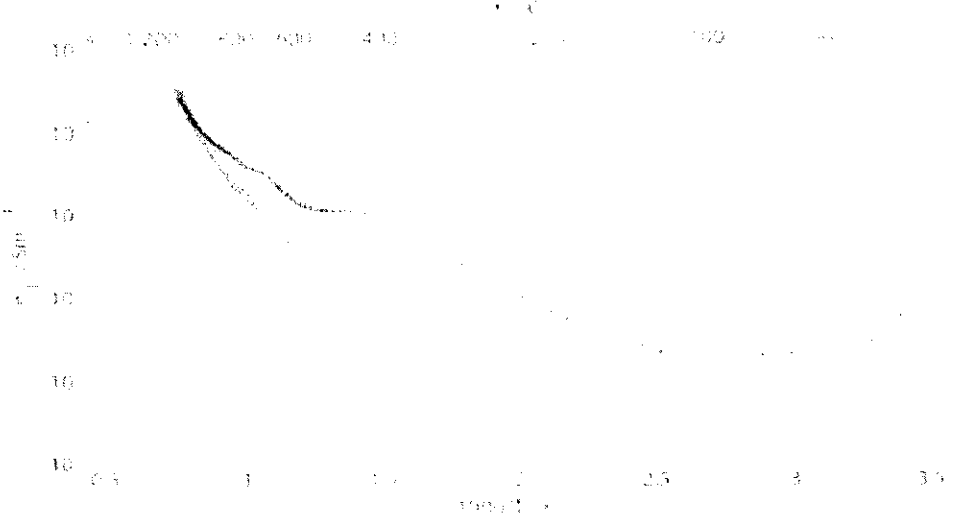

Fig. 4: Temperature dependences of the DC conductivity, in the 2nd run, for samples: M30 (○), M60 (□), M90 (◇), and M120 (✳)

Up to 450 °C, the conduction energy is equal to 0.7 eV. However, the dependence of the conductivity on the milling time is not systematic. The conductivity is highest after 120 min milling. For all milling times, DC conductivity of fired samples is much lower than that of green samples. However, at 1050 °C, the DC conductivity of all samples, green and fired, milled for arbitrary milling times, is equal.

Conclusions

The illitic clay (80 % illite, 4 % montmorillonite, 4 % orthoclase and 12 % quartz) was milled in a ball mill for 0, 30, 60, 90, 120 and 180 min. From the milled clay, samples for thermoelectrometry, TGA and DSC were prepared. It was found

- Dehydroxylation of illite is a 2-step process as confirmed by DSC and DTG.
- The dehydroxylation is shifted to lower temperatures with increasing time of milling.
- The dehydroxylation mass loss does not depend on the milling time.
- The DC conductivity of green samples increases with increasing time of milling.
- The DC conductivity of the fired samples is significantly lower than the DC conductivity of the green samples.
- Up to ~250 °C, H^+ and OH^- ions are dominant charge carriers. When physically bound water is removed, a concentration of the H^+ and OH^- ions decreases and dominant charge carriers become mainly K^+ and Na^+.

Acknowledgement

This work has been supported by the grant VEGA 1/0162/15. The authors are also indebted to Mr. J. Biber (Inter-ILI Engineering Office, Hungary) for illitic clay.

References

[1] M.N. Rahaman: *Ceramic processing and sintering*, Marcel Dekker Inc. New York 2003

[2] S. Ferrari, A.F. Gualtieri: The use of illitic clays in the production of stoneware tile ceramics. *Applied Clay Science*, **32** (2006) 73-81

[3] S. Kavaici, E. Yalmar, S. Akkurt: Effects of boron addition and intensive grinding on synthesis of anorthite ceramics. *Ceramics International*, **34** (2008) 1629-1635

[4] L.A. Gömze: Mechanochemical phenomena during fine comminution of clay minerals for ceramic bricks and roof-tiles. *Materials Science Forum* **659** (2010) 19-24

[5] R.L. Frost, E. Horvath, E. Makó, J. Kristóf: Modification of low- and high- defect kaolinite surfaces: implications for kaolinite mineral processing. *Journal of Colloid and Interface Science*, **270** (2004) 337-346

[6] R. Hamzaoui, F. Muslim, S. Guessasma, A. Bennabi, J. Guilin: Structural and thermal beghavior of proclay kaolinite using high energy ball milling process. *Powder Technology*, **271** (2015) 228-237

[7] J. Dubois, M. Murat, A. Amroune, X. Carbonneau, R. Garcon: High-temperature transformation in kaolinite: the role of the crystallinity and of the firing atmosphere. *Applied Clay Science*, **10** (1995) 187-198.

[8] M. Nakahara, Y. Kondo, K. Hamano: Effect of particle size of powders ground by ball milling on densification of cordierite ceramics. *Journal of the Ceramic Society of Japan* **107** (1999) 308-312

[9] J. Ranogajec, M. Djuric, M. Radeka, P. Jovanic: Influence of particle size and furnace atmosphere on the sintering of powder for tiles production. *Ceramics-Silikáty* **44** (2000) 71-77

[10] S.N. Monteiro, C.M.F. Vieira: Solid state sintering of red ceramics at lower temperatures. *Ceramics International* 30 (2004) 381-387.

[11] O.V. Andryushkova, O.A. Kirichenko, V.A. Ushakov, V.A. Poluboyarov: Effect of mechanical activation on phase transformations in transition aluminas. *Solid State Ionics* 101-103 (1997) 647-653.

[12] P. Ptáček, T. Opravil, J. Wasserbauer, J. Masilko, J. Baráček, The influence of structure order on the kinetics of dehydroxylation of kaolinite. *Journal of the European Ceramic Society* **33** (2013) 2793-2799

[13] P.J. Sánachez-Soto, M. Del Carmen Jimenez de Haro, L.A. Pérez-Magueda, I. Varona, J. L. Perez-Rodriguez, Effects of dry grinding on the structural changes of kaolinite powders. *Journal of the American Ceramic Society*, **83** (2000) 1649-1657

[14] I. Štubňa, G. Varga, A. Trnik, Investigation of kaolinite dehydroxylation is still interesting, *Építőanyag*, **58** (2006) 6-9.

[15] E. Elmas, K. Yildiz, N. Toplan, H.O. Toplan, Effect of mechanica activation on mullite formation in an alumina-quartz ceramics system. *Materiali in Tehnologije*, **47** (2013) 413-416

[16] S. Koc, N. Toplan, K. Yildiz, H.O Toplan, Effects of mechanical activation on the non-isothermal kinetics of mullite formation from kaolinite. *J. Thermal Analysis and Calorimetry* **103** (2011) 791-796.

[17] J. Ondruška, M. Jankula, Influence of the sieving process on thermophysical properties of brick clay. In: *Conf. Proceedings 18th Thermophysics 2013*, Podkylava, SAV Bratislava 2013, 90-95

[18] R. Podoba, I. Štubňa, V. Trnovcová, A. Trnik, Temperature dependence of DC electrical conductivity of kaolin.*J. of Thermal Analysis and Calorimetry*, **118** (2014) 597-601

[19] I. Štubňa, V. Trnovcová, L. Vozár, Š. Csáki, Uncertainty of the measurement of DC conductivity of ceramics at elevated temperatures. *Journal of Electrical Engineering* **66** (2015) 33-38

[20] A.F. Gualtieri, S. Ferrari, Kinetics of illite dehydroxylation. *Physics and Chemistry of Minerals*, **33** (2006) 490-501.

[21] T. Hülan, I. Štubňa, A. Trnik, P. Bačík, T. Kaljuvee, L. Vozár, Thermomechanical analysis of illite from Füzerradvány, *Materials Science (Medžiagotyra)* submitted article

[22] Z. Pécskay, F. Molnár, T. Itaya, T. Zelenka, Geology and K-Ar geochronology of illite from the clay deposit at Füzérradvány, Tokaj mts., Hungary. *Acta Mineralogica-Petrographica* **46** (2005) 1-7

[23] R. Ori, *The mineralogical and technological characterization of illite from Füzérradvany (Hungary) as a raw material for traditional ceramics*. PhD thesis University of Modena and Emilia Region, Modena, (2003) (in Italian).

PRÍLOHA Č. 11


Názov projektu: Environmentálne aspekty urbanizovaného prostredia
"dopytovo-orientovaný projekt"
OPVaV "Podporujeme výskumné aktivity na Slovensku / Projekt je spolufinancovaný zo zdrojov EÚ"
ITMS 26220220110
Operačný program VÝSKUM a VÝVOJ
ASFEU
Európska únia
Európsky fond regionálneho rozvoja


Európska únia
ASFEU
Názov projektu: Environmentálne aspekty urbanizovaného prostredia
Operačný program VÝSKUM a VÝVOJ
ASFEU
Európska únia

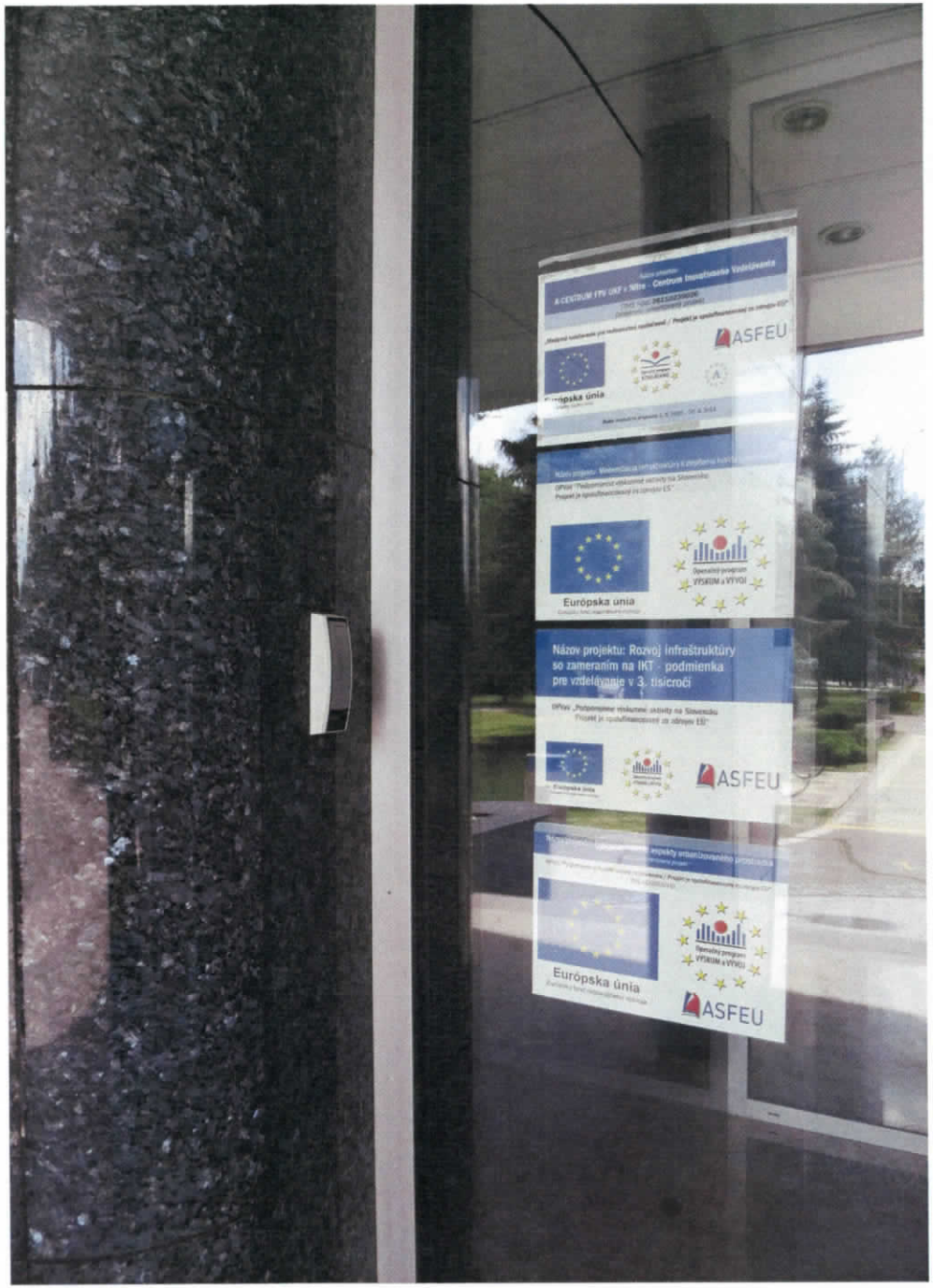
Európska únia
Názov projektu: Rozvoj infraštruktúry so zameraním na IKT - podmienka pre vzdelávanie v 3. tisícroči
ASFEU
Európska únia


ASFEU
Európska únia
INFORMÁCIE
Názov projektu: Rozvoj infraštruktúry so zameraním na IKT - podmienka pre vzdelávanie v 3. tisícroči
ASFEU
Európska únia
ASFEU

PRÍLOHA č. 12

UNIVERZITA KONŠTANTÍNA FILOZOFA V NITRE

číslo účtovného dokladu KDF

LIKVIDAČNÝ LIST FAKTÚRY 10N 000 6709

Dátum vystavenia faktúry: 16.12.2014	číslo knihy faktúr 2014107294
Dodávateľ: 100133	číslo faktúry (var. symbol): 9872008084
	splatnosť dňa 01.01.2015 KS 3558
ALLIANZ-SLOVENSKÁ POISŤOVŇA	spolu za faktúru 11.744,74 EUR
Dostojevského rad 4	predmet dodávky
815 74 Bratislava	*Allianz-poistenie majetku r. 2015

Predbežná finačná kontrola v zmysle zákona č. 502/2001 Z.z. v znení neskorších predpisov:

1. Výber dodávateľa je v súlade so zákonom č. 25/2006 Z.z. o verejnom obstarávaní a o zmene a doplnení niektorých zákonov v znení neskorších predpisov a smernicou č. 12/2014 o obstarávaní tovarov, prác a služieb na UKF v Nitre

Zmluva/objednávka č. ZML-2014-1/2845-2845 Allianz je v súlade s výsledkom verejného obstarávania

Použitý postup vo verejnom obstarávaní a referentské číslo spisu 18.12.2014

dátum vedúci OOB/~~vedúci UJ~~

2. Dodávka (práca) zodpovedá objednávke / zmluve č. ZML-2014-1/2845-2845 Allianz a potvrdzujem účelnosť vynaloženia finačných prostriedkov

19.12.2014

dátum vedúci projektu dátum vedúci objedn. pracoviska

3. Finačná operácia je v súlade:
- s rozpočtom projektu/zmluvou č.:

dátum vedúci projektu

- s rozpočtom pracoviska 19.12.2014

dátum vedúci pracoviska

- s rozpočtom ~~fakulty~~ /R,CUP
- so smernicou č. 14/2010 o obehu ekon. dokladov
- s interným predpisom č.:
- je finančne krytá 19. DEC. 2014

dátum vedúci FO/~~tajomník~~

4. Finačná operácia v zmysle bodov 1, 2. a 3 spĺňa podmienky hospodárnosti, efektívnosti, účelnosti a účinnosti použitia fin. prostriedkov

dátum

kvestor

Platobný príkaz:

z účtu: 7000240831 / 8180

na účet: 2626006702 / 1100

kód firemnej banky: 1000

čiastka k úhrade: 11.744,74

Schválenie platby: 19. DEC. 2014

dátum vedúci FO

ID ŠP:

Dátum úhrady v ŠP:

zodpovedný zamestnanec FO

Účtovací predpis:

	Účet HK	F	FO	FP	Program	FS	NS	PU	Čiastka
D	321110			T6				1900	11 744,74
MD	381100	111	0942	637015	0771199	191099		1900	11 744,74

predkontoval: 17. DEC. 2014 — dátum, podpis

zaúčtoval: 19. DEC. 2014 — dátum, podpis

schválil: 19. JAN. 2015 — dátum, podpis

Zaevidované v dlhodobom majetku áno - nie / inv. číslo

Zaevidované v drobnom majetku áno - nie / inv. číslo

dátum / podpis

Allianz
Slovenská poisťovňa

Allianz – Slovenská poisťovňa, a. s
Ústredie

Univerzita Konštantína Filozofa v Nitre
Trieda Andreja Hlinku 1
Nitra
94901

Dátum: 01.12.2014
Kontakt: R.I.C. Slovakia, s.r.o.
Tel.:
Vec: **Výmer poistného k poistnej zmluve** 9872008084

V zmysle poistnej zmluvy poistenia podnikateľov, zasielame údaje pre úhradu poistného bankovým prevodom.

Poistné: 11744,74 EUR za obdobie od 01.01.2015 do 31.12.2015 .

Na úhradu poistného môžete použiť predtlačený príkaz na úhradu. Platbu môžete uskutočniť aj vkladom na účet v Tatra banke číslo SK17 1100 0000 0026 2600 6702, BIC: TATRSKBX, s variabilným symbolom 9872008084.

S pozdravom

Ing. Miroslav Pacher
člen predstavenstva

Branislav Martinka
riaditeľ odboru firemných klientov

Dostojevského rad 4
SK-815 74 Bratislava
Slovenská republika

IČO: 00 151 700
IČ DPH: SK2020374862
DIČ: 2020374862

Okr. Súd Bratislava I, Obch. register
Oddiel: Sa, Vložka číslo: 196/B

Príkaz k úhrade

Banke Pobočke

Bankové spojenie		Mena	Symbol		
IBAN - číslo účtu platiteľa	BIC - kód banky platiteľa				
IBAN - číslo účtu príjemcu	BIC - kód banky príjemcu	Čiastka EUR	Variabilný	Konštantný	Špecifický
SK1711000000002626006702	TATRSKBX	11744.74	9872008084	3558	
Doplňujúce údaje banky		Údaje pre vnútornú potrebu príkazcu			
		Univerzita Konštantína Filozofa v Nitre			

Dátum splatnosti

V dňa

Finančné oddelenie
16. 12. 2014
UKF v Nitre

pečiatka a podpis

Allianz - Slovenská poisťovňa, a.s.

Allianz
Slovenská poisťovňa

SÚHRNNÝ NÁVRH POISTNEJ ZMLUVY
PP01

Poistná zmluva je uzavretá podpisom tohto návrhu oboma zmluvnými stranami

☒ Nová poistná zmluva

☐ Zmena poistnej zmluvy číslo

uzatvorenej dňa . .

V prípade dojednania zmeny poistnej zmluvy, uveďte dôvod zmeny:

☐ Náhrada poistnej zmluvy číslo

Nahrádzaná poistná zmluva zaniká dňom, ktorý predchádza dňu vzniku poistenia novej poistnej zmluvy. Uveďte dôvod náhrady:

Nespotrebované poistné z nahrádzanej poistnej zmluvy sa [illegible] vráti poistníkovi

Poistenie majetku

Miesto poistenia:

Ulica č.: viď prílohu č. 1 a 2

Miesto: Nitra PSČ: 94974

Popis miesta poistenia:

Popis miesta poistenia

1. Miesto poistenia sa nachádza: × vo vnútri obce ☐ v priem. zóne ☐ na okraji obce ☐ na samote

2. Bol v mieste poistenia alebo v jeho bezprostrednej blízkosti zaznamenaný zosuv pôdy? ☐ áno × nie ak áno, výluka podľa VPP-M

3. Bola v mieste poistenia povodeň v uplynulých 10 rokoch častejšie ako jedenkrát? ☐ áno × nie

a) Poistenie budov

Popis predmetu poistenia:

Predmet poistenia - popis — kód činnosti: 81000

	Objekt č.	Popis (číslo JKSO príp. KS)	Poistná suma [EUR]
× budova ☐ časť budovy ☐ stav. úpravy	1	zoznam budov	40 536 239.00 a1)

Rok uvedenia do prevádzky/celkovej rekonštrukcie:

Vedľajšie budovy, stavby, technologické zariadenia, nezahrnuté v poistnej sume objektu: a2)

Č. listu vlastníctva: Katastrálne úz.:

Spôsob využitia stavebného objektu (podiel plochy jednotlivých prevádzok na celkovej ploche): a3)

× ≥ 50 % školy, škôlky a4)

☐ do 50 %

☐ do 25 %

☐ do 10 %

Celková plocha objektu (m²): ..... alebo obstarávaný priestor (m²): .....

Požiarna odolnosť konštrukcie: × A odolná, B čiastočne odolná ☐ C neodolná

Základné poistenie:

Celková poistná suma: 40 536 239.00 EUR (súčet a1), a2), a3), a4)) × v novej hodnote ☐ v časovej hodnote

Poistené riziko:	požiar ×	voda ×	víchrica ×	živel ×	ostatné ×	Poistné spolu [EUR]
sadzba [‰]:	0.09	0.14	0.09	0.15	0.05	
poistné [EUR]:	3 648.26	5 675.07	3 648.26	6 080.44	2 026.81	21 078.84
spoluúčasť [EUR]:	100	100	100	100	100	

Spoluúčasť:

Prirážky /zľavy:

Dotazník (otázka č. 1 a 2 sa vypĺňajú vždy):
Prirážky/zľavy (uplatňujú sa iba pre poistnú sumu nad 200 000 EUR):
(poistné za prirážku sa uvádza s kladnou, za zľavu so zápornou hodnotou)

			Poistené riziko: požiar	voda	víchrica	živel	ostatné	Poistné spolu [EUR]
1. Je v budove viac ako 50% nevyužívanej plochy, resp. je budova viac ako 1 mesiac neobývaná / nepoužívaná?	☐ áno × nie	prirážka [%]:	0.00					0,00
		poistné [EUR]:						
2. Je budova vo výstavbe, v rekonštrukcii alebo na svoj účel nepoužiteľná?	☐ áno × nie	prirážka [%]:						0,00
		poistné [EUR]:						
3. Je dojazd profesionálnych hasičov do 5 minút, bez prekážok príjazdu? Najbližší hasičský zbor – miesto: NR vzdialenosť (v km): 5	× áno ☐ nie	zľava [%]:	10.00	x	x	x	x	-364,83
		poistné [EUR]:	-364,83	x	x	x	x	
4. Je budova na mieste s nočným osvetlením/oplotením alebo prístup do budovy je trvalo (24 hod. denne) kontrolovaný (vrátnik, strážnik, SBS)?	× áno ☐ nie	zľava [%]:	10.00	x	x	x	x	-364,83
		poistné [EUR]:	-364,83	x	x	x	x	
5. Platí zákaz fajčenia v celej budove?	× áno ☐ nie	zľava [%]:	5.00	x	x	x	x	-182,41
		poistné [EUR]:	-182,41	x	x	x	x	
6. Je v budove funkčná elektrická požiarna signalizácia s napojením na miesto pod stálou kontrolou osoby schopnej reagovať na prijaté hlásenie?	☐ áno × nie	zľava [%]:		x	x	x	x	0,00
		poistné [EUR]:		x	x	x	x	
7. Sú v budove inštalované sprinklerové hasiace zariadenia?	☐ áno × nie	zľava [%]:		x	x	x	x	0,00
		poistné [EUR]:		x	x	x	x	
8. Zlomkové poistenie - limity plnenia (čl. 6 ods. 6 ZD-M) × voda, 12 160 872,00 EUR, t.j. 30 % z poistnej sumy × víchrica, 12 160 872,00 EUR, t.j. 30 % z poistnej sumy		zľava [%]:	x	5.00	5.00	x	x	-466,16
		poistné [EUR]:	x	-283,75	-182,41	x	x	
9. Zľava za vyššiu spoluúčasť: ×		zľava [%]:	0.00	0.00	0.00	0.00	0.00	0,00
		poistné [EUR]:	0.00	0.00	0.00	0.00	0.00	

Prirážky/zľavy: -1 379,29

- Poistenie pre prípad nákazy hydiny,
- Poistenie pre prípad jednotlivých škôd,
- Poistenie pre prípad jednotlivých škôd na plemenných zvieratách

2.1.16. Poistenie zodpovednosti za environmentálnu škodu dojednať ako:
- zodpovednosť za škodu - čl. 3 VPP-EZ a čl. 4 VPP-EZ, čl. 3 ZD-EZ.

2.2 Výhody produktu
- možnosť dojednať v jednej poistnej zmluve viacero druhov poistenia,
- v každom druhu poistenia je možné zohľadniť individuálne požiadavky poisteného,
- niektoré pripoistenia poskytované bezplatne,
- možnosť nahlasovania poistnej udalosti cez telefón alebo internet,
- obchodná zľava a bonus zohľadňuje komplexnosť poistenia,
- technické zľavy v závislosti od prístupu poisteného k minimalizácii rizika.

2.3. Všeobecná charakteristika poistného plnenia
- 2.3.1. Poistenie budov - čl. 16 VPP-M,
- 2.3.2. Poistenie hnuteľných vecí - čl. 16 VPP-M,
- 2.3.3. Poistenie prerušenia prevádzky - čl. 16 VPP-M, čl.7 ZD-PP a čl. 7 ZD-PP-SE,
- 2.3.4. Poistenie strojov a elektroniky - čl. 9 VPP-SE,
- 2.3.5. Poistenie nákladu - čl. 11 VPP-N,
- 2.3.6. Poistenie prevádzkovej zodpovednosti za škodu - čl. 5 VPP-Z,
- 2.3.7. Poistenie zodpovednosti za škodu cestného dopravcu - čl. 5 VPP-D,
- 2.3.8. Poistenie profesijnej zodpovednosti za škodu - lekári - čl. 5 VPP-L,
- 2.3.9. Poistenie profesijnej zodpovednosti za škodu - ekonomické, právne profesie - čl. 5 VPP-P,
- 2.3.10. Poistenie profesijnej zodpovednosti za škodu - IT - čl. 5 VPP-IT,
- 2.3.11. Stavebné poistenie - čl. 15 VPP-CAR-COM,
- 2.3.12. Poistenie bytových domov - čl. 16 VPP-M a čl. 8 ZD-BD,
- 2.3.13. Poistenie vozidiel autosalónov - čl. 16 VPP-M a čl. 4 ZD-A,
- 2.3.14. Poistenie plodín - čl. 15 VPP-PL,
- 2.3.15. Poistenie Hospodárskych zvierat- čl.17 VPP-HZ,
- 2.3.16 Poistenie zodpovednosti za environmentálnu škodu - čl. 7 VPP-EZ.

2.4. Výluky z poistenia
- 2.4.1. Poistenie budov - čl. 10, 11 a články poistných rizík VPP-M,
- 2.4.2. Poistenie hnuteľných vecí - čl. 10, 11 a články poistných rizík VPP-M,
- 2.4.3. Poistenie prerušenia prevádzky - čl. 10, 11 a články poistných rizík VPP-M čl. 4 ZD-PP a čl. 4 ZD-PP-SE,
- 2.4.4. Poistenie strojov a elektroniky - čl. 4 VPP-SE,
- 2.4.5. Poistenie nákladu - čl. 6 VPP-N,
- 2.4.6. Poistenie prevádzkovej zodpovednosti za škodu - čl. 4 VPP-Z , čl. 3 ods. 5 a čl. 4 ZD-Z,
- 2.4.7. Poistenie zodpovednosti za škodu cestného dopravcu - čl. 4 VPP-D
- 2.4.8. Poistenie zodpovednosti za škodu - lekári - čl. 4 VPP-L,
- 2.4.8. Poistenie zodpovednosti za škodu - profesie - čl. 4 VPP-P,
- 2.4.9. Poistenie profesijnej zodpovednosti za škodu - IT - čl. 4 VPP-IT,
- 2.4.7. Stavebné poistenie - čl. 5 a čl. 13 VPP-CAR-COM,
- 2.4.8. Poistenie bytových domov - čl. 10, 11 a články poistných rizík VPP-M,
- 2.4.9. Poistenie vozidiel autosalónov - čl. 10, 11 a články poistných rizík VPP-M,
- 2.4.10. Poistenie plodín - čl. 5 VPP-PL,
- 2.4.11. Poistenie Hospodárskych zvierat - čl. 2 -7 VPP-HZ,
- 2.4.12. Poistenie zodpovednosti za environmnetálnu škodu - čl. 6 VPP-EZ, čl. 3 ZD-EZ.

2.5. Upozornenie na možnosť sankcií a postihov spojených s poistným plnením
Poisťovateľ je oprávnený znížiť, zamietnuť alebo odmietnuť poistné plnenie, ak poistený porušil povinnosti uvedené v nasledovných ustanoveniach:
- 2.5.1. Poistenie budov - čl. 20 a článkoch poistených rizík VPP-M,
- 2.5.2. Poistenie hnuteľných vecí - čl. 20 a článkoch poistených rizík VPP-M,
- 2.5.3. Poistenie prerušenia prevádzky - čl. 20 a článkoch poistených rizík VPP-M, čl.10 ZD-PP a čl. 10 ZD-PP-SE,
- 2.5.4. Poistenie strojov a elektroniky - čl. 13 VPP-SE,
- 2.5.5. Poistenie nákladu - čl. 15 VPP-N,
- 2.5.6. Poistenie prevádzkovej zodpovednosti za škodu - čl. 9 VPP-Z,
- 2.5.7 Poistenie zodpovednosti za škodu cestného dopravcu - čl. 9 VPP-D,
- 2.5.8. Poistenie zodpovednosti za škodu - lekári - čl. 11 VPP-L,
- 2.5.9. Poistenie profesijnej zodpovednosti za škodu - IT - čl. 11 VPP-IT,
- 2.5.7. Stavebné poistenie - čl. 8 VPP-CAR-COM,
- 2.5.8. Poistenie bytových domov - čl. 20 a články poistných rizík VPP-M,
- 2.5.9. Poistenie vozidiel autosalónov - čl. 20 a články poistných rizík VPP-M,
- 2.5.10. Poistenie plodín - čl. 12 VPP-PL, čl. 19 VPP-PL a čl. 20 VPP-PL,
- 2.5.11. Poistenie Hospodárskych zvierat:
  - poistenie hospodárskych zvierat pre prípad nákazy čl. 8 ods. 9, 10, 11, 12, 13 ZD,
  - poistenie hydiny pre prípad nákazy čl. 8 ods. 8, 9, 10, 11, 12 ZD,
  - poistenie pre prípad jednotlivých škôd na zvieratách čl. 8 ods. 6, 7, 8, 9, 10 ZD.
  - poistenie pre prípad jednotlivých škôd na plemenných [illegible] čl. 8 [illegible] 7, [illegible]

2. [illegible] Poistenie [illegible]

3. Oboznámenie o dôsledkoch nezaplatenia poistného
Poistenie zanikne, ak poistné za prvé poistné obdobie alebo jednorazové poistné nebolo zaplatené do troch mesiacov odo dňa jeho splatnosti. Poistenie zanikne aj tak, že poistné za ďalšie poistné obdobie nebolo zaplatené do jedného mesiaca odo dňa doručenia výzvy poisťovateľa na jeho zaplatenie, ak nebolo poistné zaplatené pred doručením tejto výzvy. Výzva poisťovateľa obsahuje upozornenie, že poistenie zanikne, ak nebude zaplatené. To isté platí, ak bola zaplatená len časť poistného.

4. Doplnkové administratívne služby, ktoré nie sú zahrnuté v cene poistenia a poplatky s nimi spojené a spôsob sprístupňovania informácií o ich zmene
V poistení nie sú uplatňované žiadne ďalšie poplatky súvisiace s doplnkovými administratívnymi službami.

5. Upozornenie na ustanovenia poistnej zmluvy, ktoré umožňujú poisťovateľovi vykonávať zmeny podmienok poistenia bez súhlasu druhej zmluvnej strany

5.1. Poistenie budov - čl. 4 ZD-M umožňuje v prípade dojednania poistenia na novú hodnotu automaticky aktualizovať poistnú sumu budov pre ďalšie poistné obdobie o hodnotu indexu stavebných prác a materiálov.

5.2. Poistenie hnuteľných vecí - čl. 4 ZD-M umožňuje v prípade dojednania poistenia na novú hodnotu automaticky aktualizovať poistnú sumu výrobných a prevádzkových zariadení a cudzích vecí pre ďalšie poistné obdobie o hodnotu indexu spotrebiteľských cien.

6. Podmienky odstúpenia od poistnej zmluvy a vypovedania poistnej zmluvy

6.1. Pri vedomom porušení povinností uvedených v ustanoveniach § 793 Občianskeho zákonníka môže poisťovateľ od poistnej zmluvy odstúpiť, ak pri pravdivom a úplnom zodpovedaní otázok by poistnú zmluvu neuzavrel. Toto právo môže poisťovateľ uplatniť do troch mesiacov odo dňa, keď takú skutočnosť zistil; inak právo zanikne.

6.2. Poistenie zanikne vypovedou:
- 6.2.1 jednej zo zmluvných strán do dvoch mesiacov po uzavretí poistnej zmluvy. Výpovedná lehota je osemdenná, jej uplynutím poistenie zanikne,
- 6.2.2 ku koncu poistného obdobia: výpoveď sa musí dať aspoň 6 týždňov pred jeho uplynutím,
- 6.2.3 jednej zo zmluvných strán do jedného mesiaca odo dňa poskytnutia poistného plnenia alebo jeho zamietnutia. Výpovedná lehota je osemdenná, jej uplynutím poistenie zanikne,
- 6.2.4 do dvoch mesiacov odo dňa, kedy sa poisťovateľ dozvedel o zmene v skutočnostiach, ktoré boli podkladom pri uzavieraní poistnej zmluvy, pokiaľ zmluvné strany neakceptujú uvedené zmeny úpravou poistnej zmluvy; poistenie v takom prípade zanikne doručením výpovede druhej zmluvnej strane.

7. Spôsob vybavovania sťažností

7.1. Poisťovateľ prijíma a rieši sťažnosti podané, proti jeho postupu, ústne alebo písomne. Sťažovateľ môže ústnu a písomnú sťažnosť podať osobne na pracoviskách servisu klientom a v agentúrnych kanceláriách poisťovateľa. Ústnu sťažnosť môže sťažovateľ podať aj na telefónnom čísle 0800 122 222. Ústne podanú sťažnosť poisťovateľ zaznamená. Písomnú sťažnosť môže sťažovateľ zaslať aj emailom na dialog@allianzsp.sk alebo poštou na adresu sídla poisťovateľa.

7.2. Zo sťažnosti musí byť zrejmý dátum jej podania, kto ju podáva, čoho sa týka (predmet sťažnosti) a čoho sa sťažovateľ domáha. Ak je sťažovateľom fyzická osoba, sťažnosť musí obsahovať meno, priezvisko a adresu bydliska fyzickej osoby. Ak je sťažovateľom právnická osoba, sťažnosť musí obsahovať názov alebo obchodné meno a adresu sídla právnickej osoby.

7.3. Poisťovateľ je povinný prešetriť sťažnosť a informovať sťažovateľa o spôsobe vybavenia jeho požiadaviek či dôvodoch ich zamietnutia do 30 dní odo dňa jej doručenia. Ak si vybavenie sťažnosti vyžaduje dlhšie obdobie, je možné lehotu podľa predchádzajúcej vety predĺžiť, o čom bude sťažovateľ bezodkladne upovedomený.

7.4. V prípade, že je sťažnosť podaná opakovane, tým istým sťažovateľom, v rovnakej veci a neobsahuje nové skutočnosti, poisťovateľ nie je povinný sťažnosť vybaviť a sťažovateľa o tom upovedomiť.

Upozornenie poistníka

Informácie uvedené v tomto formulári neobsahujú úplný rozsah práv a povinností, ktorý poistníkovi vyplýva z uzavretia poistnej zmluvy a nenahrádzajú informačné povinnosti ustanovené všeobecne záväznými právnymi predpismi pri predaji [illegible]

Allianz
Slovenská poisťovňa

Doložka
k súhrnnému poisteniu hnuteľných vecí

Poistený (obchodný názov a adresa) Univerzita Konštantína Filozofa v Nitre, Tr. A. Hlinku 1, 94901 Nitra IČO: 00 157 716

Osobitné zmluvné dojednania pre poistenie hnuteľných vecí na viacerých miestach poistenia

1. V prípade poistnej udalosti poisťovateľ poskytne poistné plnenie aj za poškodené, zničené alebo odcudzené poistené veci, ktoré sa nachádzali v niektorom z uvedených miest poistenia.

2. Hornou hranicou poistného plnenia pre predmet poistenia bude súčet poistných súm pre daný predmet poistenia zo všetkých miest poistenia. Poistený je v takomto prípade povinný preukázať druh a hodnotu presunutých vecí.

3. Článok 17 VPP-M sa bude uplatňovať len pre súčty poistných súm jednotlivých predmetov poistenia zo všetkých miest poistenia.

4. Miesta poistenia sú nasledovné adresy:

   a) B.Slančíkovej 1, Nitra
   b) Nábrežie mládeže 91, Nitra
   c) Hodžova 1, Nitra
   d) Kraskova 1, Nitra
   e) Drážovská cesta 2 a 4, Nitra
   f) Tr. A. Hlinku 1, Nitra
   g) Štefánikova ulica 67, Nitra
   h) ŠD UKF Brezový Háj

5. Ostatné ustanovenia VPP-M zostávajú touto doložkou nedotknuté.

V Nitre dňa 9.12.2014

podpis a pečiatka poistiteľa / poisťovníka

...a Konštantína Filozofa v Nitre, Trieda A. Hlinku 1, 949 74 Nitra

...ostatných hnuteľných vecí súčasť prílohy č. 1 k návrhu poistnej zmluvy 9872008084

Projekt (kód ITMS):

	26120130028 - zarad.	26110230026 - zarad.	26220120042 - zarad.	26110230080 - zarad.	26220220110 - zarad.	26250120001 - zarad.	26250120041 - zarad.	26220220033 - zarad.	26110230041 - zarad.	26110230096		26110230050 - zarad.	26110230014 - zarad.	26110230081 - zarad.	26220120051 - zarad.	26110230033 - zarad.	261?0230012 - zarad.	26220220180 - zarad.	26110230022 - zarad.	26250120049		26250120063		26110230114		SPOLU
										zaradený majetok	predpoklad majetku zaradeného v roku 2015									zaradený majetok	predpoklad majetku zaradeného v roku 2015	zaradený majetok	predpoklad majetku zaradeného v roku 2015	zaradený majetok	predpoklad majetku zaradeného v roku 2015	
	1A	2A	3A	4A	5A	6A	7A	8A	9A	10A	10B	11A	12A	13A	14A	15A	16A	17A	18A	19A	19B	20A	20B	21A	21B	×
	47 057,16	45 719,79	283 776,11	6 544,08	712 446,48	2 377 449,04	2 552 022,69	13 595,00	37 082,09	98 847,53	×	84 197,61	26 002,01	26 259,17	53 358,12	26 902,09	56 622,21	2 613,60	66 691,78	120 000,00	×	648,00	×	26 053,62	×	6 663 928,18
	×	×	×	×	×	×	×	×	×	×	1 892,52	×	×	×	×	×	×	×	×	×	88 610,00	×	517 282,25	×	1 582,80	607 475,05
	1.1, 1.2, 1.3, 1.4, 1.5	1.1, 1.2, 1.3, 1.4, 1.5	1.1, 1.2, 1.3, 1.4, 1.5	1.1, 1.2, 1.3, 1.4, 1.5	1.1, 1.2, 1.3, 1.4, 1.5	1.1, 1.2, 1.3, 1.4, 1.5	1.1, 1.2, 1.3, 1.4, 1.5	1.1, 1.2, 1.3, 1.4, 1.5	1.1, 1.2, 1.3, 1.4, 1.5	1.1, 1.2, 1.3, 1.4, 1.5	1.1, 1.2, 1.3, 1.4, 1.5	1.1, 1.2, 1.3, 1.4, 1.5	1.1, 1.2, 1.3, 1.4, 1.5	1.1, 1.2, 1.3, 1.4, 1.5	1.1, 1.2, 1.3, 1.4, 1.5	1.1, 1.2, 1.3, 1.4, 1.5	1.1, 1.2, 1.3, 1.4, 1.5	1.1, 1.2, 1.3, 1.4, 1.5	1.1, 1.2, 1.3, 1.4, 1.5	1.1, 1.2, 1.3, 1.4, 1.5	1.1, 1.2, 1.3, 1.4, 1.5	1.1, 1.2, 1.3, 1.4, 1.5	1.1, 1.2, 1.3, 1.4, 1.5	1.1, 1.2, 1.3, 1.4, 1.5	1.1, 1.2, 1.3, 1.4, 1.5	×
	2.1; 2.3; 2.4; 2.5	2.1; 2.3; 2.4; 2.5	2.1; 2.3; 2.4; 2.5	2.1; 2.3; 2.4; 2.5	2.1; 2.3; 2.4; 2.5	2.1; 2.3; 2.4; 2.5	2.1; 2.3; 2.4; 2.5	2.1; 2.3; 2.4; 2.5	2.1; 2.3; 2.4; 2.5	2.1; 2.3; 2.4; 2.5	2.1; 2.3; 2.4; 2.5	2.1; 2.3; 2.4; 2.5	2.1; 2.3; 2.4; 2.5	2.1; 2.3; 2.4; 2.5	2.1; 2.3; 2.4; 2.5	2.1; 2.3; 2.4; 2.5	2.1; 2.3; 2.4; 2.5	2.1; 2.3; 2.4; 2.5	2.1; 2.3; 2.4; 2.5	2.1; 2.3; 2.4; 2.5	2.1; 2.3; 2.4; 2.5	2.1; 2.3; 2.4; 2.5	2.1; 2.3; 2.4; 2.5	2.1; 2.3; 2.4; 2.5	2.1; 2.3; 2.4; 2.5	×
	16,55	16,07	99,75	2,30	250,42	835,67	897,04	4,78	13,03	34,74	0,67	29,59	9,14	9,23	18,76	9,46	19,90	0,92	23,44	42,17	31,14	0,23	181,82	9,16	0,56	2536,52

Základná sadzba poistného **0,3516 €**

1.1 požiar + komplexný živel - spoluúčasť 100 EUR
1.2 poistenie skiel - spoluúčasť 100 EUR
1.3 škody na stavebných súčastiach budovy vrátane krádeže na 1. riziko na sumu 5 000 EUR, spoluúčasť 100 EUR
1.4 vandalizmus - spoluúčasť 100 EUR, nezistený páchateľ
1.5 krádež - spoluúčasť 100 EUR

...ma vstupov:
2.1 základné mechanické zabezpečenie pevnými dverami uzamykateľnými bezpečnostnou profilovou cylindrickou vložkou
2.2 základné mechanické zabezpečenie pevnými dverami uzamykateľnými visiacim zámkom
2.3 elektrické posuvné dvere s elektromechanickým zámkom
2.4 pripojenie na pult centrálnej ochrany
2.5 bežné stavebné prvky, cez ktoré nie je možné vniknúť bez ich poškodenia

dňa 9.12.2014

Meno a podpis oprávneného zástupcu

22003705	0	Kvapalinový chromatograf s hmotn.spektrom Agilen	EA	103309	NMA00070		DEABM02023	327 840,00	-273 200,00	54 640,00	13.09.2011
22003706	0	Výškomer s laser.a ultrazvuk. diaľkomerom Vertex	EA	103303	THC00200		202826	2 484,00	-2 071,00	413,00	13.09.2011
22003707	0	Zberač údajov pre termálny komfort so snímačmiQT	EA	103304	THA00140	Mitterpach Klement	TKK080018	60 960,00	-50 800,00	10 160,00	13.09.2011
22003708	0	Laboratórny guľový mlyn PM100	EA	103304	THA0115A	Trník Anton RNDr. PhD.	1211030858H	8 088,00	-6 741,00	1 347,00	13.09.2011
22003709	0	Sitovací stroj s analytickými sitami	EA	103304	THA0115A	Trník Anton RNDr. PhD.	1211110816	7 296,00	-6 081,00	1 215,00	13.09.2011
22003725	0	Kopírovací stroj dig.Sharp MX-2310U,farebný	EA	103303	THC00200		1500623Y	4 549,61	-2 941,00	1 608,61	19.06.2012
22003729	0	Fotoaparát Nikon D300s+prísluš.	EA	103303	OS.KARTY	Rózová Zdenka prof. Ing. CSc.	6103504	3 439,27	-2 008,00	1 431,27	10.09.2012
22003745	0	Tablet profesion.PANASONIC Toughbook CF	EA	103304	THA00140	Mitterpach Klement	3CKCA09023	3 960,00	-1 735,00	2 225,00	22.04.2013
22003746	0	Tablet profesion.PANASONIC Toughbook CF	EA	103309	OS.KARTY	Petrovičová ida doc. Ing. PhD.	3CKCA09026	3 960,00	-1 735,00	2 225,00	22.04.2013
22003747	0	Tablet profesion.PANASONIC Toughbook CF	EA	103303	OS.KARTY	Rózová Zdenka prof. Ing. CSc.	3CKCA09170	3 960,00	-1 735,00	2 225,00	22.04.2013
22003748	0	Tablet profesion.PANASONIC Toughbook CF	EA	103303	OS.KARTY	Pucherová Zuzana Mgr. PhD.	3CKCA09153	3 960,00	-1 735,00	2 225,00	22.04.2013
22003781	0	Prijímač prof.GPS Topcon GRS-1	EA	103303	THC00200		596-20058	9 999,60	-3 751,00	6 248,60	02.07.2013
22003788	0	Binokulárny mikroskop B353LD2 Optika	EA	103303	THC00200		368402	3 283,60	-1 233,00	2 050,60	15.07.2013
22003789	0	Skener FOCUS 3D-S120	EA	103303	THC00200		LLS061202556	38 000,00	-14 251,00	23 749,00	24.07.2013
								712 446,48			

Projekt: Enviromentálne aspekty urbanizovaného prostredia
Kód ITMS: 26220220110

Príloha č. 5A

Inv.majetok	Podč	Označenie IM	DI	Nákl.str.	Lokalita	Zodpovedná osoba	Sériové číslo	Obstarávacia cena	Bežný odpis	Akt.účt.hod.	Dátum zaradenia
90053971	0	Profi meteo stanica	EA	103303	THC00200			588,00	0,00	588,00	29.09.2011
90053972	0	Profi meteo stanica	EA	103304	THA00140	Mitterpach Klement		588,00	0,00	588,00	29.09.2011
90053973	0	Bezkontaktný infračervený teplomer s vlhkomerom	EA	103303	THC00200		1333196/1107	1 500,00	0,00	1 500,00	29.09.2011
90053974	0	Bezkontaktný infračervený teplomer s vlhkomerom	EA	103303	THC00200		1333200/1107	1 500,00	0,00	1 500,00	29.09.2011
90053975	0	Sektorová priemerka	EA	103303	THC00200		403625	480,00	0,00	480,00	29.09.2011
90053976	0	Technické váhy	EA	103303	THC00200		W1107033	480,00	0,00	480,00	29.09.2011
90053977	0	USB Data Logger	EA	103303	THC00200		11030125	96,00	0,00	96,00	29.09.2011
90053978	0	USB Data Logger	EA	103303	THC00200		11030091	96,00	0,00	96,00	29.09.2011
90053979	0	USB Data Logger	EA	103303	THC00200		11030092	96,00	0,00	96,00	29.09.2011
90053980	0	USB Data Logger	EA	103303	THC00200		11030088	96,00	0,00	96,00	29.09.2011
90053981	0	USB Data Logger	EA	103303	THC00200		11030189	96,00	0,00	96,00	29.09.2011
90053982	0	USB Data Logger	EA	103303	THC00200		11030087	96,00	0,00	96,00	29.09.2011
90053983	0	USB Data Logger	EA	103303	THC00200		11030023	96,00	0,00	96,00	29.09.2011
90053984	0	USB Data Logger	EA	103303	THC00200		11030098	96,00	0,00	96,00	29.09.2011
90053985	0	USB Data Logger	EA	103303	THC00200		11030005	96,00	0,00	96,00	29.09.2011
90053986	0	USB Data Logger	EA	103303	THC00200		11030090	96,00	0,00	96,00	29.09.2011
90053987	0	USB Data Logger	EA	103303	THC00200		11030041	96,00	0,00	96,00	29.09.2011
90053988	0	USB Data Logger	EA	103303	THC00200		11030096	96,00	0,00	96,00	29.09.2011
90057453	0	Tablet WACOM Intuos4 XL CAD	EA	103303	THC00200			756,00	0,00	756,00	29.04.2013
90057514	0	Notebook Dell Latitude E5530	EA	103303	OS.KARTY	Rózová Zdenka prof. Ing. CSc	7NHFZW1	999,60	0,00	999,60	29.04.2013
90000062	0	SW: ArcGIS Desktop Advanced Single Use	EA	103303	OS.KARTY	Rózová Zdenka prof. Ing. CSc		4 752,00	2 278,00	2 474,00	01.02.2013
90000064	0	SW: SAS Education Analytical Suite	EA	103303	THC00200			3 999,60	1 751,00	2 248,60	26.04.2013
90000065	0	SW: AutoCAD 2013 new	EA	103308	OS.KARTY	Ďuriš Viliam RNDr. PhD.		6 499,20	2 844,00	3 655,20	26.04.2013
90003692	0	Plnoautomatický spektrofluorimeter s príslušenstvo	EA	103303	OS.KARTY	Rózová Zdenka prof. Ing. CSc		39 360,00	32 800,00	6 560,00	13.09.2011
90003693	0	Termometrická kamera Guide Infrared TP8	EA	103306	THC00170		FL1109M004	24 480,00	20 400,00	4 080,00	13.09.2011
90003694	0	Planimeter LI-3100C Area Meter	EA	103303	THC00200		8516	17 940,00	14 951,00	2 989,00	13.09.2011
90003695	0	Anemometer s multifunkč. sondami VelociCalc 9555	EA	103303	THC00200		LAM1875	2 160,00	1 800,00	360,00	13.09.2011
90003696	0	Stolný digestor Ekostar Flow HF-V	EA	103303	THC00200		9565P1130014	2 880,00	2 400,00	480,00	13.09.2011
90003697	0	Digitálna priemerka Digitech Professional Haglof	EA	103303	THC00200		70/2011-A	3 480,00	2 901,00	579,00	13.09.2011
90003698	0	Elektronický dendrometer Criterion RD 1000	EA	103303	THC00200		24582	2 484,00	2 071,00	413,00	13.09.2011
90003699	0	Autokláv Tuttnauer 2540 EL	EA	103303	THC00200		RD000882	5 160,00	2 868,00	2 292,00	13.09.2011
90003700	0	Multikompon.analyzátor a plynové senzory AQM60	EA	103303	THC00200		2809859	90 192,00	75 161,00	15 031,00	13.09.2011
90003701	0	Prenosné kompaktné laboratorium s testami	EA	103303	OS.KARTY	Vanková Viera Ing. PhD	8533113013	2 076,00	1 732,00	344,00	13.09.2011
90003702	0	Luxmeter Testo 545	EA	103303	THC00200		1.11151.0001HC0797	2 340,00	1 951,00	389,00	13.09.2011
90003703	0	Luxmeter Testo 545	EA	103304	THA00140	Mitterpach Klement	2132320	2 340,00	1 951,00	389,00	13.09.2011
90003704	0	Izomet s prídavými sondami M2114	EA	103304	THA0115A	Trnik Anton RNDr. PhD.	2132363	12 480,00	10 400,00	2 080,00	13.09.2011
							9511030105				

Univerzita Konštantína Filozofa v Nitre, Trieda A. Hlinku 1, 949 74 Nitra

Predmet zákazky: Poistenie nehnuteľného a hnuteľného majetku na UKF v Nitre na rok 2015

Návrh na plnenie kritérii:

Majetok	Základná sadzba poistného	Ročné poistné
Nehnuteľný	0,2267	9 188,22 €
Hnuteľný	0,3516	2 556,52 €
SPOLU	x	**11 744,74 €**

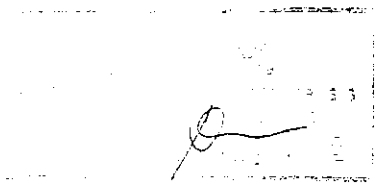

Klient/VOJ: Univerzita Konštantína Filozofa v Nitre
ID klienta/VOJ: 2882
IČO klienta/VOJ: 00157716
Adresa klienta/VOJ: Tr. Andreja Hlinku 1, 94974 Nitra

TATRA BANKA
POKLADNICA

Výpis číslo: 241
Dátum výpisu: 22.12.2014
Účet: SK84 8180 0000 0070 0024 0831
BIC: SPSRSKBA
Názov účtu: Bežný účet neúročený dotačný UKF v Nitre
Produkt: BÚ neúročený
Mena účtu: EUR

Obdobie výpisu: 22.12.2014 - 22.12.2014
Začiatočný stav:
Konečný stav:

Obraty na výpise	Počet	Suma
Obraty debet:		
Obraty kredit:		
Obraty spolu:		

Sumarizácia poplatkov

Názov	Počet	Suma
Poplatok za prevod ZPS	1	5.00 EUR

22.12.2014	408143437	SK17 1100 0000 0026 2600 6702	TATRSKBXXXX	ALLIANZ-SLOVENSKA POISTOVNA	
22.12.2014	Hrom. PP na úhradu				
22.12.2014	9872008084				
Allianz-poistenie majetku r. 2015		3558		-11 744,74 EUR	-11 744,74 EUR

INTERNÝ PREVOD

PRÍLOHA č. 13

UNIVERZITA KONŠTANTÍNA FILOZOFA V NITRE

číslo účtovného dokladu KDF

LIKVIDAČNÝ LIST FAKTÚRY

Dátum vystavenia faktúry: 22.12.2015	číslo knihy faktúr:	2015106577	
Dodávateľ: 100133	číslo faktúry (var. symbol):	9873010993	
	splatnosť dňa:	31.12.2015	KS: 3558
ALLIANZ-SLOVENSKÁ POISŤOVŇA	spolu za faktúru:	10.252,68 EUR	
Dostojevského rad 4	predmet dodávky:		
815 74 Bratislava	*Allianz-poistenie majetku a budov r.2016		

Predbežná finančná kontrola v zmysle zákona č. 502/2001 Z.z. o finančnej kontrole a vnútornom audite a o zmene a doplnení niektorých zákonov v znení neskorších predpisov:

1. Výber dodávateľa je / ~~nie je~~ v súlade so zákonom č. 25/2006 Z.z. o verejnom obstarávaní a o zmene a doplnení niektorých zákonov v znení neskorších predpisov a smernicou č. ....13/15.. o verejnom obstarávaní a nákupe tovarov, služieb a prác na UKF v Nitre.

Zmluva/objednávka č. ZoL-2015-2/3991-2094: 9100 6

je / ~~nie je~~ v súlade s výsledkom verejného obstarávania.

Použitý postup vo verejnom obstarávaní a referentské číslo spisu: CP199/15 — 22. DEC. 2015 (dátum) — vedúci OOB/vedúci UJ

2. Finančná operácia alebo jej časť je / ~~nie je~~ z hľadiska formálnej, vecnej, číselnej stránky, úplnosti a správnosti dokladov v súlade s uzatvorenou zmluvou č.: ..... objednávkou č.:

...esp. iným dokladom a potvrdzujem účelnosť vynaloženia finančných prostriedkov

dátum	vedúci projektu (za vecnú správnosť)	dátum	vedúci objed. pracoviska (za vecnú správnosť)	dátum	zamestnanec FO (za formálnu správnosť)
.....	.....	21.12.2015	.....	22. DEC. 2015	.....

3. Finančná operácia alebo jej časť je / ~~nie je~~ v súlade:

- s rozpočtom projektu/zmluvou č.: ..... dátum ..... vedúci projektu
- s rozpočtom pracoviska ..... dátum ..... vedúci pracoviska
- s rozpočtom ~~fakulty~~ /R,CUP
- so smernicou o obehu ekon. dokladov č. 17/2015
- s interným predpisom č.: .....
- je finančne krytá

22. DEC. 2015 (dátum) — vedúci FO/~~tajomník~~

4. Finačná operácia alebo jej časť v zmysle bodov 1., 2. a 3. spĺňa / nespĺňa podmienky hospodárnosti, efektívnosti, účelnosti a účinnosti použitia fin. prostriedkov

22 DEC. 2015 (dátum) — kvestor

Platobný príkaz:

z účtu: **7000240831 / 8180**

na účet: **2626006702 / 1100**

kód firemnej banky: **1000**

čiastka k úhrade: 10.252,68

Schválenie platby: 22. DEC. 2015 (dátum) — vedúci FO

ID ŠP:

Dátum úhrady v ŠP: 23 DEC. 2015

zodpovedný zamestnanec FO

Účtovací predpis:

	Účet HK	F	FO	FP	Program	FS	NS	PU	Čiastka
D	321110			T6				1900	10.252,68
MD	381100	111	09412	637015	0771199	191099		1900	8.016,22
MD	381100	111	09412	637015	0771199	191099		1900	2.236,46

predkontoval:		zaúčtoval:		schválil:	
22 DEC. 2015		22. DEC. 2015		- 7. JAN. 2016	
dátum	podpis	dátum	podpis	dátum	podpis

Zaevidované v dlhodobom majetku / inv. číslo:

Zaevidované v drobnom majetku / inv. číslo:

dátum / podpis

Príloha č.2

Univerzita Konštantína Filozofa v Nitre, Trieda A. Hlinku 1, 949 74 Nitra

…tenie hnuteľného majetku na UKF v Nitre na rok 2016

	Projekt (kód ITMS):																				
	26120130028	26110230026	26220120042	26110230080	26220220110	26250120041	26220220033	26110230041	26110230096	26110230050	26110230014	26110230081	26220120051	26110230033	26110230012	26220220180	26110230022	26250120049	26250120063	26110230114	SPOLU
…nota …teného …etku	47 097,16	45 719,79	283 776,11	6 544,08	712 446,48	2 554 933,89	13 595,00	37 158,90	105 323,49	84 413,41	26 002,01	26 259,17	53 358,17	26 902,59	34 526,18	3 124 728,00	66 691,78	168 888,[illegible]	500 755,76	27 636,42	7 946 756,56
…né poistné	13,25 €	12,87 €	79,86 €	1,84 €	200,50 €	719,04 €	3,83 €	10,46 €	[illegible]	23,76 €	7,32 €	7,39 €	15,02 €	7,57 €	9,72 €	879,39 €	18,77 €	[illegible]	140,93 €	7,78 €	**2 236,46 €**

…né riziká   požiar do výšky poistovaného majetku   spoluúčasť 300 EUR   Základná sadzba poistného 0,2814 €

…akter hnuteľného majetku:
Informačno-komunikačné technológie, prístroje, kancelárske zariadenia, nábytok, učebné pomôcky a pod.

…sob zabezpečenia vstupov do budov, v ktorých sa nachádza poistovaný hnuteľný majetok
do budovy: základné mechanické zabezpečenie pevnými dverami uzamykateľnými bezpečnostnou profilovou cylindrickou vložkou
elektrické posuvné dvere s elektromechanickým zámkom
pripojenie na pult centrálnej ochrany
…né otvory: bežné stavebné prvky, cez ktoré nie je možné vniknúť bez ich poškodenia

V …tre   dňa 15.12.2015

Kristína Divinčová

Obchodné meno: Allianz SP a.s.   Meno a podpis oprávneného zástupcu

za FPV celková suma … €

46 09412 0-06-103/0001-00 109399

Allianz
Slovenská poisťovňa

Allianz – Slovenská poisťovňa, a. s
Ústredie

Univerzita Konštantína Filozofa v Nitre
Trieda Andreja Hlinku 1
Nitra
94901

Dátum: 15.12.2015
Kontakt: R.I.C. Slovakia, s.r.o.
Tel.:
Vec: **Výmer poistného k poistnej zmluve** 9873010993

V zmysle poistnej zmluvy poistenia podnikateľov, zasielame údaje pre úhradu poistného bankovým prevodom.

Poistné: 10252,68 EUR za obdobie od 01.01.2016 do 31.12.2016 .

Na úhradu poistného môžete použiť predtlačený príkaz na úhradu. Platbu môžete uskutočniť aj vkladom na účet v Tatra banke číslo SK17 1100 0000 0026 2600 6702, BIC: TATRSKBX, s variabilným symbolom 9873010993.

S pozdravom

Finančné oddelenie
22. 12. 2015
UKF v Nitre

Ing. Miroslav Pacher
člen predstavenstva

Branislav Martinka
riaditeľ odboru firemných klientov

Príkaz k úhrade

Banke Pobočke

Bankové spojenie		Mena	Symbol		
IBAN - číslo účtu platiteľa	BIC - kód banky platiteľa				
IBAN - číslo účtu príjemcu	BIC - kód banky príjemcu	Čiastka EUR	Variabilný	Konštantný	Špecifický
SK1711000000002626006702	TATRSKBX	10252,68	9873010993	3558	
Doplňujúce údaje banky		Údaje pre vnútornú potrebu príkazcu			
		Univerzita Konštantína Filozofa v Nitre			

Dátum splatnosti

V dňa pečiatka a podpis:

SÚHRNNÝ NÁVRH POISTNEJ ZMLUVY
PP01

Poistná zmluva je uzavretá podpisom tohto návrhu oboma zmluvnými stranami

× Nová poistná zmluva

☐ Zmena poistnej zmluvy číslo

uzatvorenej dňa . .

V prípade dojednania zmeny poistnej zmluvy, uveďte dôvod zmeny:

☐ Náhrada poistnej zmluvy číslo

Nahrádzaná poistná zmluva zaniká dňom, ktorý predchádza dňu vzniku poistenia novej poistnej zmluvy. Uveďte dôvod náhrady:

Nespotrebované poistné z nahrádzanej poistnej zmluvy sa: ☐ vráti poistníkovi

☐ prevedie na nahradzujúcu poistnú zmluvu

9873010993

Rekapitulácia poistného

☒ Poistenie majetku	počet príloh: 1	poistné celkom:	24 123,95	EUR
☐ Poistenie strojov - technické riziká	počet príloh: 0	poistné celkom:	0,00	EUR
☐ Poistenie prerušenia prevádzky	počet príloh: 0	poistné celkom:	0,00	EUR
☐ Poistenie nákladu	počet príloh: 0	poistné celkom:	0,00	EUR
☐ Poistenie vozidiel autosalónov	počet príloh: 0	poistné celkom:	0,00	EUR
☐ Poistenie hospodárskych zvierat	počet príloh: 0	poistné celkom:	0,00	EUR
☐ Poistenie plodín	počet príloh: 0	poistné celkom:	0,00	EUR
☐ Prevádzková zodpovednosť za škodu	počet príloh: 0	poistné celkom:	0,00	EUR
☐ Zodpovednosť za environmentálnu škodu	počet príloh: 0	poistné celkom:	0,00	EUR
☐ Zodpovednosť za škodu cestného dopravcu	počet príloh: 0	poistné celkom:	0,00	EUR
☐ Profesijná zodpovednosť za škodu - lekári	počet príloh: 0	poistné celkom:	0,00	EUR
☐ Profesijná zodpovednosť za škodu - ekonom., právne profesie	počet príloh: 0	poistné celkom:	0,00	EUR
☐ Profesijná zodpovednosť za škodu - IT	počet príloh: 0	poistné celkom:	0,00	EUR
☐ Poistenie bytových domov	počet príloh: 0	poistné celkom:	0,00	EUR
☐ Stavebné poistenie	počet príloh: 0	poistné celkom:	0,00	EUR

Výpočet poistného

Celkové poistné: 24 123,95 EUR

(V prípade nepriaznivého škodového priebehu v predchádzajúcom poistnom období bonus na nasledujúce poistné obdobie zaniká v plnej výške).

Obchodná zľava: 37,5 % + Bonus: 20 % = 57,5 %

Minimálne poistné: 100,00 EUR

Celkové poistné po zľave (CP): 10 252,68 EUR

Vznik a zánik poistenia /zmena poistenia

Vznik poistenia / Zmena poistenia od 01.01.2016 00:00 hodín

☐ Poistenie je dlhodobé na dobu neurčitú. *(Poistné obdobie je 1 rok a predlžuje sa o ďalší rok, pokiaľ nedôjde k výpovedi poistenia.)*

☒ Poistenie je na dobu určitú do: 31.12.2016

Bežné poistné

Poistné obdobie: ☐ bežný rok ☐ kalendárny rok Výročný deň (deň a mesiac): . .

(Prvý deň dojednaného poistného obdobia. Pre kalendárny rok: 01.01.)

☐ ročná splátka CP ☐ polročné splátky 1/2 CP x prirážka 3% ☐ štvrťročné splátky 1/4 CP x prirážka 5% Ľahotné poistné: 10 252,68 EUR

Jednorazové poistné

☒ splátka naraz ☐ splátka v splátkach - 1. splátka: . . vo výške: EUR

2. splátka: . . vo výške: EUR

3. splátka: . . vo výške: EUR

Údaje pre platbu poistného

☒ Bankovým prevodom ☐ V hotovosti - doklad č.: 333

Bankové spojenie: SK17 1100 0000 0026 2600 6702 BIC: TATRSKBX

Pre platbu prvého poistného uvádzajte ako variabilný symbol číslo tohto návrhu na poistenie (uvedené vyššie). Pre platbu následného poistného uvádzajte ako variabilný symbol číslo poistnej zmluvy, ktoré Vám bude oznámené na tlačive Poistka. Bežné poistné je splatné prvým dňom poistného obdobia a jednorazové poistné dňom vzniku poistenia. V prípade dojednania platenia bežného poistného vo forme ročných/polročných /štvrťročných splátok, prvá splátka poistného je splatná v deň vzniku poistenia. Každá ďalšia splátka poistného je splatná v deň, ktorý sa svojim číselným označením zhoduje s výročným dňom poistenia, a to dvanásteho/šiesteho/tretieho mesiaca nasledujúceho po splatnosti predchádzajúcej splátky poistného.V prípade dojednania platenia jednorazového poistného vo forme individuálnych splátok sú splátky splatné v dojednaných termínoch splatnosti.

Vyhlásenie oprávneného zástupcu poistovateľa

Vyhlasujem, že som overil totožnosť klienta podľa dokladu totožnosti.

Miesto uzavretia poistnej zmluvy/zmeny poistnej zmluvy

Nitra

Dátum uzavretia poistnej zmluvy/zmeny poistnej zmluvy

15.12.2015

Allianz - Slovenská poisťovňa, a.s.

podpis a otlačok pečiatky poistníka

podpis a otlačok pečiatky oprávneného zástupcu poistovateľa

Kristina Divincova

Poistenie majetku

Miesto poistenia:

Ulica č.: vid' prílohu č. 1 a 2

Miesto: Nitra PSČ: 94974

Popis miesta poistenia:

Popis miesta poistenia

1. Miesto poistenia sa nachádza: × vo vnútri obce ☐ v priem. zóne ☐ na okraji obce ☐ na samote

2. Bol v mieste poistenia alebo v jeho bezprostrednej blízkosti zaznamenaný zosuv pôdy? ☐ áno × nie — ak áno, výluka podľa VPP-V

3. Bola v mieste poistenia povodeň v uplynulých 10 rokoch častejšie ako jedenkrát? ☐ áno × nie

a) Poistenie budov

Popis predmetu poistenia:

Predmet poistenia - popis — kód činnosti: 81000

	Objekt č.	Popis (číslo JKSO prip. KS)	Poistná suma [EUR]
× budova ☐ časť budovy ☐ stav. úpravy	1	zoznam budov	38 942 783,73

Rok uvedenia do prevádzky/celkovej rekonštrukcie:

Vedľajšie budovy, stavby, technologické zariadenia, nezahrnuté v poistnej sume objektu:

Č. listu vlastníctva: Katastrálne úz.:

Spôsob využitia stavebného objektu (podiel plochy jednotlivých prevádzok na celkovej ploche):

× > 50 % školy, škôlky

☐ do 50 %

☐ do 25 %

☐ do 10 %

Celková plocha objektu (m²): ... alebo obstavaný priestor (m³): ...

Požiarna odolnosť konštrukcie: × A odolná, B čiastočne odolná ☐ C neodolná

Základné poistenie:

Celková poistná suma: 38 942 783,73 EUR (súčet a1), a2), a3), a4)) × v novej hodnote ☐ v časovej hodnote

Poistené riziko:	požiar ×	voda ×	víchrica ×	živel ×	ostatné ×	Poistné spolu [EUR]
sadzba [‰]:	0,09	0,14	0,09	0,15	0,05	
poistné [EUR]:	3 504,85	5 451,99	3 504,85	5 841,42	1 947,14	20 250,25
spoluúčasť [EUR]:	100	100	100	100	100	

Spoluúčasť:

Prirážky /zľavy:

Dotazník (otázka č. 1 a 2 sa vypĺňajú vždy):
Prirážky/zľavy (uplatňujú sa iba pre poistnú sumu nad 200 000 EUR):
(poistné za prirážku sa uvádza s kladnou, za zľavu so zápornou hodnotou)

			Poistené riziko: požiar	voda	víchrica	živel	ostatné	Poistné spolu [EUR]
1. Je v budove viac ako 50% nevyužívanej plochy, resp. je budova viac ako 1 mesiac neobývaná / nepoužívaná?	☐ áno × nie	prirážka [%]:	0,00					0,00
		poistné [EUR]:						
2. Je budova vo výstavbe, v rekonštrukcii alebo na svoj účel nepoužiteľná?	☐ áno × nie	prirážka [%]:						0,00
		poistné [EUR]:						
3. Je dojazd profesionálnych hasičov do 5 minút, bez prekážok príjazdu? Najbližší hasičský zbor – miesto: NR vzdialenosť (v km): 5	× áno ☐ nie	zľava [%]:	10,00	x	x	x	x	-350,49
		poistné [EUR]:	-350,49	x	x	x	x	
4. Je budova na mieste s nočným osvetlením/oplotením alebo prístup do budovy je trvalo (24 hod. denne) kontrolovaný (vrátnik, strážnik, SBS) ?	× áno ☐ nie	zľava [%]:	10,00	x	x	x	x	-350,49
		poistné [EUR]:	-350,49	x	x	x	x	
5. Platí zákaz fajčenia v celej budove?	× áno ☐ nie	zľava [%]:	5,00	x	x	x	x	-175,24
		poistné [EUR]:	-175,24	x	x	x	x	
6. Je v budove funkčná elektrická požiarna signalizácia s napojením na miesto pod stálou kontrolou osoby schopnej reagovať na prijaté hlásenie?	☐ áno × nie	zľava [%]:		x	x	x	x	0,00
		poistné [EUR]:		x	x	x	x	
7. Sú v budove inštalované sprinklerové hasiace zariadenia?	☐ áno × nie	zľava [%]:		x	x	x	x	0,00
		poistné [EUR]:		x	x	x	x	
8. Zlomkové poistenie - limity plnenia: (čl. 6 ods. 6 ZD-M) × voda, 1 947 139,00 EUR, t.j. 5 % z poistnej sumy × víchrica, 11 682 835,00 EUR, t.j. 30 % z poistnej sumy		zľava [%]:	x	20,00	5,00	x	x	-1 265,64
		poistné [EUR]:	x	-1 090,40	-175,24	x	x	
9. Zľava za vyššiu spoluúčasť: ×		zľava [%]:	0,00	0,00	0,00	0,00	0,00	0,00
		poistné [EUR]:	0,00	0,00	0,00	0,00	0,00	

Poistné za prirážky/zľavy: -2 141,86

Poistné za časť a) poistenie budov: 18 108,39

c) Pripoistenia

Pripoistenia:

Pripoistenia: (dojednávajú sa na prvé riziko v zmysle čl. 14 ods. 4 VPP-M)	Poistná suma [EUR] (zvýšenie hornej hranice plnenia)		Poistené riziko: požiar	voda	víchrica	krádež	živel	ostatné	Poistné spolu [EUR]
1. Vypratávacie náklady (čl. 6 ods. 1 písm. a) ZD-M) v základnom poistení kryté do 1 000 EUR	1 000	sadzba [‰]:	1,50	0,50	0,50	0,15	0,50	0,15	3,30
		poistné [EUR]:	1,50	0,50	0,50	0,15	0,50	0,15	
2. Stavebné súčasti budovy-krádež, vandalizmus (čl. 6 ods. 1 písm. b) ZD-M) v základnom poistení kryté do 1 000 EUR	10 000	sadzba [‰]:	x	x	x	50,00	x	x	500,00
		poistné [EUR]:	x	x	x	500,00	x	x	
3. Zvonku budovy umiestnené predmety (čl. 6 ods. 1 písm. c) ZD-M) v základnom poistení kryté do 1 000 EUR	0	sadzba [‰]:	x	x	0,00	x	x	x	0,00
		poistné [EUR]:	x	x	0,00	x	x	x	
4. Demontáž, remontáž nepoškodených stavebných súčastí (čl. 6 ods. 1 písm. d) ZD-M) v zákl. poistení kryté do 1 000 EUR	0	sadzba [‰]:	0,00	0,00	0,00	0,00	0,00	0,00	0,00
		poistné [EUR]:	0,00	0,00	0,00	0,00	0,00	0,00	
5. Cennosti v trezore (čl. 6 ods. 2 písm. a) ZD-M) v základnom poistení hnut. vecí kryté do 1 000 EUR	0	sadzba [‰]:	0,00	0,00	0,00	0,00	0,00	0,00	0,00
		poistné [EUR]:	0,00	0,00	0,00	0,00	0,00	0,00	
6. Cennosti pri preprave (čl. 6 ods. 2 písm. a) ZD-M) v základnom poistení hnut. vecí kryté do 1 000 EUR	0	sadzba [‰]:	x	x	x	0,00	x	x	0,00
		poistné [EUR]:	x	x	x	0,00	x	x	
7. Umelecké predmety (čl. 6 ods. 2 písm. b) ZD-M) v základnom poistení hnut. vecí kryté do 1 000 EUR	0	sadzba [‰]:	0,00	0,00	0,00	0,00	0,00	0,00	0,00
		poistné [EUR]:	0,00	0,00	0,00	0,00	0,00	0,00	
8. Výstavné modely (čl. 6 ods. 2 písm. b) ZD-M) v základnom poistení hnut. vecí kryté do 1 000 EUR	0	sadzba [‰]:	0,00	0,00	0,00	0,00	0,00	0,00	0,00
		poistné [EUR]:	0,00	0,00	0,00	0,00	0,00	0,00	
9. DPH (iba ak poistený je platcom DPH) (čl. 10 ods. 5 písm. b) VPP-M)	0	sadzba [‰]:	x	x	x	0,00	x	x	0,00
		poistné [EUR]:	x	x	x	0,00	x	x	
10. Obnova dát (čl. 6 ods. 2 písm. c) ZD-M) v základnom poistení hnut. vecí kryté do 1 000 EUR	2 000	sadzba [‰]:	1,00	0,25	0,10	7,50	0,50	0,15	19,00
		poistné [EUR]:	2,00	0,50	0,20	15,00	1,00	0,30	
11. Výmena zámkov vstup. dverí po strate kľúča (čl. 6 ods. 3 ZD-M) v základnom poistení hnut. vecí kryté do 1 000 EUR	0	sadzba [‰]:	x	x	x	0,00	x	x	0,00
		poistné [EUR]:	x	x	x	0,00	x	x	
12.	0	sadzba [‰]:	0,00	0,00	0,00	0,00	0,00	0,00	0,00
		poistné [EUR]:	0,00	0,00	0,00	0,00	0,00	0,00	

Poistné za časť c) pripoistenia: 522,30

d) Poistenie skla

Sklo:

Poistenie rizika rozbitia skla:	Poistná suma [EUR]		sadzba [‰]	spoluúčasť [EUR]	Poistné [EUR]
	5 000,00	☐ stanovená paušálne z poistnej sumy budovy ☐ stanovená súborom (vonkajšie, vnútorné sklá) × stanovená na 1. riziko	50,00	100,00	250,00

Zľavy:	zľava [%]	
1. Dojednaná vyššia spoluúčasť	0,00	0,00
2.	0,00	0,00

Pripoistenia (dojednávajú sa na prvé riziko v zmysle čl. 14 ods. 4 VPP-M):	Poistná suma [EUR]	sadzba [‰]	Poistné [EUR]
13. Firemné štíty, povrchová úprava zasklenia, provizórna oprava zasklenia, lešenie a iné stavebné prostriedky, de- /remontáž stavebných súčastí (čl. 10 ods. 6 písm. b) až f) VPP-M)	0,00	0,00	0,00

Poistné za časť d) poistenie skla: 250,00

Súhrnné poistné za časti a), b), c), d): (poistné za celú prílohu) 24 123,95

Poistné podmienky

Obsah poistenia upravujú:
Všeobecné poistné podmienky pre poistenie majetku právnických a podnikajúcich fyzických osôb, účinné od 1.5.2012 (ďalej len "VPP-M")
Zmluvné dojednania pre poistenie majetku, účinné od 1.5.2012 (ďalej len "ZD-M").
Doložky:
a dokumenty: Zoznam HV, zoznam nehnuteľností , Doložka M-LP ,

Vznik /zmena poistenia

Vznik/zmena poistenia na tejto prílohe od: 01.01.2016 00:00:00 00:00 hod.

Dôvod zmeny:

Dátum uzavretia poistenia/zmeny poistenia na tejto prílohe: 15.12.2015 00:00:00

podpis a odtlačok pečiatky poistníka

Allianz - Slovenská poisťovňa, a.s. Regionálne riaditeľstvo [illegible] 1

podpis a odtlačok pečiatky oprávneného zástupcu poisťovateľa

- Poistenie pre prípad nákazy hydiny,
- Poistenie pre prípad jednotlivých škôd,
- Poistenie pre prípad jednotlivých škôd na plemenných zvieratách.

2.1.16. Poistenie zodpovednosti za environmentálnu škodu dojednať ako:
- zodpovednosť za škodu - čl. 3 VPP-EZ a čl. 4 VPP-EZ, čl. 3 ZD-EZ.

2.2. Výhody produktu
- možnosť dojednať v jednej poistnej zmluve viacero druhov poistenia,
- v každom druhu poistenia je možné zohľadniť individuálne požiadavky poisteného,
- niektoré pripoistenia poskytované bezplatne,
- možnosť nahlasovania poistnej udalosti cez telefón alebo internet,
- obchodná zľava a bonus zohľadňuje komplexnosť poistenia,
- technické zľavy v závislosti od prístupu poisteného k minimalizácii rizika.

2.3. Všeobecná charakteristika poistného plnenia
2.3.1. Poistenie budov - čl. 16 VPP-M,
2.3.2. Poistenie hnuteľných vecí - čl. 16 VPP-M,
2.3.3. Poistenie prerušenia prevádzky - čl. 16 VPP-M, čl.7 ZD-PP a čl. 7 ZD-PP-SE,
2.3.4. Poistenie strojov a elektroniky - čl. 9 VPP-SE,
2.3.5. Poistenie nákladu - čl. 11 VPP-N,
2.3.6. Poistenie prevádzkovej zodpovednosti za škodu - čl. 5 VPP-Z,
2.3.7. Poistenie zodpovednosti za škodu cestného dopravcu - čl. 5 VPP-D,
2.3.8. Poistenie profesijnej zodpovednosti za škodu - lekári - čl. 5 VPP-L,
2.3.9. Poistenie profesijnej zodpovednosti za škodu - ekonomické, právne profesie - čl. 5 VPP-P,
2.3.10. Poistenie profesijnej zodpovednosti za škodu - IT - čl. 5 VPP-IT,
2.3.11. Stavebné poistenie - čl. 15 VPP-CAR-COM,
2.3.12. Poistenie bytových domov - čl. 16 VPP-M a čl. 8 ZD-BD,
2.3.13. Poistenie vozidiel autosalónov - čl. 16 VPP-M a čl. 4 ZD-A,
2.3.14. Poistenie plodín - čl. 15 VPP-PL,
2.3.15. Poistenie Hospodárskych zvierat- čl.17 VPP-HZ,
2.3.16. Poistenie zodpovednosti za environmentálnu škodu - čl. 7 VPP-EZ.

2.4. Výluky z poistenia
2.4.1. Poistenie budov - čl. 10, 11 a články poistných rizík VPP-M,
2.4.2. Poistenie hnuteľných vecí - čl. 10, 11 a články poistných rizík VPP-M,
2.4.3. Poistenie prerušenia prevádzky - čl. 10, 11 a články poistných rizík VPP-M čl. 4 ZD-PP a čl. 4 ZD-PP-SE,
2.4.4. Poistenie strojov a elektroniky - čl. 4 VPP-SE,
2.4.5. Poistenie nákladu - čl. 6 VPP-N,
2.4.6. Poistenie prevádzkovej zodpovednosti za škodu - čl. 4 VPP-Z , čl. 3 ods. 5 a čl. 4 ZD-Z,
2.4.7. Poistenie zodpovednosti za škodu cestného dopravcu - čl. 4 VPP-D,
2.4.8. Poistenie zodpovednosti za škodu - lekári - čl. 4 VPP-L,
2.4.8. Poistenie zodpovednosti za škodu - profesie - čl. 4 VPP-P,
2.4.9. Poistenie profesijnej zodpovednosti za škodu - IT - čl. 4 VPP-IT,
2.4.7 Stavebné poistenie - čl. 5 a čl. 13 VPP-CAR-COM,
2.4.8. Poistenie bytových domov - čl. 10, 11 a články poistných rizík VPP-M,
2.4.9. Poistenie vozidiel autosalónov - čl. 10, 11 a články poistných rizík VPP-M,
2.4.10. Poistenie plodín - čl. 5 VPP-PL,
2.4.11. Poistenie Hospodárskych zvierat - čl. 2 -7 VPP-HZ,
2.4.12. Poistenie zodpovednosti za environmnetálnu škodu - čl. 6 VPP-EZ, čl. 3 ZD-EZ.

2.5. Upozornenie na možnosť sankcií a postihov spojených s poistným plnením
Poistovateľ je oprávnený znížiť, zamietnuť alebo odmietnuť poistné plnenie, ak poistený porušil povinnosti uvedené v nasledovných ustanoveniach:
2.5.1. Poistenie budov - čl. 20 a článkoch poistených rizík VPP-M,
2.5.2. Poistenie hnuteľných vecí - čl. 20 a článkoch poistených rizík VPP-M,
2.5.3. Poistenie prerušenia prevádzky - čl. 20 a článkoch poistených rizík VPP-M, čl.10 ZD-PP a čl. 10 ZD-PP-SE,
2.5.4. Poistenie strojov a elektroniky - čl. 13 VPP-SE,
2.5.5. Poistenie nákladu - čl. 15 VPP-N,
2.5.6. Poistenie prevádzkovej zodpovednosti za škodu - čl. 9 VPP-Z,
2.5.7. Poistenie zodpovednosti za škodu cestného dopravcu - čl. 9 VPP-D,
2.5.8. Poistenie zodpovednosti za škodu - lekári - čl. 11 VPP-L,
2.5.9. Poistenie profesijnej zodpovednosti za škodu - IT - čl. 11 VPP-IT,
2.5.7. Stavebné poistenie - čl. 8 VPP-CAR-COM,
2.5.8. Poistenie bytových domov - čl. 20 a články poistných rizík VPP-M,
2.5.9. Poistenie vozidiel autosalónov - čl. 20 a články poistných rizík VPP-M,
2.5.10. Poistenie plodín - čl. 12 VPP-PL, čl. 19 VPP-PL a čl. 20 VPP-PL,
2.5.11. Poistenie Hospodárskych zvierat:
- poistenie hospodárskych zvierat pre prípad nákazy čl. 8 ods. 9, 10, 11, 12, 13 ZD,
- poistenie hydiny pre prípad nákazy čl. 8 ods. 8, 9, 10, 11, 12 ZD,
- poistenie pre prípad jednotlivých škôd na zvieratách čl. 8 ods. 6, 7, 8, 9, 10 ZD,
- poistenie pre prípad jednotlivých škôd na plemenných zvieratách čl. 8 ods. 6, 7, 8, 9 ZD.

2.5.12. Poistenie zodpovednosti za environmentálnu škodu - čl. 13 VPP-EZ.

3. Upozornenie o následkoch omeškania s úhradou poistného
Poistenie zaniká, ak poistné za prvé poistné obdobie alebo jednorazové poistné nebolo zaplatené do troch mesiacov odo dňa jeho splatnosti. Poistenie zanikne aj tak, že poistné za ďalšie poistné obdobie nebolo zaplatené do jedného mesiaca odo dňa doručenia výzvy poistovateľa na jeho zaplatenie, ak nebolo poistné zaplatené pred doručením tejto výzvy. Výzva poistovateľa obsahuje upozornenie, že poistenie zanikne, ak nebude zaplatené. To isté platí, ak bola zaplatená len časť poistného.

4. Doplnkové administratívne služby, ktoré nie sú zahrnuté v cene poistenia a poplatky s nimi spojené a spôsob sprístupňovania informácií o ich zmene
V poistení nie sú uplatňované žiadne ďalšie poplatky súvisiace s doplnkovými administratívnymi službami.

5. Upozornenie na ustanovenia poistnej zmluvy, ktoré umožňujú poisťovateľovi vykonávať zmeny podmienok poistenia bez súhlasu druhej zmluvnej strany

5.1. Poistenie budov - čl. 4 ZD-M umožňuje v prípade dojednania poistenia na novú hodnotu automaticky aktualizovať poistnú sumu budov pre ďalšie poistné obdobie o hodnotu indexu stavebných prác a materiálov.
5.2. Poistenie hnuteľných vecí - čl. 4 ZD-M umožňuje v prípade dojednania poistenia na novú hodnotu automaticky aktualizovať poistnú sumu výrobných a prevádzkových zariadení a cudzích vecí pre ďalšie poistné obdobie o hodnotu indexu spotrebiteľských cien.

6. Podmienky odstúpenia od poistnej zmluvy a vypovedania poistnej zmluvy

6.1. Pri vedomom porušení povinností uvedených v ustanoveniach § 793 Občianskeho zákonníka môže poisťovateľ od poistnej zmluvy odstúpiť, ak pri pravdivom a úplnom zodpovedaní otázok by poistnú zmluvu neuzavrel. Toto právo môže poistovateľ uplatniť do troch mesiacov odo dňa, keď takú skutočnosť zistil; inak právo zanikne.
6.2. Poistenie zanikne výpoveďou:
6.2.1 jednej zo zmluvných strán do dvoch mesiacov po uzavretí poistnej zmluvy. Výpovedná lehota je osemdenná, jej uplynutím poistenie zanikne,
6.2.2 ku koncu poistného obdobia: výpoveď sa musí dať aspoň 6 týždňov pred jeho uplynutím,
6.2.3 jednej zo zmluvných strán do jedného mesiaca odo dňa poskytnutia poistného plnenia alebo jeho zamietnutia. Výpovedná lehota je osemdenná, jej uplynutím poistenie zanikne,
6.2.4 do dvoch mesiacov odo dňa, kedy sa poistovateľ dozvedel o zmene v skutočnostiach, ktoré boli podkladom pri uzavieraní poistnej zmluvy, pokiaľ zmluvné strany neakceptujú uvedené zmeny úpravou poistnej zmluvy; poistenie v takom prípade zanikne doručením výpovede druhej zmluvnej strane.

7. Spôsob vybavovania sťažností

7.1. Poisťovateľ prijíma a rieši sťažnosti podané, proti jeho postupu, ústne alebo písomne. Sťažovateľ môže ústnu a písomnú sťažnosť podať osobne na pracoviskách servisu klientom a v agentúrnych kanceláriách poisťovateľa. Ústnu sťažnosť môže sťažovateľ podať aj na telefónnom čísle 0800 122 222. Ústne podanú sťažnosť poistovateľ zaznamená. Písomnú sťažnosť môže sťažovateľ zaslať aj emailom na dialog@allianzsp.sk alebo poštou na adresu sídla poisťovateľa.
7.2. Zo sťažnosti musí byť zrejmý dátum jej podania, kto ju podáva, čoho sa týka (predmet sťažnosti) a čoho sa sťažovateľ domáha. Ak je sťažovateľom fyzická osoba, sťažnosť musí obsahovať meno, priezvisko a adresu bydliska fyzickej osoby. Ak je sťažovateľom právnická osoba, sťažnosť musí obsahovať názov alebo obchodné meno a adresu sídla právnickej osoby.
7.3. Poisťovateľ je povinný prešetriť sťažnosť a informovať sťažovateľa o spôsobe vybavenia jeho požiadaviek či dôvodoch ich zamietnutia do 30 dní odo dňa jej doručenia. Ak si vybavenie sťažnosti vyžaduje dlhšie obdobie, je možné lehotu podľa predchádzajúcej vety predĺžiť, o čom bude sťažovateľ bezodkladne upovedomený.
7.4. V prípade, že je sťažnosť podaná opakovane, tým istým sťažovateľom, v rovnakej veci a neobsahuje nové skutočnosti, poisťovateľ nie je povinný sťažnosť vybaviť a sťažovateľa o tom upovedomiť.

Upozornenie poistníka

Informácie uvedené v tomto formulári neobsahujú úplný rozsah práv a povinností, ktorý poistníkovi vyplýva z uzavretia poistnej zmluvy a nenahrádzajú informačné povinnosti ustanovené všeobecne záväznými právnymi predpismi pri predaji alebo sprostredkovaní poistných produktov.

Tlačivo „Informácia o podstatných častiach uzatváranej poistnej zmluvy bolo schválené dňa 1.6.2012.

Allianz Slovenská poisťovňa

Doložka M – LP: **Osobitné dojednania pre poistenie na viacerých miestach poistenia**

1. Táto doložka tvorí neoddeliteľnú súčasť horeuvedenej poistnej zmluvy.
2. Touto doložkou sa dojednáva, že limity poistného plnenia pre pripoistenia dojednané na prílohe č. 1 horeuvedenej NPZ/poistnej zmluvy sa vzťahujú na všetky prílohy horeuvedenej NPZ/ poistnej zmluvy.
3. Ostatné ustanovenia VPP-M a ZD-M zostávajú touto doložkou nedotknuté.

Miesta poistenia:

a) B.Slančíkovej 1, Nitra
b) Nábrežie mládeže 91, Nitra
c) Hodžova 1, Nitra
d) Kraskova 1, Nitra
e) Drážovská cesta 2 a 4, Nitra
f) Tr. A. Hlinku 1, Nitra
g) Štefániková ulica 67, Nitra
h) ŠD UKF Brezový Háj

V Nitre , dňa 15.12.2015

podpis a otlačok pečiatky poistníka

poisťovňa, a.s.
Bratislava

podpis a otlačok pečiatky zástupcu poisťovateľa

Doložka M: **Doplnenie podmienok poistenia na základe požiadavky zadávateľa požiadavky na vypracovanie ponuky poistenia**

Táto doložka tvorí neoddeliteľnú súčasť horeuvedenej poistnej zmluvy. V súlade s VPP-M sa dojednávajú nasledovné podmienky:

1. Poistná zmluva alebo jej dodatky nadobúdajú platnosť po ich podpisaní štatutárnymi zástupcami oboch zmluvných strán a účinnosť po dni zverejnenia podľa platných právnych predpisov

2. Poisťovateľ je povinný strpieť výkon kontroly/auditu/overovania súvisiaceho s predmetom zmluvy kedykoľvek počas platnosti a účinnosti zmluvy oprávnenými osobami a je povinný im poskytnúť všetku potrebnú súčinnosť. Oprávnené osoby na výkon kontroly/auditu/overovania na mieste sú najmä:

   - poskytovateľ NFP a ním poverené osoby. Poskytovateľom NFP je agentúra Ministerstva školstva , vedy, výskumu a športu Slovenskej republiky pre štrukturálne fondy EÚ, Hanulova 5/B, 841 02 Bratislava
   - Najvyšší kontrolný úrad SR, príslušná správa finančnej kontroly, Certifikačný orgán a nimi poverené osoby
   - orgán auditu, jeho spolupracujúce orgány a nimi poverené osoby
   - splnomocnení zástupcovia Európskej komisie a Európskeho dvora audítorov
   - osoby prizvané vyššie uvedenými orgánmi v súlade s príslušnými právnymi predpismi SR a ES

3. Poisťovateľ súhlasí so zverejnením textu tejto zmluvy

4. Poisťovateľ dodá najneskôr do jedného pracovného dňa po podpise zmluvy znenie zmluvy vrátane príloh v elektronickej forme vo formáte pdf pre zverejnenie zmluvy v Centrálnom registri zmlúv vedenom Úradom vlády SR.

V Nitre dňa 15.12.2015

podpis a otlačok pečiatky poistníka

Allianz Slovenská poisťovňa, a.s.

podpis a otlačok pečiatky zástupcu poisťovateľa

Príloha č.2

Univerzita Konštantína Filozofa v Nitre, Trieda A. Hlinku 1, 949 74 Nitra

Poistenie hnuteľného majetku na UKF v Nitre na rok 2016

	Projekt (kód ITMS):																	
	26120130028	26110230026	26220120042	26110230080	26220220110	26250120041	26220220033	26110230041	26110230096	26110230050	26110230014	26110230081	26220120051	26110230033	26110230012	26220220180	26110230022	26250120049	26250120063	26110230114	SPOLU
Hodnota poisteného majetku	47 097,16	45 719,79	283 776,11	6 544,08	712 446,48	2 554 933,89	13 595,00	37 158,90	105 323,49	84 413,41	26 002,01	26 259,17	53 358,12	26 902,09	34 526,18	3 124 728,00	66 691,78	168 888,72	500 755,76	27 636,42	7 946 756,56
Ročné poistné	13,25 €	12,87 €	79,86 €	1,84 €	200,50 €	719,04 €	3,83 €	10,46 €	29,64 €	23,76 €	7,32 €	7,39 €	15,02 €	7,57 €	9,72 €	879,39 €	18,77 €	47,53 €	140,93 €	7,78 €	2 236,46 €

Poistné riziká: požiar do výšky poisťovaného majetku - spoluúčasť 100 EUR

Základná sadzba poistného 0,2814 €

Charakter hnuteľného majetku:

Informačno-komunikačné technologie, prístroje, kancelárske zariadenia, nábytok, učebné pomôcky a pod.

Spôsob zabezpečenia vstupov do budov, v ktorých sa nachádza poisťovaný hnuteľný majetok

Vstup do budovy: základné mechanické zabezpečenie pevnými dverami uzamykateľnými bezpečnostnou profilovou cylindrickou vložkou
elektrické posuvné dvere s elektromechanickým zámkom
pripojenie na pult centrálnej ochrany

Ostatné otvory: bežné stavebné prvky, cez ktoré nie je možné vniknúť bez ich poškodenia

V Nitre dňa 15.12.2015

Allianz
Slovenská poisťovňa
Allianz - Slovenská poisťovňa, a.s.
Regionálne riaditeľstvo
Chorvátska 9
949 01 NITRA 1

Kristina Divincová

.....

Meno a podpis oprávneného zástupcu

Obchodné meno: Allianz SP a.s.

Klient/VOJ: Univerzita Konštantína Filozofa v Nitre
Výpis číslo: 239 **Dátum výpisu:** 23.12.2015
Účet: SK84 8180 0000 0070 0024 0831 **BIC:** SPSRSKBA
Mena účtu: EUR

ŠTÁTNA POKLADNICA

Dátum sprac.	Trans.ID	Účet			BIC	Platiteľ/Príjemca	
Dátum splat.	Popis			Kurz MO	Kurz MÚ	Suma v mene operácie	Suma v mene účtu
Dátum odpis.	VS	ŠS	KS		Referencia odosielateľa		
Správa pre prijímateľa							

23.12.2015	459074282	SK17 1100 0000 0026 2600 6702		TATRSKBXXXX	ALLIANZ-SLOVENSKA POISTOVNA	
23.12.2015	Hrom. PP na úhradu				-10 252,68 EUR	-10 252,68 EUR
23.12.2015	9873010993		3558			
Allianz-poistenie majetku a budov r.2016						

Klient/VOJ: Univerzita Konštantína Filozofa v Nitre
ID klienta/VOJ: 2882
IČO klienta/VOJ: 00157716
Adresa klienta/VOJ: Tr. Andreja Hlinku 1, 94974 Nitra

ŠTÁTNA POKLADNICA

Výpis číslo: 239 **Dátum výpisu:** 23.12.2015
Účet: SK84 8180 0000 0070 0024 0831 **BIC:** SPSRSKBA
Názov účtu: Bežný účet neúročený dotačný UKF v Nitre
Produkt: BÚ neúročený
Mena účtu: EUR

31 139

Obdobie výpisu: 23.12.2015 - 23.12.2015
Začiatočný stav:
Konečný stav:

Obraty na výpise
Obraty debet:
Obraty kredit:
Obraty spolu: